USGS
science for a changing world

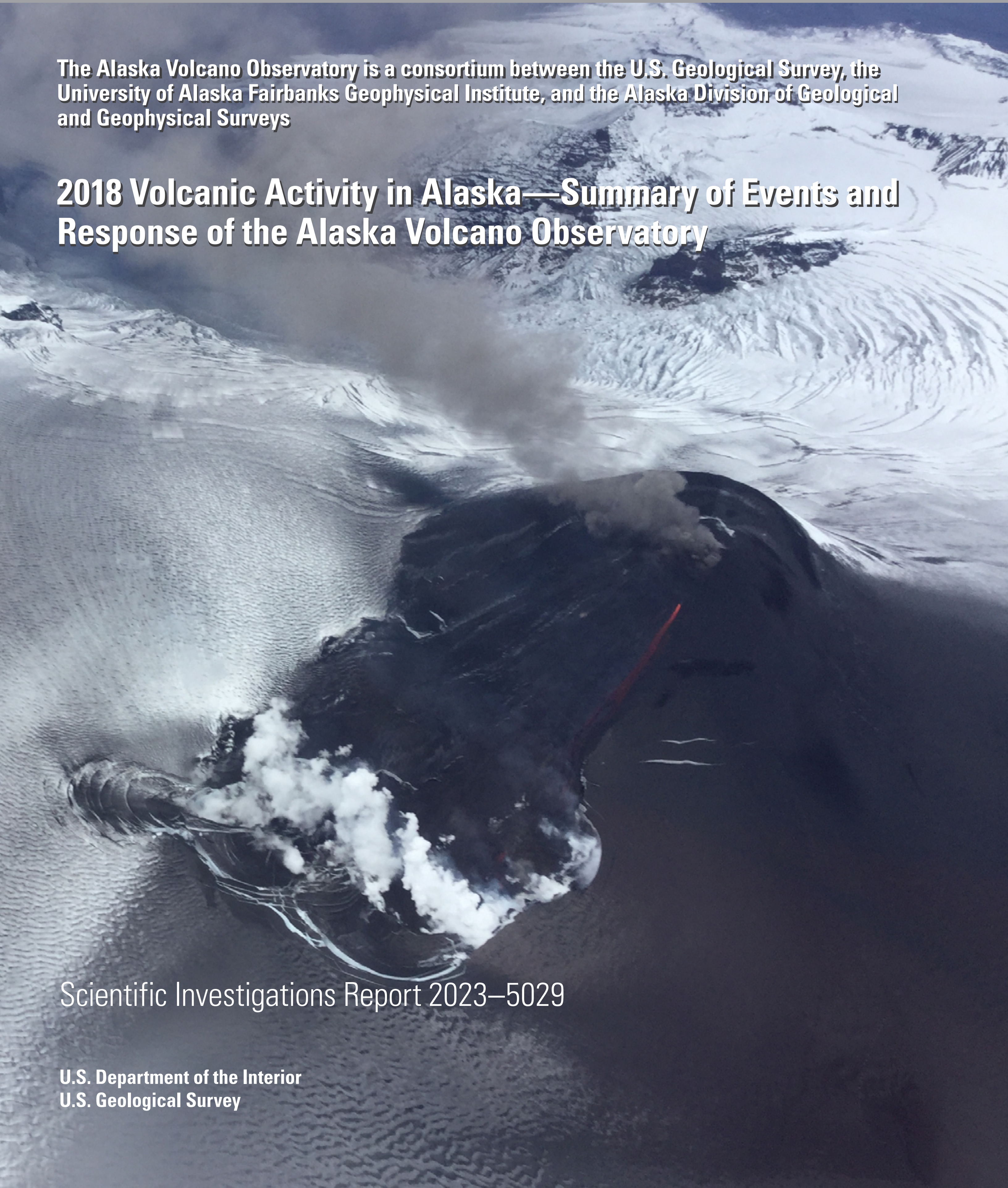

The Alaska Volcano Observatory is a consortium between the U.S. Geological Survey, the University of Alaska Fairbanks Geophysical Institute, and the Alaska Division of Geological and Geophysical Surveys

# 2018 Volcanic Activity in Alaska—Summary of Events and Response of the Alaska Volcano Observatory

Scientific Investigations Report 2023–5029

**U.S. Department of the Interior**
**U.S. Geological Survey**

**Cover.** Oblique aerial photograph, taken September 26, 2018, showing active lava flows from the intracaldera cone of Mount Veniaminof, which erupted from September through December. Ash deposits from explosive phases of the eruption blanket the intracaldera ice field downwind from the cone. Aerial photograph by M. Laker, U.S. Fish and Wildlife Service.

# 2018 Volcanic Activity in Alaska—Summary of Events and Response of the Alaska Volcano Observatory

By Cheryl E. Cameron, Tim R. Orr, James P. Dixon, Hannah R. Dietterich, Christopher F. Waythomas, Alexandra M. Iezzi, John A. Power, Cheryl Searcy, Ronni Grapenthin, Gabrielle Tepp, Kristi L. Wallace, Taryn M. Lopez, Kimberly DeGrandpre, and John M. Perreault

The Alaska Volcano Observatory is a consortium between the U.S. Geological Survey, the University of Alaska Fairbanks Geophysical Institute, and the Alaska Division of Geological and Geophysical Surveys

Scientific Investigations Report 2023–5029

**U.S. Department of the Interior**
**U.S. Geological Survey**

U.S. Geological Survey, Reston, Virginia: 2023

For more information on the USGS—the Federal source for science about the Earth, its natural and living resources, natural hazards, and the environment—visit https://www.usgs.gov or call 1–888–ASK–USGS (1–888–275–8747).

For an overview of USGS information products, including maps, imagery, and publications, visit https://store.usgs.gov.



Suggested citation:
Cameron, C.E., Orr, T.R., Dixon, J.P., Dietterich, H.R., Waythomas, C.F., Iezzi, A.M., Power, J.A., Searcy, C., Grapenthin, R., Tepp, G., Wallace, K.L., Lopez, T.M., DeGrandpre, K., and Perreault, J.M., 2023, 2018 Volcanic activity in Alaska—Summary of events and response of the Alaska Volcano Observatory: U.S. Geological Survey Scientific Investigations Report 2023–5029, 68 p., https://doi.org/10.3133/sir20235029.

ISSN 2328-0328 (online)

# Acknowledgments

This report represents work of the entire Alaska Volcano Observatory staff, colleagues from other U.S. Geological Survey volcano observatories, cooperating State and Federal agencies, and members of the public. This publication greatly benefited from thoughtful technical reviews by Ninfa Bennington and Brandon Browne, who improved the content and presentation. We particularly thank those who contributed to maintaining the internal chronologies of activity at active volcanic centers. The Alaska Volcano Observatory is funded by the U.S. Geological Survey Volcano Hazards Program and the State of Alaska.

# Contents

## Figures

## Tables

# Conversion Factors

U.S. customary units to International System of Units

| Multiply | By | To obtain |
|---|---|---|
| | Length | |
| foot (ft) | 0.3048 | meter (m) |
| foot (ft) | 0.000305 | kilometer (km) |

International System of Units to U.S. customary units

| Multiply | By | To obtain |
|---|---|---|
| | Length | |
| centimeter (cm) | 0.3937 | inch (in.) |
| meter (m) | 3.281 | foot (ft) |
| meter (m) | 1.0936 | yard (yd) |
| kilometer (km) | 3,281 | foot (ft) |
| kilometer (km) | 0.6214 | mile (mi) |
| | Area | |
| square meter ($m^2$) | 10.76 | square foot ($ft^2$) |
| square kilometer ($km^2$) | 0.3861 | square mile ($mi^2$) |
| | Volume | |
| cubic meter ($m^3$) | 35.31 | cubic foot ($ft^3$) |
| cubic meter ($m^3$) | 1.308 | cubic yard ($yd^3$) |
| cubic kilometer ($km^3$) | 0.2399 | cubic mile ($mi^3$) |
| | Mass | |
| metric ton (t) | 1.102 | ton, short [2,000 pounds] |
| metric ton (t) | 0.9842 | ton, long [2,240 pounds] |
| | Mass flow | |
| metric ton per day (t/d) | 1.102 | ton, short [2,000 pounds] per day |
| metric ton per day (t/d) | 0.9842 | ton, long [2,240 pounds] per day |

Temperature in degrees Celsius (°C) may be converted to degrees Fahrenheit (°F) as follows:

$$°F = (1.8 \times °C) + 32.$$

## Datum

Altitude, as used in this report, refers to distance above sea level of a location in the air.

Elevation, as used in this report, refers to distance above sea level of a location on the land surface.

Depth, as used in this report, refers to distance below sea level.

Locations in latitude and longitude are presented in decimal degrees referenced to the World Geodetic System 1984 (WGS84) datum, unless otherwise noted.

## Abbreviations

| | |
|---|---|
| AKDT | Alaska daylight time; UTC–8 hours |
| AKST | Alaska standard time; UTC–9 hours |
| ASL | above sea level |
| AVO | Alaska Volcano Observatory |
| GPS | Global Positioning System |
| GVP | Smithsonian Institution Global Volcanism Program |
| LP | long-period |
| # | number |
| OMI | Ozone Mapping Instrument |
| OMPS | Ozone Mapping and Profile Suite |
| PIREP | pilot weather report |
| RSAM | real-time seismic amplitude measurement |
| Suomi-NPP | Suomi National Polar-Orbiting Partnership satellite |
| UAFGI | University of Alaska Fairbanks Geophysical Institute |
| USGS | U.S. Geological Survey |
| UTC | coordinated universal time; same as Greenwich mean time |
| VT | volcano-tectonic |

# 2018 Volcanic Activity in Alaska—Summary of Events and Response of the Alaska Volcano Observatory

By Cheryl E. Cameron,[1] Tim R. Orr,[2] James P. Dixon,[2] Hannah R. Dietterich,[2] Christopher F. Waythomas,[2] Alexandra M. Iezzi,[3] John A. Power,[2] Cheryl Searcy,[2] Ronni Grapenthin,[3] Gabrielle Tepp,[2] Kristi L. Wallace,[2] Taryn M. Lopez,[3] Kimberly DeGrandpre,[4] and John M. Perreault[1]

## Abstract

The Alaska Volcano Observatory responded to eruptions, considerable and minor volcanic unrest, and seismic events at 15 volcanic centers in Alaska during 2018. The most notable volcanic activity came from Mount Cleveland, which had continuing intermittent dome growth and ash eruptions, and Mount Veniaminof, Great Sitkin Volcano, and Semisopochnoi Island, the three of which had minor eruptions. This report also documents landslides at Iliamna Volcano; resuspended ash from the 1912 Novarupta-Katmai eruption; anomalous seismicity and heightened degassing at Pavlof Volcano; seismic unrest at Shishaldin Volcano; long-term inflation at Westdahl volcano, Akutan Volcano, and Mount Okmok; steam plumes, anomalous seismicity, and anomalous gas measurements at Makushin Volcano; elevated seismicity at Mount Gareloi; seismic signals possibly related to icequakes at Mount Spurr; and new mud flows at Shrub mud volcano.

## Introduction

The Alaska Volcano Observatory (AVO) is responsible for monitoring, studying, and warning of hazards associated with volcanic unrest in Alaska (fig. 1). This report summarizes notable volcanic activity in Alaska during 2018 (tables 1, 2) and briefly describes AVO's response. Information about all volcanic unrest is included, even if no formal public notification was issued. Observations, images, and data that are typically not published elsewhere are included in this report. Similar summaries of volcanic unrest and AVO's response have been published annually since 1992 (appendix 1).

The AVO volcano monitoring program includes daily analysis of satellite imagery, webcam imagery, seismicity, and infrasound and other acoustic detections. The program also analyzes data from occasional overflights, takes airborne and ground-based gas measurements, and compiles visual reports from aircraft pilots (pilot weather reports), observatory personnel, local residents, and mariners. AVO receives real-time deformation data from permanent Global Positioning System (GPS) stations at eight Alaskan volcanoes: Akutan Volcano, Augustine Volcano, Makushin Volcano, Mount Okmok, Redoubt Volcano, Shishaldin Volcano, Mount Spurr, and Westdahl volcano. These deformation data are supplemented with Interferometric Synthetic Aperture Radar (InSAR) imagery (for example, Lee and others, 2010).

AVO scientists produce daily reports through weekly duty scientist and duty remote sensing rotations. The duty remote sensor produces a daily remote sensing report, whereas the duty scientist summarizes all observations (including remote sensing and seismicity) at volcanoes with elevated Aviation Color Codes and Volcano Alert Levels. The reports also include descriptions of any notable satellite and webcam observations at the other volcanoes AVO monitors. These observations are archived in an internal database structure to assist in retrieving past records. A second rotation of scientists from AVO and the U.S. Geological Survey National Earthquake Information Center monitors the volcanoes that have local seismometers and analyzes activity detected on regional infrasound sensors. Each day, this team compiles three separate reports, spaced approximately eight hours apart. These reports are also catalogued within a relational database.

Thirty-three of the historically active volcanoes and volcanic fields in Alaska were instrumented with seismometers operated by AVO as of December 31, 2018. Included in this formal list are two volcanoes with insufficient seismic instrumentation to compute reliable earthquake hypocenters and magnitudes, and four whose real-time telemetry was not reliable enough to produce a complete record of earthquake activity. For example, owing to the small size and remote location of Bogoslof Island, installing a network that could be used to locate earthquakes at Bogoslof volcano is not possible. To increase AVO's capability to monitor this volcano, a broadband seismograph station was installed on the island in the summer of 2018. Mount Cleveland, in contrast, is on a larger island but had only two seismograph stations in operation in 2018, so it lacked the minimum number of local stations to locate earthquakes. Little Sitkin Island, Semisopochnoi Island, and Mount Wrangell are also considered to have been unmonitored

[1]Alaska Division of Geological & Geophysical Surveys.

[2]U.S. Geological Survey.

[3]University of Alaska Fairbanks.

[4]Southern Methodist University.

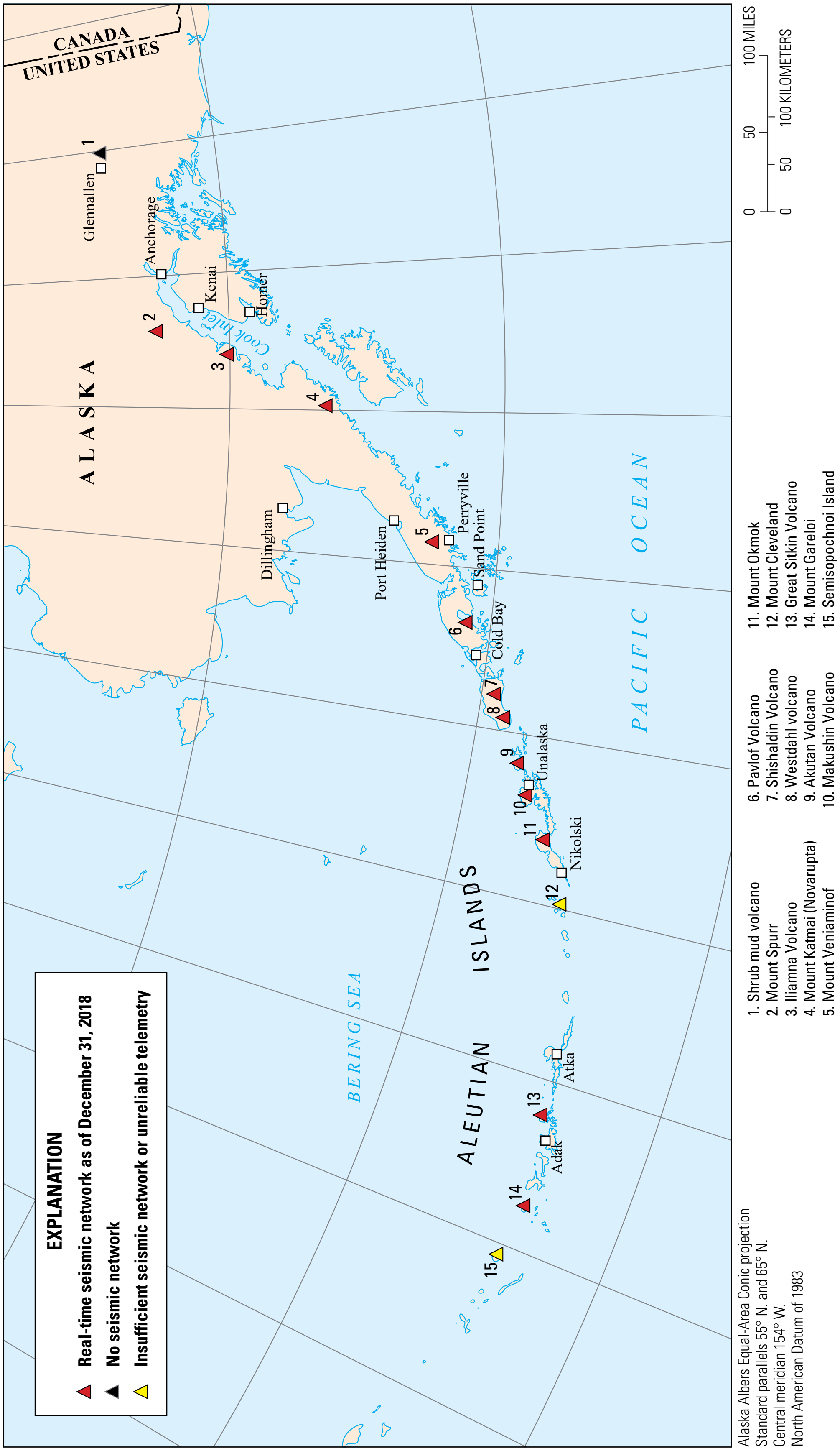


**Figure 1.** Map of volcanoes discussed in this report and their monitoring statuses. In addition, the map shows Shrub mud volcano, which produced new mud flows in 2018.

**Table 1.** Summary of 2018 monitoring highlights at Alaskan volcanoes, including but not limited to confirmed eruptions, possible eruptions, increases in seismicity, observations of fumarolic activity, and other notable events.

[Volcano locations shown in figure 1. See appendix tables 2.1 and 2.2 for lists of volcanic activity described in past Alaska Volcano Observatory annual summaries, sorted by year and by volcano]

| Volcano | Month of activity | Type of activity |
|---|---|---|
| Shrub mud volcano | October–December | New mud flows from flank |
| Mount Spurr | June | Seismicity, likely related to glacial movement |
| Iliamna Volcano | July | Minor snow and debris flow |
| Mount Katmai (Novarupta) | September | Resuspension of ash from 1912 eruption |
| Mount Veniaminof | September–December | Intermittent minor eruption |
| Pavlof Volcano | Year-round | Elevated seismic activity |
| Shishaldin Volcano | January | Declining volcanic unrest |
| Westdahl volcano | Year-round | Long-term inflation |
| Akutan Volcano | Year-round | Inflation |
| Makushin Volcano | Year-round | Earthquake swarms; gas plumes |
| Mount Okmok | Year-round | Inflation |
| Mount Cleveland | Year-round | Intermittent explosions and dome growth |
| Great Sitkin Volcano | January–June | Earthquake swarm; explosions |
| Mount Gareloi | June–September | Increased seismicity |
| Semisopochnoi Island | September–December | Minor eruption |

**Table 2.** Alaska volcanoes with Aviation Color Code and Volcano Alert Level changes in 2018.

[See appendix 3 for definitions of Aviation Color Codes and Volcano Alert Levels. Dates shown as month/day/year. Times shown as HH:MM in coordinated universal time (UTC)]

| Aviation Color Code/Volcano Alert Level | Date and time of change (UTC) |
|---|---|
| Mount Veniaminof | |
| **GREEN/NORMAL** | Beginning of year |
| **YELLOW/ADVISORY** | 09/03/2018 (19:29) |
| **ORANGE/WATCH** | 09/04/2018 (21:09) |
| **RED/WARNING** | 11/21/2018 (19:15) |
| **ORANGE/WATCH** | 11/22/2018 (20:05) |
| Shishaldin Volcano | |
| **YELLOW/ADVISORY** | Beginning of year |
| **GREEN/NORMAL** | 02/07/2018 (23:01) |
| Mount Cleveland | |
| **ORANGE/WATCH** | Beginning of year |
| **YELLOW/ADVISORY** | 02/09/2018 (22:44) |
| **ORANGE/WATCH** | 03/02/2018 (15:38) |
| **YELLOW/ADVISORY** | 03/05/2018 (22:14)[1] |
| **ORANGE/WATCH** | 04/04/2018 (12:35) |
| **YELLOW/ADVISORY** | 04/06/2018 (18:31) |
| **ORANGE/WATCH** | 05/05/2018 (06:20) |
| **YELLOW/ADVISORY** | 05/06/2018 (20:16) |

| Aviation Color Code/Volcano Alert Level | Date and time of change (UTC) |
|---|---|
| Mount Cleveland—Continued | |
| **ORANGE/WATCH** | 06/26/2018 (21:07) |
| **YELLOW/ADVISORY** | 08/22/2018 (19:45) |
| **ORANGE/WATCH** | 12/12/2018 (21:21) |
| Great Sitkin Volcano | |
| **YELLOW/ADVISORY** | Beginning of year |
| **GREEN/NORMAL** | 01/18/2018 (22:36) |
| **YELLOW/ADVISORY** | 06/10/2018 (21:26) |
| **GREEN/NORMAL** | 06/27/2018 (18:49) |
| **YELLOW/ADVISORY** | 07/01/2018 (18:37) |
| Semisopochnoi Island | |
| **UNASSIGNED** | Beginning of year |
| **YELLOW/ADVISORY** | 09/16/2018 (17:56) |
| **ORANGE/WATCH** | 09/17/2018 (21:33) |
| **YELLOW/ADVISORY** | 10/12/2018 (19:45) |
| **ORANGE/WATCH** | 10/26/2018 (05:35) |
| **YELLOW/ADVISORY** | 11/21/2018 (20:59) |
| **UNASSIGNED** | 12/19/2018 (20:35) |

[1]Erroneous alert notifications of a change to **GREEN** and **NORMAL** were issued and retracted on 03/06/2018.

in 2018 because the telemetry for each of their subnetworks was unreliable. Finally, the seismic network on Fourpeaked Mountain experienced an outage throughout 2018, leading to an unmonitored status for that volcano.

Volcanoes in this report are presented in geographic order from east to west along the Aleutian Arc. Each entry starts with a title block with information about that volcano, consisting of a unique identifier number (#) assigned by the Smithsonian Institution Global Volcanism Program (GVP), the volcano's latitude and longitude, its summit elevation, the name of its geographic region, and an abbreviated summary of its 2018 activity. The title block is followed by detailed information on the volcano's activity, commonly with accompanying tables, images, figures, or all three, before ending with a description of the volcano and a summary of its past activity. This information is derived from formal public AVO information products, internal online electronic logs compiled by AVO staff, and published material (such as Miller and others [1998]). Beginning with the 2013 report, AVO's annual summary has also included expanded information on seismicity at Alaskan volcanoes.

For information on the volcanic activity in past and present AVO summaries, see appendix table 2.1 for a compilation sorted by year and appendix table 2.2 for a compilation sorted by volcano. Note that AVO sometimes uses informal volcano names for clarity; the names provided by the official U.S. Board on Geographic Names (through the Geographic Names Information System) may match imprecisely with the volcanoes themselves. For example, Bogoslof volcano comprises more islands than Bogoslof Island. Alaska also has volcanoes without official place names, such as Takawangha volcano, which require the use of informal names.

Measurements are provided in the International System of Units, except for altitudes, which are reported in feet (ft) above sea level (ASL), in line with U.S. Federal aviation standards. Volcano locations, given in latitude and longitude, decimal degrees, and summit elevations (in meters [m]) are taken from AVO's database of Alaskan volcanoes (Cameron and others, 2022), and so may differ slightly from previously published compilations. General date references are given in local time unless specified otherwise. Most volcanoes in Alaska are in the Alaska standard time (AKST) or Alaska daylight time (AKDT) zones, but all Aleutian volcanoes west of Umnak Island (see the community of Nikolski, Alaska, on figure 1) are in the Hawaii-Aleutian standard time (HAST) or Hawaii-Aleutian daylight time (HADT) zones. In 2018, daylight saving time ran from March 11 to November 4.

# Volcanic Activity in Alaska, East to West Along the Aleutian Arc

## Shrub mud volcano


*Not listed in GVP database*
62.1490° N., 145.0211° W.
897 m

Copper River Basin

**NEW MUD FLOWS FROM FLANK**

In the fall of 2017, a new eruption began low on the southeast flank of Shrub mud volcano, discharging a mud flow that wrapped around the south side of the base of the cone. This was the first new activity observed at Shrub mud volcano since the late 1990s and marked its first flank eruption since 1996, when a pilot reported seeing mud erupting from a vent low on the north flank of the volcano. Satellite imagery indicates that the 2017 activity began sometime between

## What is an "eruption"?

The specific definition of the term "eruption" varies from scientist to scientist and has no universally agreed upon definition. Here, we adopt the usage of Siebert and others (2010, p. 17), who define eruptions as, "* * * events that involve the explosive ejection of fragmental material, the effusion of liquid lava, or both." The critical elements of this definition are the verbs "ejection" and "effusion," referring to dynamic surface processes that pose some level of hazard. The presence or absence of "juvenile material," or newly erupted rock, which can sometimes be ambiguous, is not relevant to this use of the term eruption, particularly when communicating a potential hazard. This definition does not, however, include passive volcanic degassing or hydrothermal fluid discharge.

## What is a "historically active volcano"?

AVO defines an active volcano as a volcanic center that has recently had an eruption (see "What is an 'eruption'? ") or a period of intense deformation, seismic activity, or fumarolic activity; these are inferred to reflect the presence of magma at shallow levels beneath the volcano. AVO considers the historical period in Alaska to be since 1741, when written records of volcanic activity began. On the basis of a rigorous reanalysis of all volcanic activity accounts in Alaska (from many sources), Cameron and others (2018) concluded that 54 Alaskan volcanoes fit these criteria. In this report, we modify the number of historically active volcanoes to 52, because we consider 1) Korovin Volcano and Mount Kliuchef to be subfeatures of Atka volcanic complex and 2) Novarupta to be a subfeature of Mount Katmai. As geologic understanding of Alaskan volcanoes improves through additional fieldwork and modern radiometric dating techniques, our list of active volcanoes will continue to evolve.

October 16 and October 20 and continued for several months, but given the poor quality of available imagery, it is equally likely that the event comprised two or more eruption episodes separated by pauses. A comparison between the mud flow extent visible in high-quality satellite imagery from June 2018 and helicopter overflight photos taken in June 2019 indicates that the eruption continued after June 2018.

Shrub mud volcano is one of the three mud volcanoes that compose the Klawasi group mud volcanoes, located in the Copper River Basin of south-central Alaska, about 26 kilometers (km) east of Glennallen, Alaska (fig. 1). Shrub mud volcano sits near the west slope of Mount Drum, a Pleistocene volcano in Wrangell-St. Elias National Park and Preserve, and occupies land administered by Ahtna, Incorporated, an Alaska Native regional corporation.

Shrub mud volcano rises 104 m above the surrounding terrain and is composed of deposits derived from the glaciolacustrine sediments that underlie the Copper River Basin (Richter and others, 1998a). Although minor mud discharge and weak gas emissions have historically been almost constant at the other two volcanoes of the Klawasi group (Upper Klawasi and Lower Klawasi mud volcanoes), Shrub mud volcano was barely active for decades, with only extremely weak activity observed in the mid-1950s (Nichols and Yehle, 1961). In the spring of 1997, however, and possibly as early as the summer of 1996, Shrub mud volcano began to vigorously erupt $CO_2$-rich gas and warm, saline mud (Richter and others, 1998a), producing mud flows from the base of its edifice. The activity waned over the next few years, eventually evolving into a bubbling mud pond at Shrub's summit. The pond made Shrub mud volcano more like Upper Klawasi and Lower Klawasi mud volcanoes, which both have similar features. The summit pond at Shrub mud volcano has remained active since it formed, with little change in behavior or appearance.

## Mount Spurr

GVP #313040
61.2989° N., 152.2539° W.
3,374 m

Cook Inlet


**SEISMICITY LIKELY RELATED TO GLACIAL MOVEMENT**

From June 6 to 9, 2018, AVO noted a sequence of seismic events on seismograph station STLK, located about 31 km east of Mount Spurr near Strandline Lake. This sequence was interpreted as glacial movement in the Strandline Lake area, but its precise source could not be located because only one station recorded the seismicity. The activity began on June 6 at 17:07 UTC (09:07 AKDT) with a series of weak, low-frequency earthquakes that increased in rate for an hour, at which point a 9-minute tremor-like signal was recorded (fig. 2). Earthquakes resumed after the tremor, and although

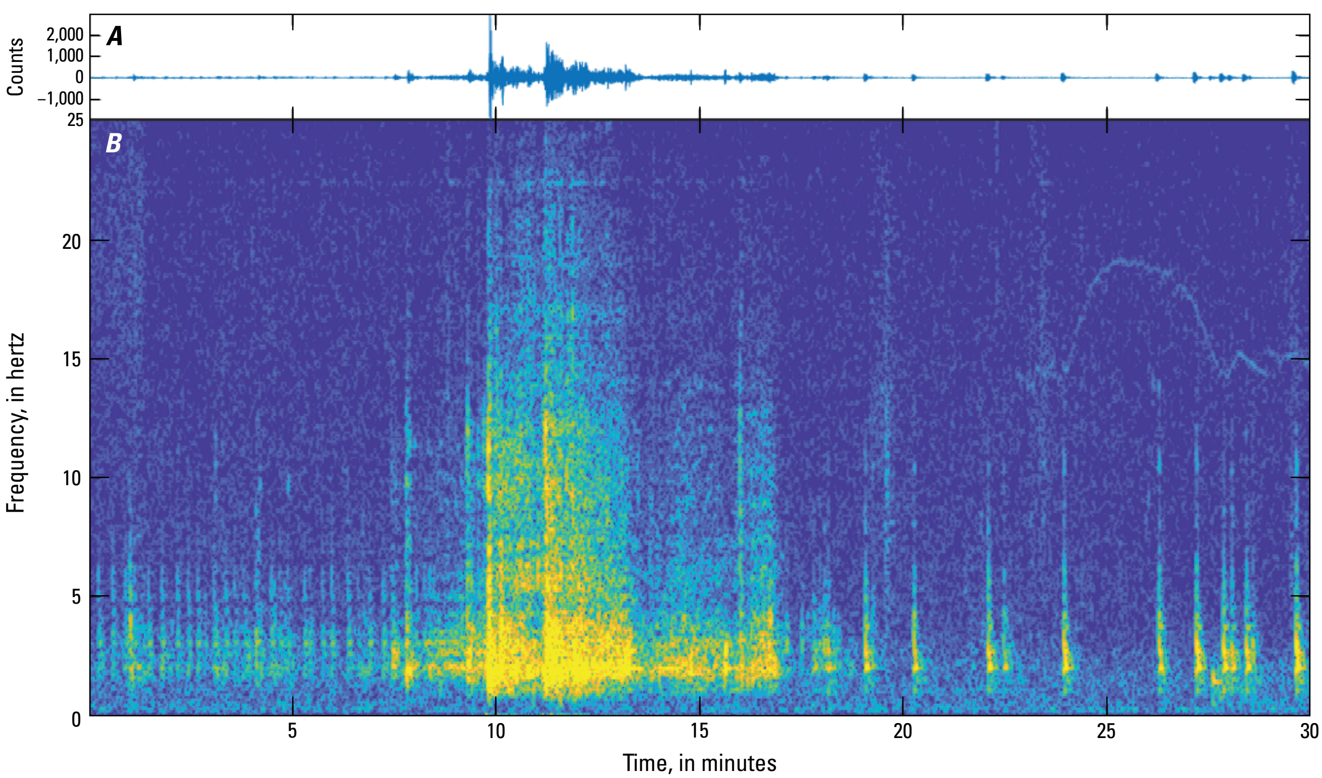


**Figure 2.** Waveform (*A*) and spectrogram (*B*) plots of part of the seismic sequence near Mount Spurr, south-central Alaska, on June 7, 2018. The tremor started at about the 8-minute mark and was both preceded and followed by earthquakes. Data from seismograph station STLK, starting at 02:00 coordinated universal time (June 6 at 18:00 Alaska daylight time). Colors represent shaking intensity at different frequencies, with warmer colors indicating higher values.

they took place at a lower event rate, they also produced the highest amplitudes of the sequence. Earthquakes decreased in amplitude considerably over the next 9 hours, but weak earthquakes continued until 15:35 UTC (07:35 AKDT) on June 9. About 950 earthquakes were detected in the entire sequence, with 90 taking place prior to the tremor. This sequence was similar to previously described seismicity produced by weather-related glacial movements (for example, Thelen and others, 2013; Allstadt and Malone, 2014), and the earthquakes likely reflected stick-slip movement of the glacier, with the tremor burst produced by a period of continuous motion. Changes in the character of the earthquakes, including increasing durations, through the sequence indicate the seismicity source was changing over time—either in location or source conditions.

Mount Spurr is a 3,374-meter-high, ice- and snow-covered stratovolcano 125 km west of Anchorage, Alaska. Its edifice may be a lava dome complex (Nye and Turner, 1990), but its last known summit eruption, calculated by correlating tephra deposits, took place about 5,200 years ago (Riehle, 1985). Mount Spurr has, however, produced many smaller eruptions since then (Kristi Wallace, U.S. Geological Survey and AVO, written commun., 2016); Crater Peak, a satellite vent 3.5 km south of the summit, produced two explosive eruptions in 1953 and 1992 (Keith, 1995, and references therein). Both eruptions created ashfalls that affected populated areas in south-central Alaska.

## Iliamna Volcano

*GVP #313020*
60.032° N., 153.092° W.
3,053 m


Cook Inlet

**MINOR SNOW AND DEBRIS FLOW**

Like in previous years, Iliamna Volcano experienced at least one large avalanche in 2018, as well as many smaller ones. The Aviation Color Code and Volcano Alert Level at the volcano remained **GREEN** and **NORMAL** throughout the year. Late in the morning of July 11, a resident from the Kenai Peninsula observed a fresh slide deposit on the east face of Iliamna Volcano (fig. 3*A*). A retrospective analysis of seismic data indicated a probable avalanche signal at 00:24 UTC on July 11, 2018 (July 10 at 14:24 AKDT). The same resident observed a deposit from a slightly larger avalanche on August 1, 2018 (fig. 3*B*), but retrospective seismic analysis did not yield a possible signal for this later event. These deposits are very similar to those of Iliamna Volcano avalanches observed in prior years (Cameron and others, 2020; Dixon and others, 2020).

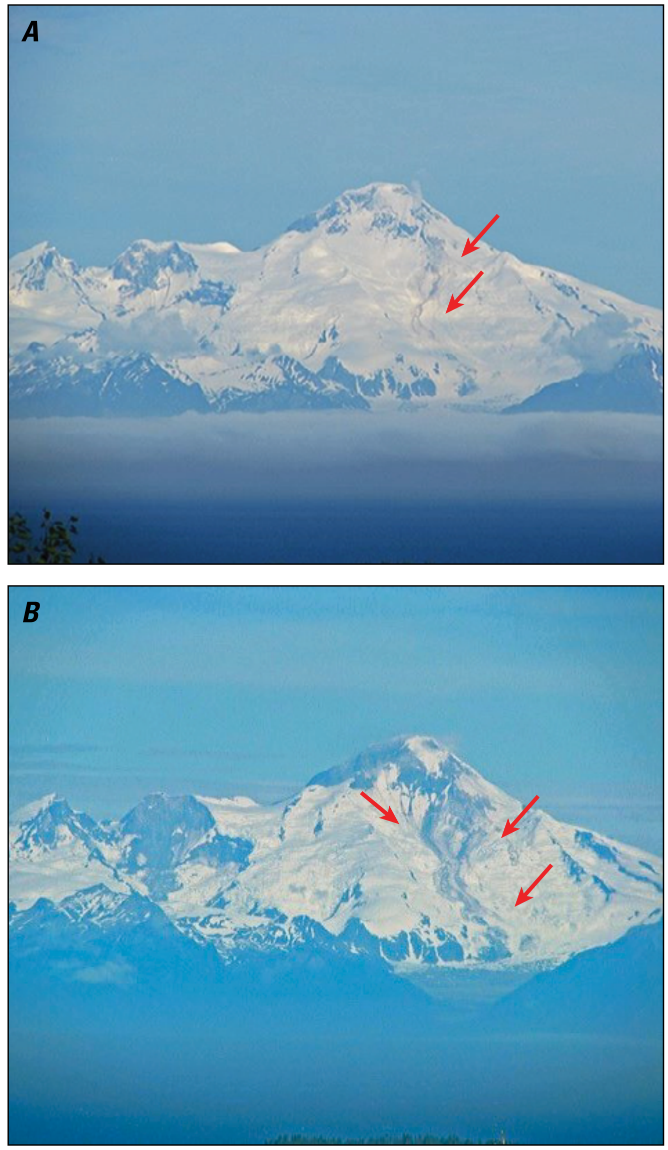


**Figure 3.** Photographs of fresh avalanches on the east side of Iliamna Volcano, south-central Alaska, as viewed from the Kenai Peninsula on July 12, 2018 (*A*), and August 1, 2018 (*B*). Locations of avalanches are shown with arrows. Photographs by Dennis Anderson.

On September 6, 2018, AVO measured the gas emissions at Iliamna Volcano during its annual overflight. These values proved largely unchanged from those of the previous year: instruments recorded an $H_2S/SO_2$ value of about 2, a $CO_2/(SO_2+H_2S)$ value of about 6, and an $SO_2$ emission rate of 45±30 metric tons per day (t/d). The large uncertainty of the $SO_2$ rate is due to a local wind field around the volcano that produces swirling air currents.

Iliamna Volcano is a glacier-carved stratovolcano on the southwest end of Cook Inlet, approximately 215 km southwest of Anchorage. Although no historical eruptions of the volcano are known, geologic studies document late Holocene explosive activity and repeated, considerable mass wasting of its steep, hydrothermally altered edifice (Waythomas and Miller, 1999). Fumaroles at an elevation of about 2,740 m on the east flank produce nearly constant plumes of steam and volcanic gas (Werner and others, 2011). In the past two decades, at least two magmatic intrusions without eruptions have taken place at Iliamna Volcano (Roman and others, 2004; Prejean and others, 2012).

## Mount Katmai (Novarupta)

*GVP #312170*
58.279° N., 154.953° W.
2,047 m


Alaska Peninsula

**RESUSPENSION OF 1912 ASH**

The resuspension and transport of fine-grained volcanic ash produced by the 1912 eruption of Mount Katmai at Novarupta (called the Novarupta-Katmai eruption) has been frequently observed and documented during at least the last several decades (Hadley and others, 2004; Wallace and Schwaiger, 2019). One such episode took place on September 29, 2018, when strong southeast winds entrained, resuspended, and transported ash northwest from the Mount Katmai (Novarupta) region. Ash was not observed in cloudy satellite data, but local pilots reported a resuspended ash cloud extending east of King Salmon, Alaska, below an altitude of 4,000 ft (1,200 m) ASL. The National Weather Service Alaska Aviation Weather Unit issued a significant meteorological weather advisory for aviators and AVO issued an information statement. AVO received no reports of ashfall on Kodiak Island (southeast of the Mount Katmai-Novarupta region). The Aviation Color Code and Volcano Alert Level remained **GREEN** and **NORMAL** for Mount Katmai (Novarupta) throughout 2018.

The 1912 Novarupta-Katmai eruption created atmospheric pyroclastic clouds that deposited approximately 17 cubic kilometers ($km^3$) of ash. It also produced ground-hugging pyroclastic currents that filled nearby valleys with 11 $km^3$ of volcanic material (Hildreth and Fierstein, 2012), creating what is today known as the Valley of Ten Thousand Smokes. Ash in this valley is as much as 200 m thick, and the valley remains almost entirely free of vegetation even more than a century after the eruption. When this landscape is snow-free, and particularly when the ground has little moisture content, strong winds can pick up the ash and create large ash clouds. During particularly strong wind conditions, the resuspended ash can be transported southeast across Shelikof Strait, Kodiak Island, and the Gulf of Alaska. These clouds are commonly seen by individuals downwind and are recorded in satellite imagery. The ash clouds commonly appear to originate broadly from the Mount Katmai (Novarupta) region rather than from a specific volcanic source, and although they look identical to dispersing volcanic ash clouds in satellite imagery, the phenomenon is not the result of volcanic activity.

## Mount Veniaminof

*GVP #312070*
56.198° N., 159.393° W.
2,507 m


Alaska Peninsula

**INTERMITTENT ERUPTION**

The 2018 eruption of Mount Veniaminof took place from early September to late December, ending a roughly 5-year repose since the end of its previous eruption in October 2013 (Dixon and others, 2015). Eruptive activity took place from a ~300-meter-high cone within the summit-defining, ice-filled caldera of Mount Veniaminof (fig. 4). All known historical eruptions have taken place at this cone, although only 5 of the 18 documented historical events produced lava flows.

Seismic unrest at Mount Veniaminof began late on September 2, 2018. AVO responded on September 3 by raising the Aviation Color Code and Volcano Alert Level from **GREEN** and **NORMAL** to **YELLOW** and **ADVISORY**, and on September 4 raised them again to **ORANGE** and **WATCH**. Lava fountaining, which likely began as early as September 6, was underway by September 7. By September 14, a lava flow extended about 800 m down the south flank of the summit cone. This flow eventually covered about 600,000 square meters ($m^2$), and intermittent ash emissions reached an altitude of 20,000 ft (6,000 m) ASL. Trace ashfall dusted nearby Perryville, Alaska, 35 km south of the volcano (table 3).

More details of the 2018 eruption are published in Loewen and others (2022) and Waythomas and others (2022). Information about the 2018 eruption is derived from geophysical instrumentation on or near the volcano, including an 8-station seismic network, regional infrasound sensors, frequent satellite images of the eruption, occasional aerial photographs taken by passing pilots, and webcam images of the volcano from Perryville (fig. 4). Overall, eruptive activity consisted of occasional explosive emissions of ash and steam, episodes of lava fountaining, and the effusion of lava flows.

Nearly continuous seismic tremor began at Mount Veniaminof late on September 2, and in response, AVO raised the Aviation Color Code from **GREEN** to **YELLOW** and the

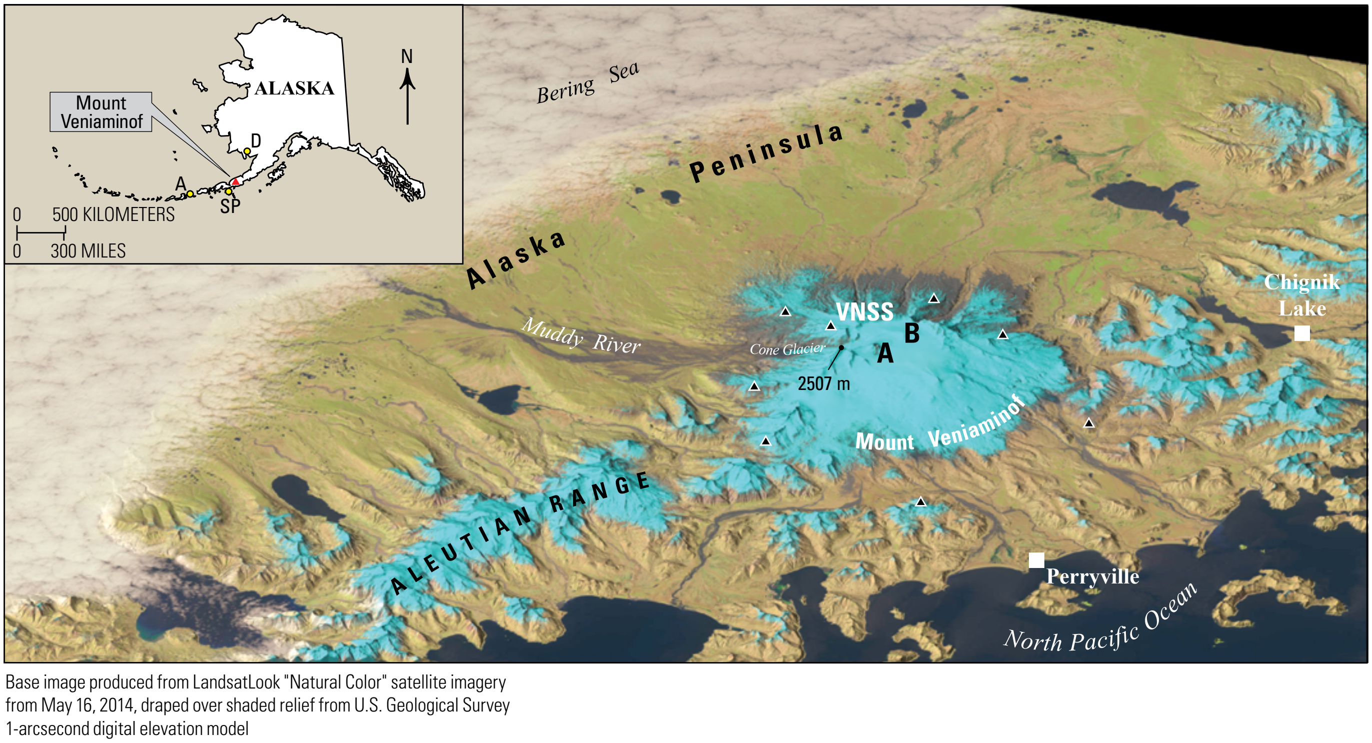


**Figure 4.** Oblique satellite view of Mount Veniaminof and the surrounding region in southwest Alaska. The intracaldera cone that is the site of all known historical eruptive activity is labeled A. An older intracaldera cone, mostly covered by ice and snow, with no known historical eruptions is labeled B. Triangles mark locations of seismic stations; station VNSS is labeled (see figure 5). The inset map shows the locations of Mount Veniaminof and infrasound arrays discussed in the report. These arrays are based in the cities of Dillingham (D), Akutan (A), and Sand Point (SP), Alaska. m, meter.

**Table 3.** Summary of activity and observations in 2018 at Mount Veniaminof, southwest Alaska.

[Dates shown in local time as month/day/year. Sept., September; AVO, Alaska Volcano Observatory; m, meter; ft, foot; $SO_2$, sulfur dioxide; ASL, above sea level (altitude); km, kilometer; Nov., November; Dec., December]

| Aviation Color Code/ Volcano Alert Level | Date | Observation description |
|---|---|---|
| YELLOW/ADVISORY | 09/03/2018 | Seismic activity increased late on Sept. 2 and continued through Sept. 3 with tremor; AVO raised the Aviation Color Code and Volcano Alert Level. |
| ORANGE/WATCH | 09/04/2018 | Minor ash emissions observed in webcam images and by residents in Perryville, Alaska; moderately elevated surface temperatures; AVO raised the Aviation Color Code and Volcano Alert Level. |
| ORANGE/WATCH | 09/05/2018 | Seismic swarm and tremor continued; minor ash emissions seen in webcam images; elevated surface temperatures seen in satellite data. |
| ORANGE/WATCH | 09/06/2018 | Minor ash emissions and elevated seismicity continued; highly elevated surface temperatures. |
| ORANGE/WATCH | 09/07/2018 | Minor ash emissions; incandescence observed in webcam images; lava fountaining. |
| ORANGE/WATCH | 09/08/2018–09/14/2018 | Lava flow extended 800 m from the vent; no sizable ash emissions. |
| ORANGE/WATCH | 09/15/2018–09/21/2018 | Lava flow paused advance on Sept. 18; no sizable ash emissions; $SO_2$ detected. |
| ORANGE/WATCH | 09/22/2018–09/28/2018 | Lava flow extended 900 m from the vent; minor ash emissions to 15,000 ft (4,600 m) ASL; $SO_2$ detected. |
| ORANGE/WATCH | 09/29/2018–10/05/2018 | Seismic tremor suggesting ongoing lava effusion; lava flow reached 1,000 m long; no sizable ash emissions; $SO_2$ detected. |
| ORANGE/WATCH | 10/06/2018–10/12/2018 | Lava effusion continued; $SO_2$ detected. |
| ORANGE/WATCH | 10/13/2018–10/19/2018 | Lava effusion continued; steam and minor ash plumes; nearly continuous seismic tremor; $SO_2$ detected. |

**Table 3.**—Continued

| Aviation Color Code/ Volcano Alert Level | Date | Observation description |
|---|---|---|
| ORANGE/WATCH | 10/20/2018–10/24/2018 | Lava effusion continued; steam and minor ash plumes; lava flow extended 1.2 km from the vent. |
| ORANGE/WATCH | 10/25/2018 | Trace ashfall at Perryville, 35 km southeast of the eruptive vent. |
| ORANGE/WATCH | 10/26/2018–11/09/2018 | Elevated surface temperatures and seismic tremor; plumes observed in satellite and webcam images. |
| ORANGE/WATCH | 11/10/2018–11/20/2018 | Elevated surface temperatures, seismic tremor, and infrasound detections; plumes visible in satellite and webcam images. Pilot reported ash to 16,000 ft (4,900 m) ASL on Nov. 16. |
| RED/WARNING | 11/21/2018 | Ash emissions increased; continuous ash plume extended 400 km southeast at 15,000 ft (4,600 m) ASL. Emissions preceded by strong rise in seismic tremor amplitude. Perryville residents heard “booming” that was likely explosions. AVO raised the Aviation Color Code and Volcano Alert Level. |
| ORANGE/WATCH | 11/22/2018 | Ash emissions and seismicity decreased. Ash plume extended 100 km from the vent, typically below 10,000 ft (3,000 m) ASL. Trace ashfall reported in Perryville on the morning of Nov. 22. AVO lowered the Aviation Color Code and Volcano Alert Level. |
| ORANGE/WATCH | 11/23/2018–11/30/2018 | Lava effusion continued; possible ash emission hiatus on Nov. 25–28. Low-level seismic tremor and small explosions detected by regional infrasound arrays. |
| ORANGE/WATCH | 12/01/2018–12/05/2018 | Lava effusion continued. |
| ORANGE/WATCH | 12/06/2018 | Seismicity changed from nearly continuous, low-level tremor to intermittent small, low-frequency events with short tremor bursts. Possible slowing or cessation of lava effusion. |
| ORANGE/WATCH | 12/07/2018–12/12/2018 | Eruption paused or slowed; reduced seismicity; no evidence of eruptive activity in webcam and satellite images through the morning of Dec. 13. |
| ORANGE/WATCH | 12/13/2018–12/21/2018 | Intermittent tremor returned, became continuous Dec. 13–16, then transitioned to discrete events. Ash plume and elevated surface temperatures observed in webcam and satellite images. Lava fountaining observed Dec. 15; $SO_2$ emissions detected in satellite data. |
| ORANGE/WATCH | 12/22/2018–12/31/2018 | Seismic tremor; highly elevated surface temperatures; lava fountaining observed Dec. 23–24. After Dec. 27, active lava effusion slowed or ceased. |

Volcano Alert Level from **NORMAL** to **ADVISORY** the next day. By the early afternoon of September 4, minor ash emissions were apparent in webcam images and were seen by observers in Perryville. This prompted AVO to raise the Aviation Color Code to **ORANGE** and the Volcano Alert Level to **WATCH** (fig. 5). Satellite imagery showed a trace amount of ashfall over the southwest sector of the caldera icefield. Webcam images obtained throughout the days of September 4–5 showed distinct, pulsatory ash emissions consistent with small Strombolian explosions. Diffuse ash emissions that reached an altitude of about 10,000–15,000 ft (3,000–4,600 m) ASL were observed by passing pilots on September 5. On September 7, incandescence was observed in early morning webcam images from Perryville, and mid-infrared satellite images showed strongly elevated surface temperatures at the intracaldera cone. These observations indicated that lava fountaining was underway by September 7, though initial lava effusion may have begun as early as September 6. Seismicity at the time was characterized by long-period events and pulsatory tremor bursts, the latter of which lasted as long as a few minutes, though it also included intermittent harmonic tremor (primarily on September 3). The tremor became more continuous around September 7.

On September 11, a passing pilot observed and photographed several thin, ribbon-like lava flows, fed by low fountaining or spattering, on the south flank of Mount Veniaminof’s intracaldera cone and coalescing at the cone’s base. A WorldView-3 satellite image acquired on the same day showed lava erupting from as many as four small vents in the same area and feeding a lava flow covering about 50,600 $m^2$. On September 16 and 18, Sentinel-2 satellite images showed definitive steam emissions associated with lava-ice interaction at the terminus of the lava flow, and on September 25, robust, vertically rising steam emissions associated with lava-ice interaction were evident in Perryville webcam images (fig. 6). Aerial photographs taken on September 26 confirmed that the lava flow had begun melting into the ice and snow on the south side of the intracaldera cone (fig. 7).

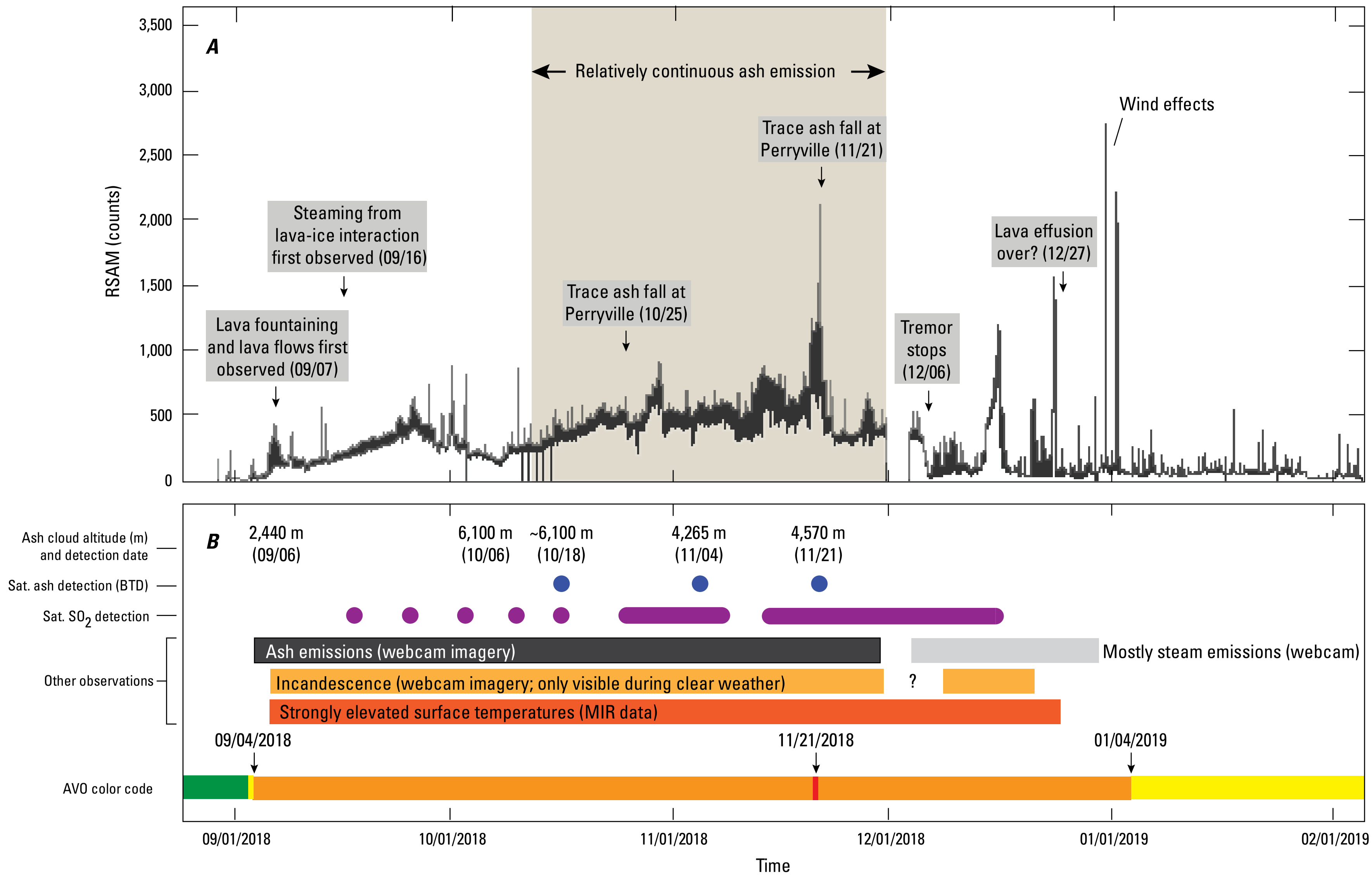


**Figure 5.** Real-time seismic amplitude measurement (RSAM) data and the chronology of major events from the 2018 eruption of Mount Veniaminof, southwest Alaska. *A*, RSAM data from seismograph station VNSS at Mount Veniaminof throughout the 2018 eruption. *B*, Simplified chronology of the eruption. Dates shown as month/day and month/day/year. PIREP, pilot weather report; sat., satellite; BTD, brightness temperature difference (an algorithm for determining the presence of volcanic ash in satellite data products); MIR, mid-infrared (light with 3,000–5,000-nanometer wavelengths, useful in measuring cloud temperatures); m, meter; ~, approximately; AVO, Alaska Volcano Observatory; $SO_2$, sulfur dioxide.


**Figure 6.** Photograph of a steam plume rising from the intracaldera cone of Mount Veniaminof, southwest Alaska, taken September 25, 2018. Plume altitude is about 15,000 feet (4,600 meters) above sea level. Image from the Federal Aviation Administration (FAA) Perryville NorthWest [sic] webcam. View direction is to the northwest.

Conspicuous concentric subsidence cracks grew around the periphery of the lava flow as the glacier responded to this melt-induced loss of mass.

Sulfur dioxide emissions were detected near Mount Veniaminof on September 20, 24, and 25 by multiple satellite sensors. The volcano emitted about 500 metric tons (t) of $SO_2$ on September 25, whereas emissions detected on September 20 and 24 were barely above background levels. Regional seismic networks detected ground-coupled airwaves on September 25–27, indicating Strombolian explosions were taking place. On September 27, an infrasound array in Dillingham, Alaska (322 km north of the volcano), also recorded explosive signals from the volcano.

Lava effusion characterized activity in early October and was associated with continuous tremor, nighttime incandescence, and persistent, strong thermal signals at the intracaldera cone. Measurements from the Ozone Monitoring Instruments (OMI) and the Infrared Atmospheric Sounding Interferometer (OMPS) detected sulfur dioxide emissions on October 4 and 10, but at amounts just above background levels (fig. 5). The total surface area of new lava flows by October 3, as determined from satellite data, was 184,000 $m^2$.

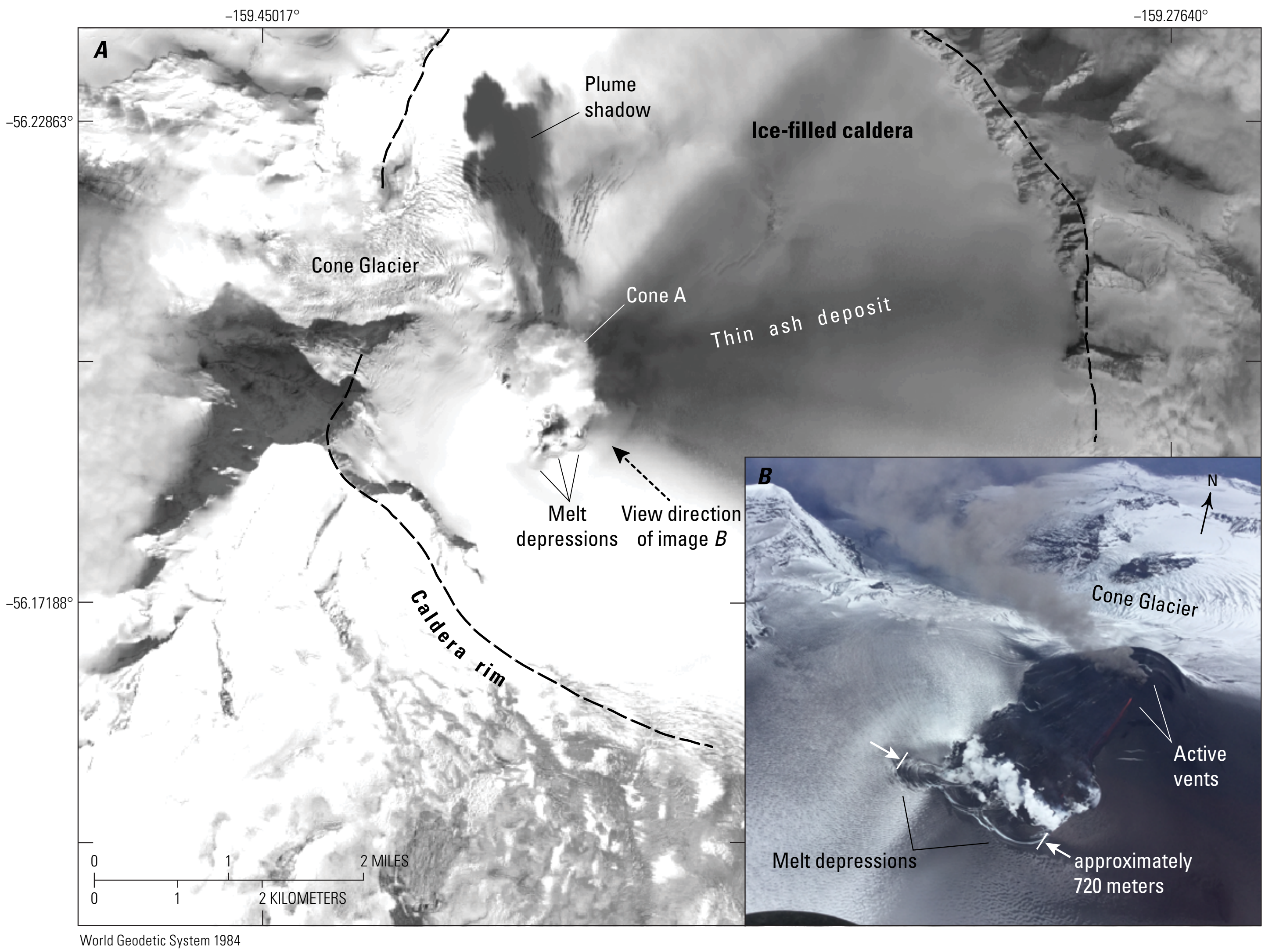


**Figure 7.** Satellite (*A*) and oblique aerial (*B*) images of lava flows and the intracaldera cone at Mount Veniaminof, southwest Alaska. Image *A* taken September 25; image *B* taken September 26, 2018. Image *B* by Mark Laker, U.S. Fish and Wildlife Service.

Visibility improved considerably on October 18 compared to the previous several weeks, allowing a webcam in Perryville to record a billowy, low-altitude ash cloud extending southeast from the intracaldera cone. Several satellites detected $SO_2$ on October 17 and 18, with OMI measuring about 270 t of $SO_2$ emitted near Mount Veniaminof on October 18. Ash emissions reached an altitude of about 20,000 ft (6,000 m) ASL on October 19, and on October 23, satellite imagery showed minor ash deposits in the summit crater. Trace ashfall was reported in Perryville on October 25. Satellite observations that day indicated that lava had covered a total area of about 385,000 $m^2$. The volcano remained restless through the end of October, with continued lava effusion and intermittent minor ash emissions. Sulfur dioxide was again detected in satellite data on October 30 and 31, but in amounts just slightly above background levels.

By about November 3, activity at Mount Veniaminof began transitioning to episodic emissions of more robust steam and ash clouds, which appeared in satellite and webcam data. Satellite imagery from the early morning of November 5 showed an east-drifting ash cloud, confirmed by a pilot's observation, extending at least 60 km beyond the vent and reaching a maximum altitude of about 14,000 ft (4,300 m) ASL. From November 6 to 19, satellite data and occasional webcam images showed a persistent volcanic cloud of steam and ash extending as far as about 64 km from the intracaldera cone at an altitude that varied from 8,000 to 12,000 ft (2,400 to 3,700 m) ASL. Satellite instruments also detected $SO_2$ near the volcano throughout early to mid-November, though the seasonal decline in ultraviolet light made the detection and accurate estimation of atmospheric $SO_2$ loading less certain.

On November 19, volcanic tremor increased in amplitude to reach the highest levels that had been measured up to that point in the eruption (fig. 5). This increase in seismicity was accompanied by infrasound detections on an array in Dillingham, which continued for the next few days (see point D on the inset map of figure 4). Satellite data from November 19 indicated that lava and tephra from the eruption now covered 540,000 $m^2$.

Conditions at the volcano escalated again on November 21, with increasing ash emissions and tremor amplitudes (fig. 5). An ash cloud detected in satellite imagery (fig. 8) now extended more than 240 km southeast from the vent, reaching an altitude of at least 15,000 ft (4,600 m) ASL. This cloud was also observed from Perryville, where residents reported distinct "booming" sounds—likely explosions—coming from the direction of the volcano. The level of seismicity and the extent of the ash cloud prompted AVO to raise the Aviation Color Code and Volcano Alert Level to **RED** and **WARNING**.

Mount Veniaminof emitted ash nearly continuously for much of November 21 as the ash cloud continued lengthening to the southeast, eventually reaching a distance of at least 400 km from the vent. Trace ashfall was again reported at Perryville on November 21 and 22. Activity began to decline by the late afternoon of November 21 (AKST), and on November 22, AVO lowered the Aviation Color Code and Volcano Alert Level to **ORANGE** and **WATCH**. Clear webcam views from Perryville on November 22 showed nearly continuous ash emissions extending as far as 100 km beyond the vent and reaching an altitude of about 10,000 ft (3,000 m) ASL. Unobstructed nighttime views showed incandescence at the summit.

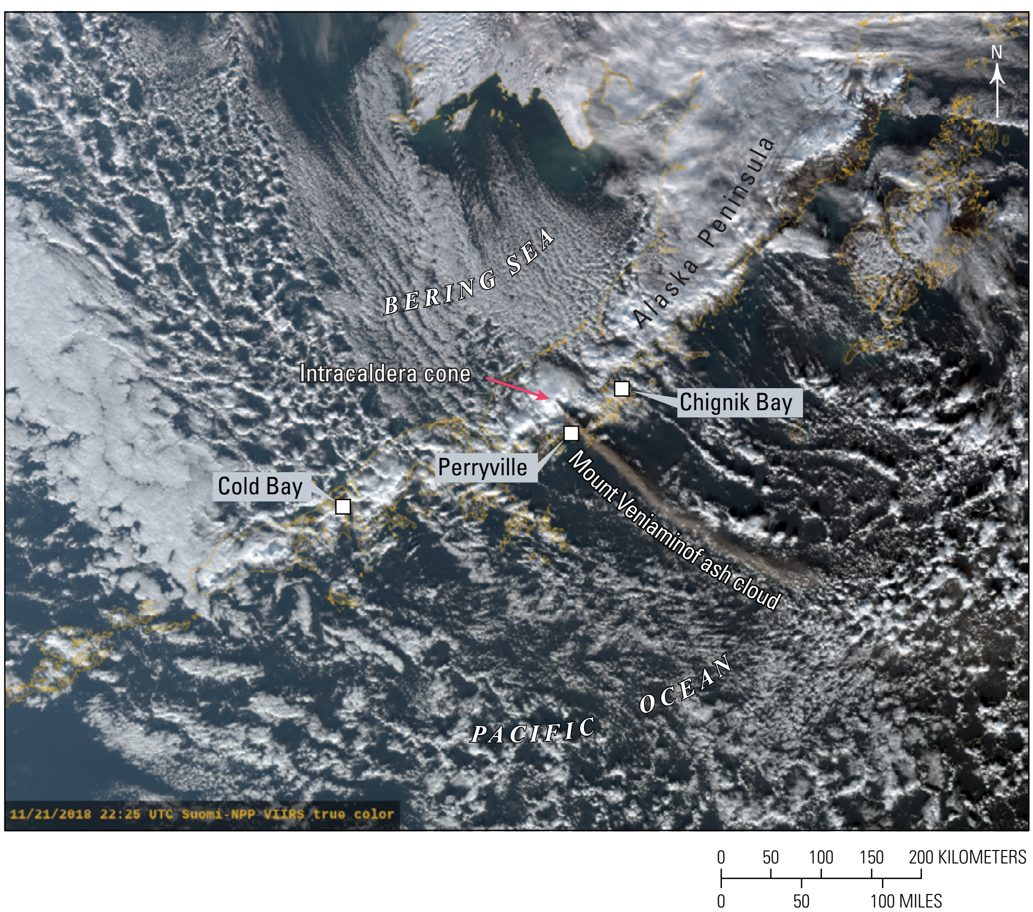


**Figure 8.** Annotated true color satellite image from November 21, 2018, showing an ash cloud extending from the intracaldera cone of Mount Veniaminof, southwest Alaska. The cloud stretched at least 400 kilometers southeast of the vent and reached an altitude of 15,000 feet (4,600 meters) above sea level. Image taken with a Visible Infrared Imaging Radiometer Suite (VIIRS) instrument on the Suomi National Polar-Orbiting Partnership (Suomi-NPP) satellite. Date shown as month/day/year. UTC; coordinated universal time.

Coincident with a gradual decline in tremor amplitude, by November 25, ash emissions were no longer evident from the intracaldera cone. On November 27, however, the RSAM of volcanic tremor increased slightly, and AVO detected occasional infrasound pulses on arrays in the Alaskan cities of Dillingham, Sand Point, and Akutan (points D, SP, and A on the inset map of figure 4). This slight increase in activity was associated with the appearance of minor ash emissions in satellite data. From November 30 to December 3, data transmission from the Mount Veniaminof remote seismic stations was interrupted, so AVO relied primarily on satellite observations and regional infrasound data to maintain surveillance. During this period, satellite data continued to show elevated surface temperatures, and small volcanic clouds were visible in some images.

By December 6, the continuous tremor signal that had been characteristic of the eruption transitioned into frequent long-period (LP) earthquakes. This change likely indicated that lava effusion had paused or ended. Over the next several days, LP earthquakes and tremor bursts lasting as long as tens of seconds took place frequently, along with occasional harmonic tremor. A partly cloudy Sentinel-2 satellite image from December 10 showed that a light snow dusting covered parts of the intracaldera lava flows, and that only minor steam emissions continued. The weakening of seismic activity, absence of continuous tremor, and apparent cooling of the lava flows further indicated that eruptive activity had ceased.

AVO detected many ground-coupled airwaves associated with LP earthquakes on December 11, but no other outward signs of unrest were observed in satellite or webcam imagery. This quiescence quickly changed as ash emissions from the intracaldera cone were again observed in Perryville webcam images on December 13 and 16. As cloud cover decreased over the volcano, satellite imagery again showed elevated surface temperatures, indicating a resumption in lava effusion, and also showed small volcanic clouds again extending from the intracaldera cone. This resumption of activity was accompanied by the return of the low-level, nearly continuous seismic tremor, which persisted until December 16, at which point the tremor signal ended and was replaced by many discrete, low-frequency events. Webcam images from Perryville showed minor ash emissions through December 17, after which the volcano was obscured by clouds. Satellite data confirmed that Mount Veniaminof emitted $SO_2$ during the brief unrest in early to mid-December; additional $SO_2$ emissions, possibly from the volcano, were also detected over the Seward Peninsula during this interval, about 966 km to the north.

A Sentinel-2 satellite image acquired on December 20, 2018, showed no active lava effusion or additional advancement of the active lava flows. Slight fluctuations in seismic tremor amplitude took place from December 21 to 28, and on December 23, strong thermal signals again appeared in satellite data. From December 23 to 24, AVO observed lava-fountain-associated incandescence in webcam images. This activity was brief, however, and by December 27, all satellite, seismic, and webcam data indicated that active lava effusion had slowed, or perhaps stopped completely. From December 27, 2018, through the end of the year, the level of unrest at Mount Veniaminof gradually declined.

By the end of the eruption, new lava flows covered 600,000 $m^2$ of land. This material came from a cluster of small vents on the upper south flank of a cinder cone within the ice-filled caldera. The flows melted into ice and snow, slowly creating melt depressions around their peripheries. However, no unusual water outflows were observed exiting the caldera through its main drainage, located northwest of the cone. The amount of lava and ash erupted from September 7 to December 27, 2018, resulted in the generation of about 1,200,000 cubic meters ($m^3$) of lava and 20,000–30,000 $m^3$ of ash, though no aircraft reported encountering ash throughout the eruptive period.

Mount Veniaminof, an ice-clad andesite and dacite stratovolcano topped by a 10-kilometer-diameter caldera, is 775 km southwest of Anchorage and 35 km north of Perryville (fig. 1). With a volume of about 350 $km^3$, Mount Veniaminof is one of the largest and most active volcanoes of the Aleutian Arc (Miller and others, 1998; Bacon and others, 2009). Extensive pyroclastic flow deposits around the volcano indicate two caldera-forming eruptions have taken place there in the Holocene (Miller and Smith, 1987), and the volcano has erupted at least 15 times in the past 200 years, all from its approximately 300-meter-tall intracaldera cone. This cone was also the site of the 2018 eruption. Prior to 2018, the last substantial magmatic eruption at the volcano took place in 2013–2014 (Cameron and others, 2017).

## Pavlof Volcano

*GVP #312030*
55.417° N., 161.894° W.
2,518 m

Alaska Peninsula

**ELEVATED SEISMIC ACTIVITY**


The number of located earthquakes at Pavlof Volcano increased in 2018 compared to previous years. Although this increase was at least in part due to improvements to the local seismic network, there are indications that seismic activity in 2018 was nonetheless above background levels. Shallow LP earthquakes are common at the volcano, and the relative amplitudes of their waveforms, as observed by the Pavlof Volcano seismic network, indicate they tend to be located at or near the volcano summit. Although these events are commonly too small to be located by AVO's routine earthquake location procedures, they are observable on spectrograms and are still noted in AVO's routine seismic checks (Power and others, 2020). Similar activity has been observed at other open-vent systems in the Aleutian Arc, such as Shishaldin Volcano (Petersen and others, 2006; Pesicek and others 2018) and Mount Veniaminof (Pesicek and others, 2018), and appears to be typical for such systems (Quezada-Reyes and others, 2013).

The Pavlof Volcano seismic network consists of three broad-band digital seismic stations (PN7A, PS1A, and PS4A), three short-period 3-component stations (PV6A, PVV, and HAG), and one short-period vertical-component station (BLHA) (fig. 9). The current configuration is fairly new; AVO carried out substantial upgrades to the network in the summer of 2017, during which PN7A, PS1A, PVV, and PS4A were upgraded to broadband digital

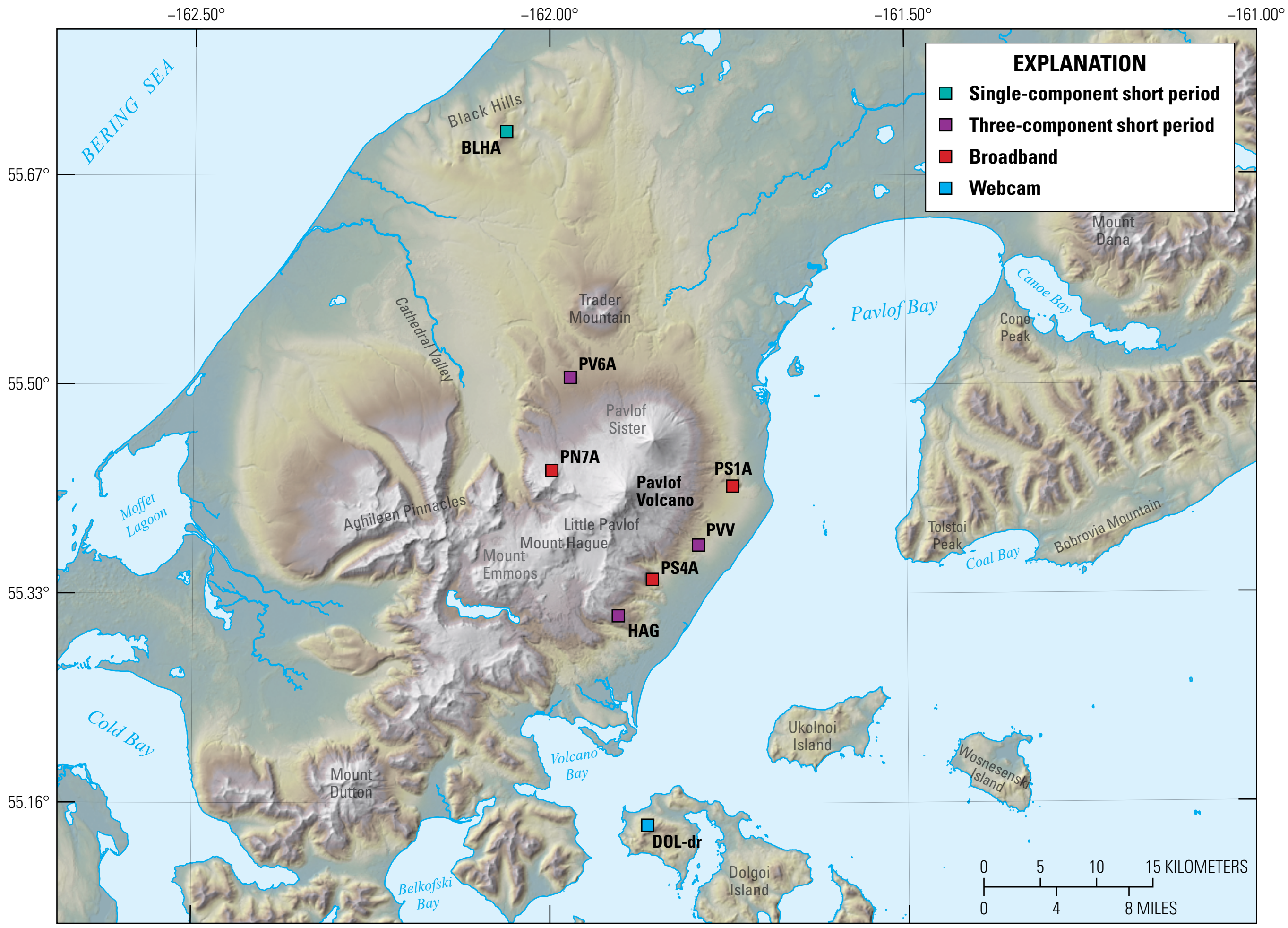


Base from U.S. Geological Survey, The National Map, 2022
State Plane, Alaska, FIPS 5007
North American datum of 1983
Transverse Mercator projection

**Figure 9.** Map of Pavlof Volcano and other volcanoes in the area, located in southwest Alaska. Nearby earthquakes are located using a surrounding array of seven seismic stations. The Alaska Volcano Observatory also uses one webcam (DOL-dr), installed on Dolgoi Island, to monitor the volcanoes.

stations, PV6 was replaced by PV6A, and HAG was upgraded from a vertical-component analog station to a 3-component station (Dixon and others, 2019).

AVO located 152 earthquakes within a 20-kilometer radius of Pavlof Volcano in 2018. Figure 10 charts the number of earthquakes located within this area per year since 2010. Throughout 2018, the volcano remained at Aviation Color Code **GREEN** and Volcano Alert Level **NORMAL**. Of the events that occurred in 2018, 111 were designated as LP earthquakes and 41 as volcano-tectonic (VT) earthquakes. Epicentral and hypocentral locations for these events are shown in figures 11 and 12. Moderately deep LP earthquakes (10–20 km deep) took place in a broad swath east of Pavlof Volcano and Pavlof Sister throughout 2018 (fig. 12), and although these events appear to be well-located based on reported root mean square errors (0.05–0.33), they often had small magnitudes.

On March 27, 2018, an unusual cluster of VT earthquakes took place about 6–8 km north-northwest of Pavlof Sister and 12–13 km north of Pavlof Volcano (figs. 11, 13). The earthquakes were 6.6–9.0 km below sea level with local magnitudes ($M_L$) between 0.3 and 1.5. Later, in early April, a sequence of deep LP earthquakes took place near Pavlof Sister (fig. 13). These events were 10.1–29.3 km below sea level with $M_L$ values between −0.37 and 1.99, but only two events from the sequence were above $M_L$ 1.0. On September 11, another series of deep LP earthquakes took place in the same

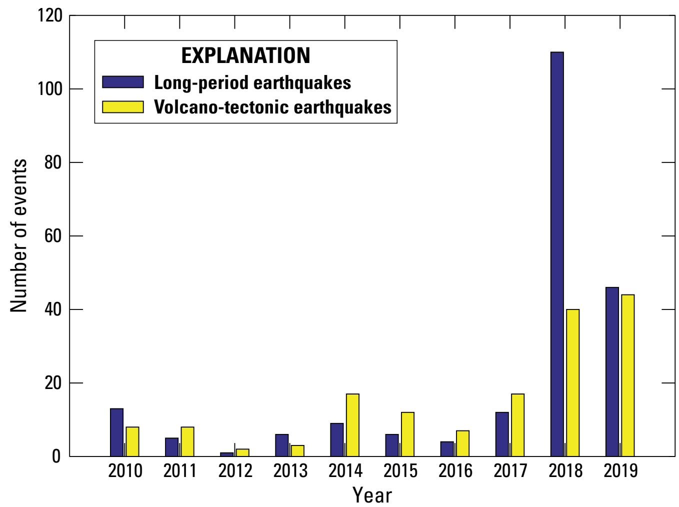


**Figure 10.** Graph showing the number of long-period and volcano-tectonic earthquakes located each year at Pavlof Volcano, southwest Alaska. The sharp increase in 2018 is chiefly due to the improved network installed during the summer of 2017.

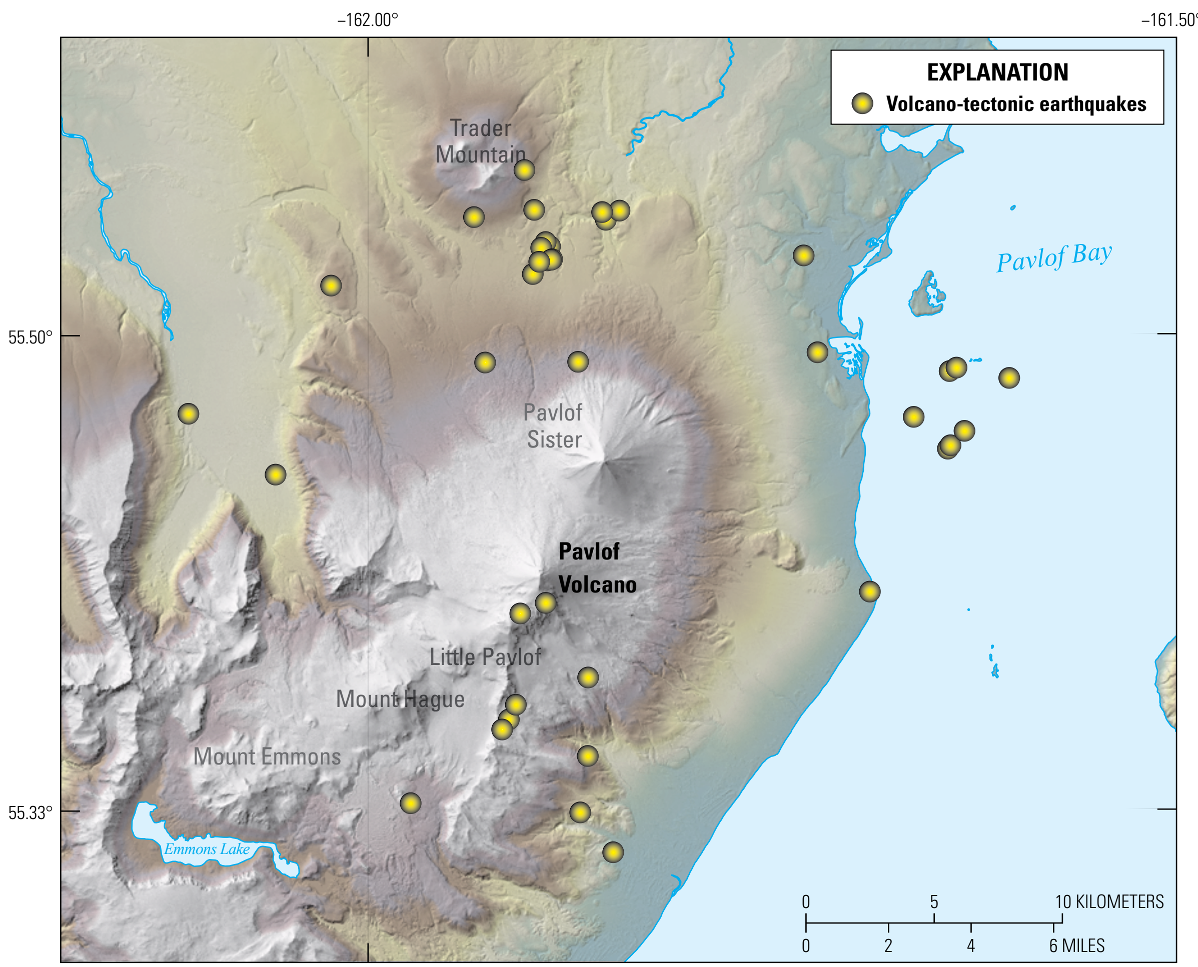


Base from U.S. Geological Survey, The National Map, 2022
State Plane, Alaska, FIPS 5007
North American datum of 1983
Transverse Mercator projection

**Figure 11.** Map of epicenters of volcano-tectonic earthquakes located near Pavlof Volcano, southwest Alaska, during 2018.

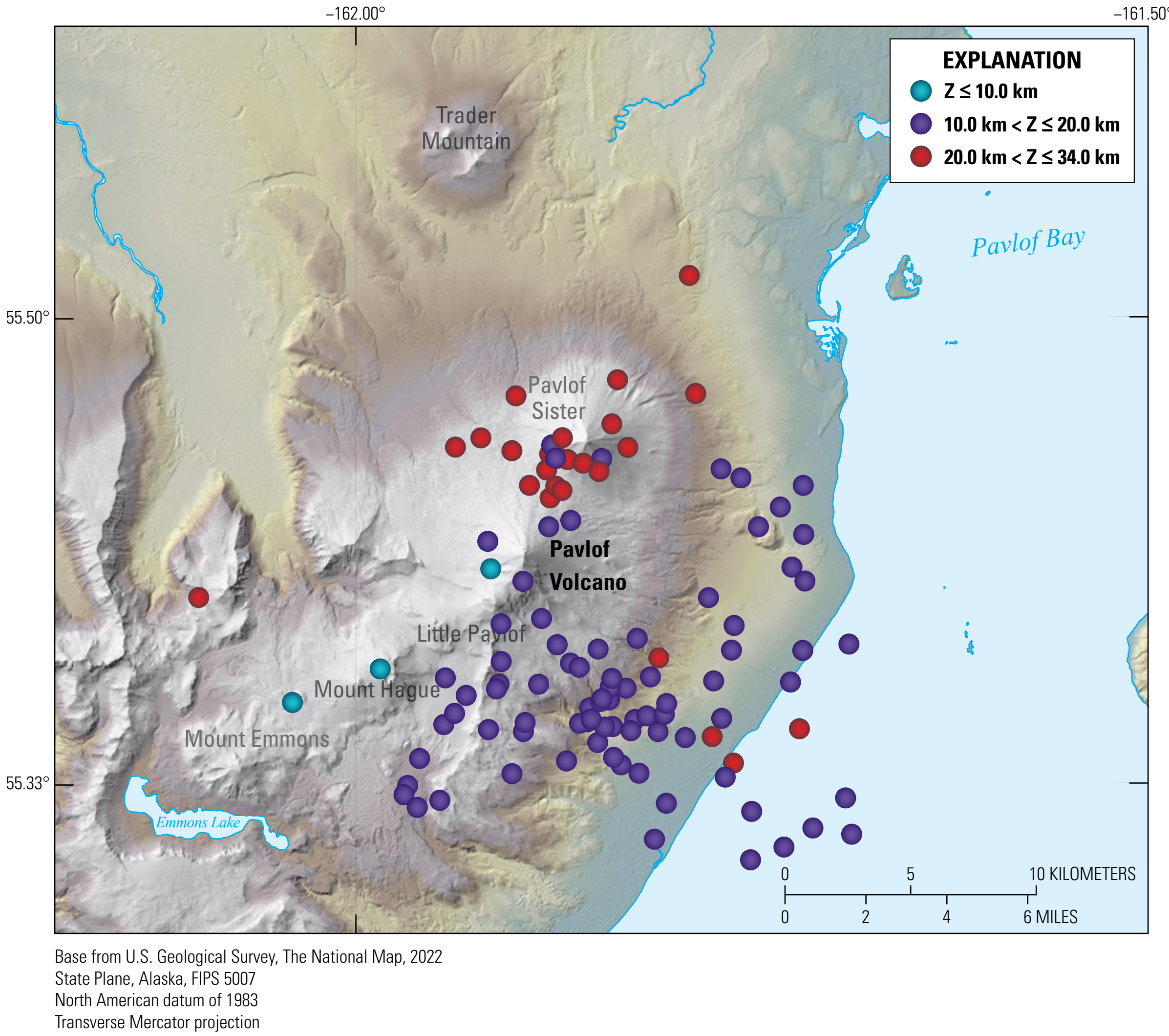


**Figure 12.** Map of hypocenters of long-period earthquakes located near Pavlof Volcano, southwest Alaska, during 2018. Z, depth; km, kilometer.

location as the March LP earthquake activity. The September 11 sequence had nine events, the two largest being $M_L$ 1.3 and 1.4 (fig. 14). The hypocentral depths of these nine events ranged from 26 to 32 km. The sequence was also accompanied by a short tremor episode lasting about four minutes, though the tremor may have actually been closely spaced LP earthquakes.

Volcano-tectonic earthquakes are not as common at Pavlof Volcano as at other volcanic systems, making the March 2018 brittle failure sequence notable. These events are assumed to have been distal VT earthquakes on the basis of their location (12–13 km from Pavlof Volcano), though they also may have been tectonically generated. AVO has not located any similar cluster in the same area since it began monitoring the volcano in 1996.

The fact that there were more located events in 2018 than in previous years (fig. 10) is not surprising given the network improvements made in 2017. Many of the 2018 events were of small magnitudes, and the increase in earthquake locations is partly due to the improved network. However, the additional presence of the March VT earthquake cluster and the LP earthquakes above $M_L$ 1.0 indicate the 2018 activity may have been above background levels for the upgraded network, suggesting increased magmatic activity at Pavlof Volcano in 2018. Alternatively, this behavior may be typical for the

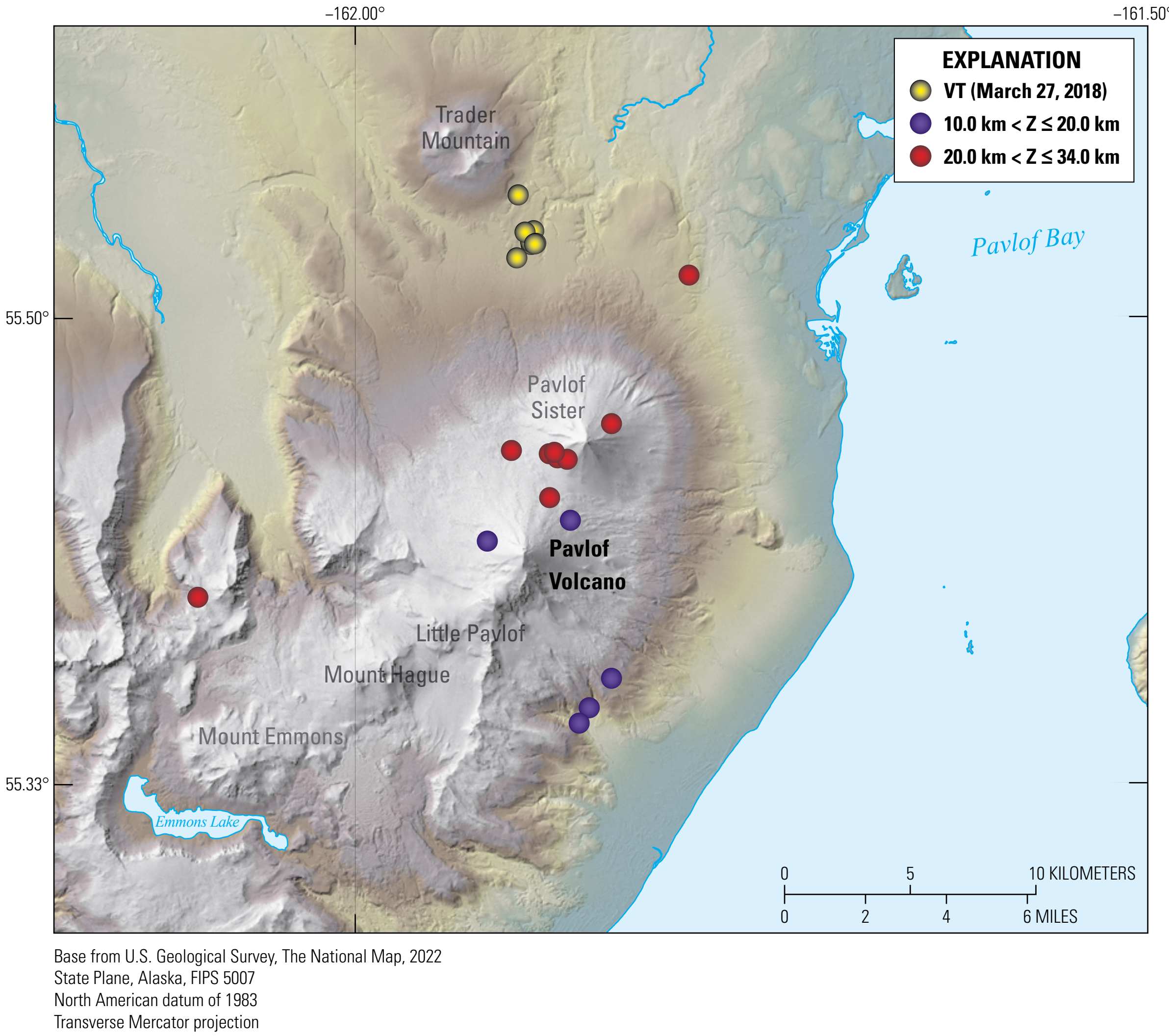


**Figure 13.** Map of hypocenters of earthquakes that took place near Pavlof Volcano, southwest Alaska, during March and April 2018. Long-period earthquakes are colored by depth. The swarm of volcano-tectonic (VT) earthquakes north-northwest of Pavlof Sister took place prior to the long-period activity. Z, depth; km, kilometer.

volcano but is only observed now because of the improved network.

Observations made by Power and others (2004) of deep LP earthquake activity throughout the Aleutian Arc suggest a link between magma movement in the lower to middle crust and eruptive activity, although the timing between these parameters appears to vary. The deep LP earthquake activity at Pavlof Volcano may indicate the presence of continued magma supply to the volcano, with 2018 a slightly more active year. Further monitoring of earthquake activity at Pavlof Volcano will likely shed light on the magmatic system that feeds eruptive activity at the volcano.

Pavlof Volcano is a cone-shaped stratovolcano composed of basaltic andesite lava flows and pyroclastic rock. The volcano is located on the Alaska Peninsula east of the City of Cold Bay, Alaska, and is considered one of the most active volcanoes in North America, with more than 40 documented historical eruptions since 1790 (Miller and others, 1998). Eruptions at Pavlof Volcano tend to be Strombolian to Vulcanian in nature (Waythomas and others, 2006), and the volcano is considered an open vent system that commonly has eruptions with little precursory seismic activity or ground deformation visible in InSAR (Lu and Dzurisin, 2014; Pesicek and others, 2018). The last substantial eruption at Pavlof Volcano began in March 2016 and was characterized by continuous

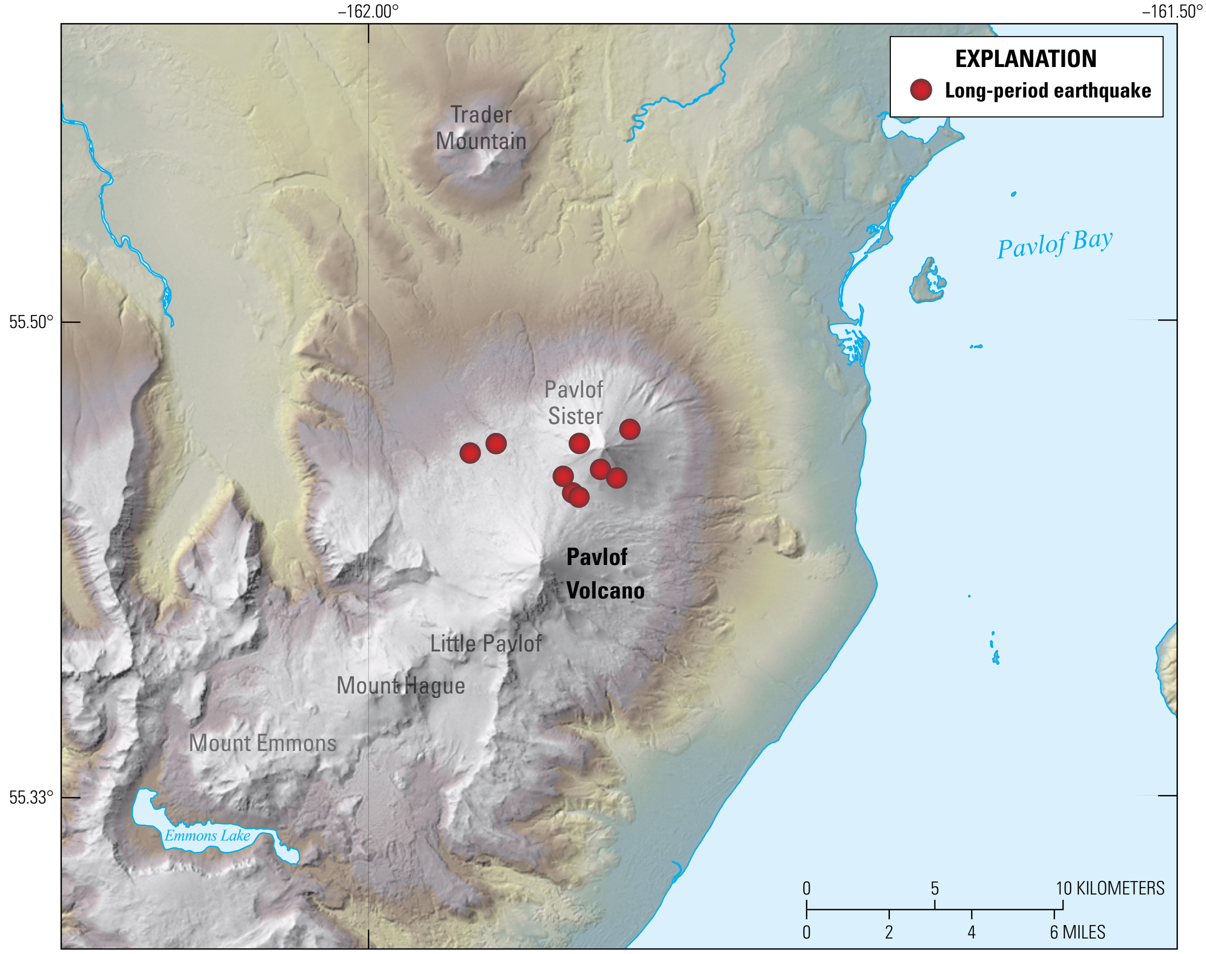


**Figure 14.** Map of epicenters of the long-period earthquake series that took place near Pavlof Volcano, southwest Alaska, on September 11, 2018. All events shown had depths between 26 and 32 kilometers.

seismic tremor, infrasound detections, and lightning. This eruption also produced an ash cloud that rose to an altitude of 20,000 ft (6,000 m) ASL (Fee and others, 2017).

## Shishaldin Volcano

*GVP #311360*
54.755° N., 163.971° W.
2,857 m


Unimak Island, Fox Islands, Aleutian Islands

**DECLINING VOLCANIC UNREST**

In the latter part of 2017, Shishaldin Volcano began producing seismic and infrasound signals consistent with small explosions and robust degassing. This behavior led the volcano to begin 2018 at an elevated Aviation Color Code and Volcano Alert Level of **YELLOW** and **ADVISORY** (Dixon and others, 2020). The overall activity at Shishaldin Volcano declined throughout January 2018, and on February 7, 2018, this continued decline triggered AVO to lower the Aviation Color Code and Volcano Alert Level of the volcano to **GREEN** and **NORMAL**. No other notable unrest took place at the volcano for the remainder of 2018.

Shishaldin Volcano, located near the center of Unimak Island in the east Aleutian Islands, is a spectacular symmetric cone with a basal diameter of approximately 16 km. The small summit crater on the volcano typically emits a noticeable gas plume, occasionally with minor amounts of ash. Shishaldin Volcano is one of the most active volcanoes in the Aleutian volcanic arc (Cameron and others, 2018).

## Westdahl volcano

*GVP #311340*
54.571° N., 164.648° W.
1,560 m


Unimak Island, Fox Islands, Aleutian Islands

**LONG-TERM INFLATION**

Throughout 2018, Westdahl volcano (an informal name that herein includes Westdahl Peak, Westdahl caldera, and associated intra- and extra-caldera features) continued its long-term steady inflation, which has persisted since the deformation was first observed after the installation of a GPS network on Unimak Island in 2008 (figs. 15, 16). An analysis of Westdahl volcano InSAR data by Lu and others (2003) indicated a shallow magma reservoir exists beneath the volcano; the continued inflation is consistent with an ongoing accumulation of magma at shallow depths. Westdahl volcano remained at **GREEN** and **NORMAL** throughout 2018.

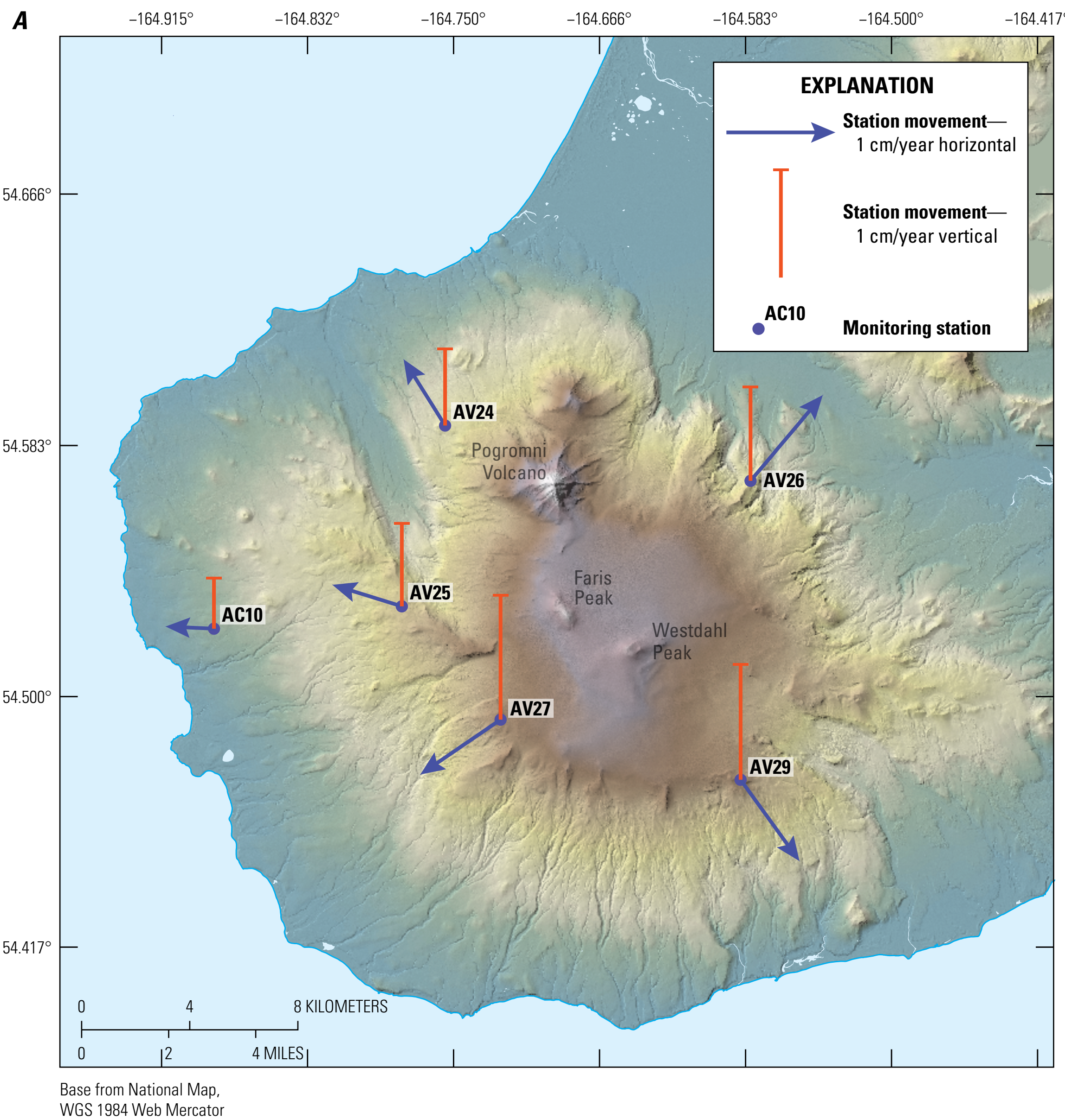


Base from National Map,
WGS 1984 Web Mercator

**Figure 15.** Global Positioning System velocity map (*A*) and displacement time series with 68 percent confidence levels for monitoring station AV26 (*B*) at Westdahl volcano, in the eastern Aleutian Islands, Alaska. The data, spanning August 30, 2008, to December 30, 2018, show long-term inflation in centimeters per year (cm/year) and in centimeters as monitoring stations moved up and away from the volcano. Velocities and displacements are given with respect to station AB06, located away from any volcanoes on the east side of Unimak Island, near the community of False Pass, Alaska. Jan., January.

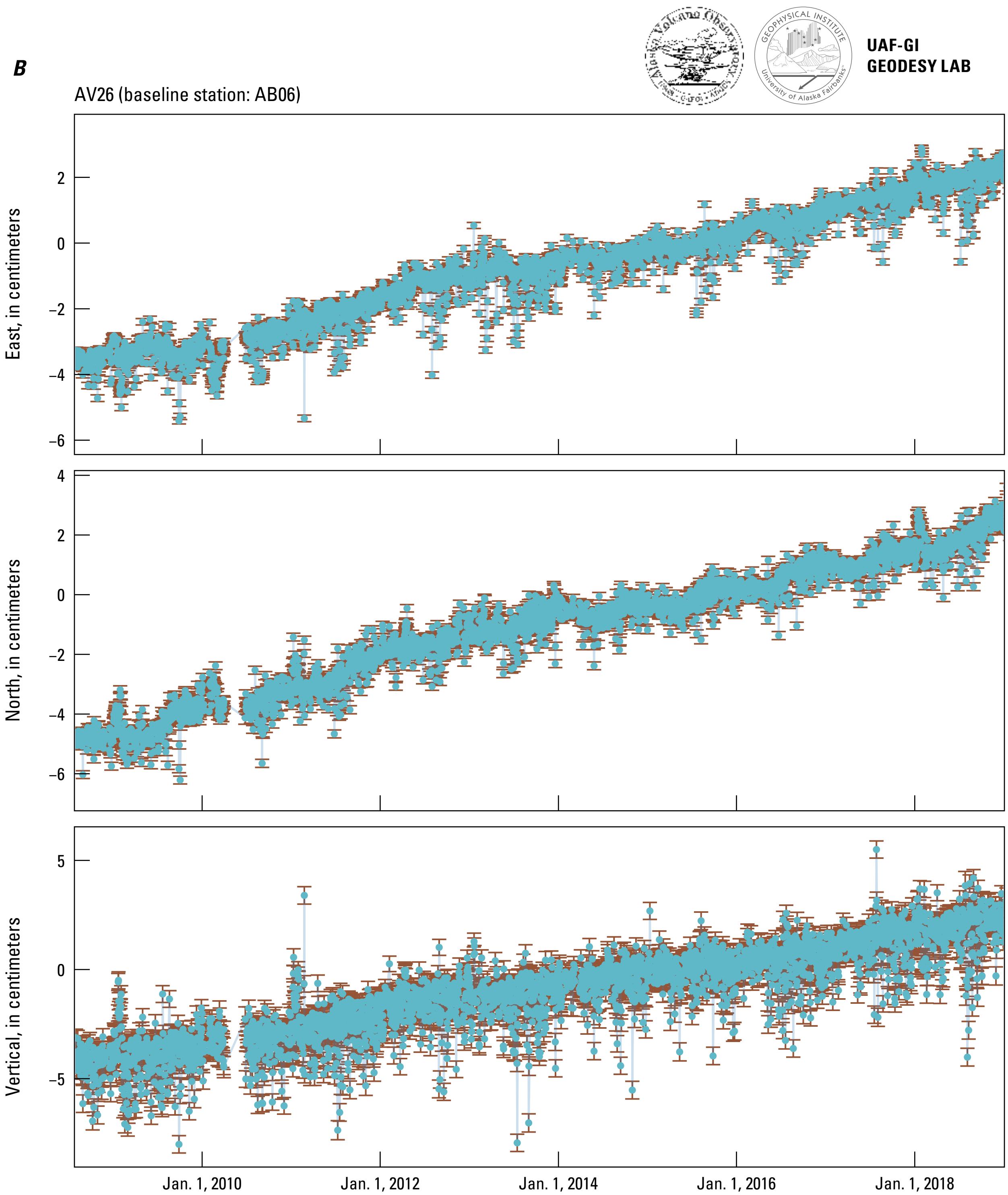


**Figure 15.** Global Positioning System velocity map (*A*) and displacement time series with 68 percent confidence levels for monitoring station AV26 (*B*) at Westdahl volcano, in the eastern Aleutian Islands, Alaska. The data, spanning August 30, 2008, to December 30, 2018, show long-term inflation in centimeters per year (cm/year) and in centimeters as monitoring stations moved up and away from the volcano. Velocities and displacements are given with respect to station AB06, located away from any volcanoes on the east side of Unimak Island, near the community of False Pass, Alaska. Jan., January.—Continued

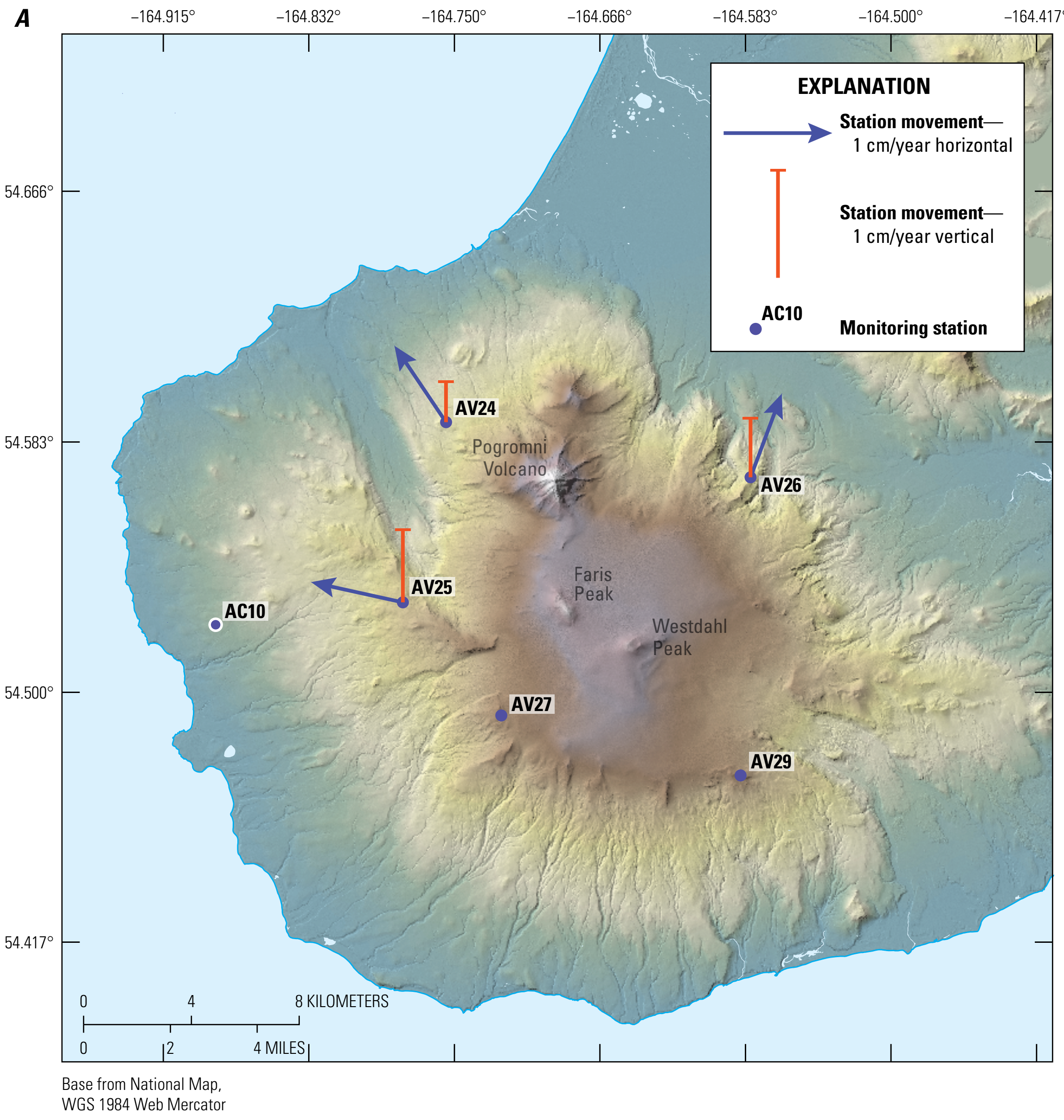


**Figure 16.** Global Positioning System velocity map (*A*) and displacement time series with 68 percent confidence levels showing movement of monitoring stations AV24 (*B*), AV25 (*C*), and AV26 (*D*) at Westdahl volcano (in the eastern Aleutian Islands, Alaska) from January 1 to December 31, 2018. Velocities and displacements are given with respect to station AB06, located away from any volcanoes on the east side of Unimak Island, near the community of False Pass, Alaska. Only AV24, AV25, and AV26 provided enough data during 2018 to reliably determine velocities, which are shown in centimeters per year (cm/year). Jan., January; Mar., March; Sept., September; Nov., November.

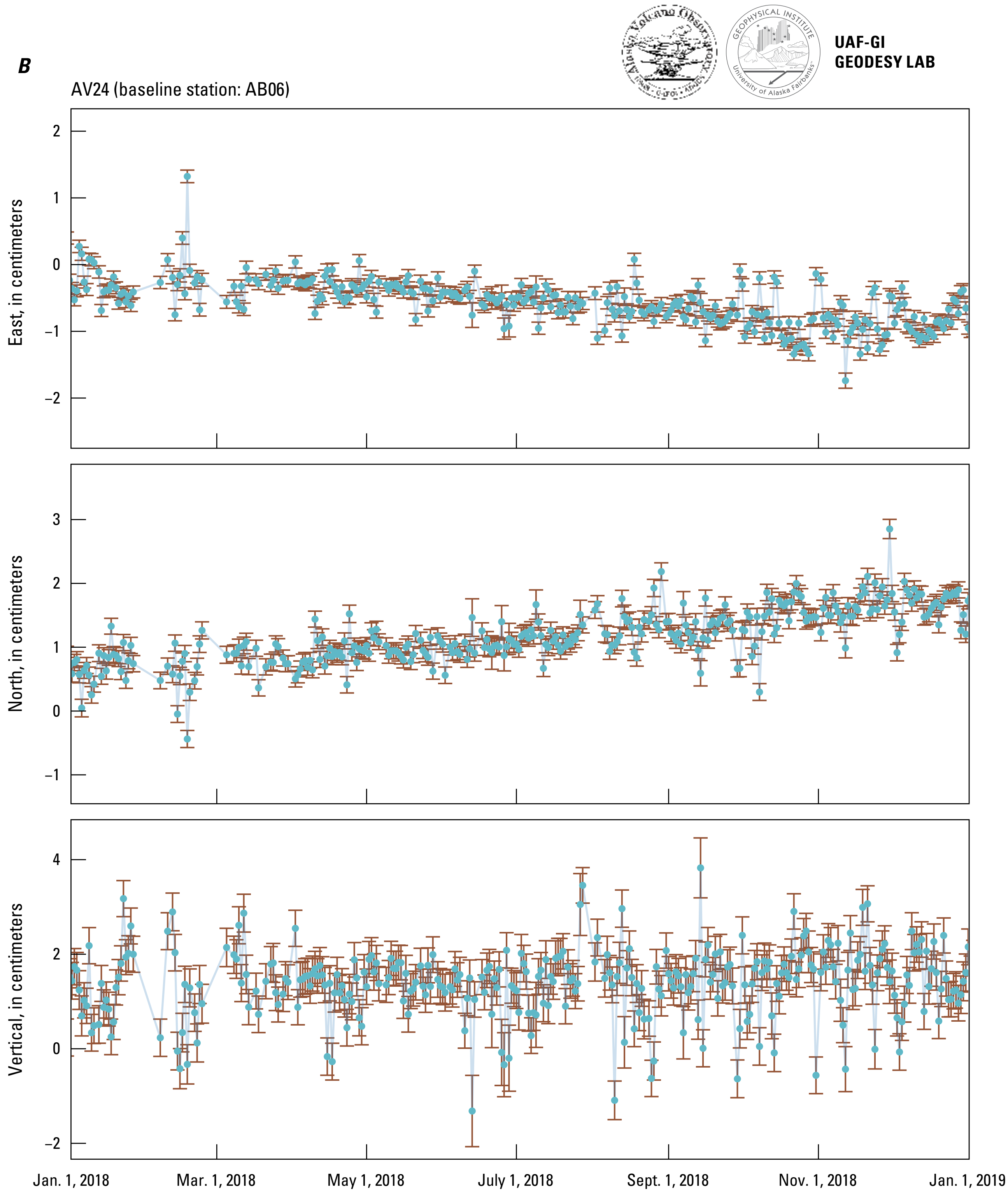


**Figure 16.** Global Positioning System velocity map (*A*) and displacement time series with 68 percent confidence levels showing movement of monitoring stations AV24 (*B*), AV25 (*C*), and AV26 (*D*) at Westdahl volcano (in the eastern Aleutian Islands, Alaska) from January 1 to December 31, 2018. Velocities and displacements are given with respect to station AB06, located away from any volcanoes on the east side of Unimak Island, near the community of False Pass, Alaska. Only AV24, AV25, and AV26 provided enough data during 2018 to reliably determine velocities, which are shown in centimeters per year (cm/year). Jan., January; Mar., March; Sept., September; Nov., November.—Continued

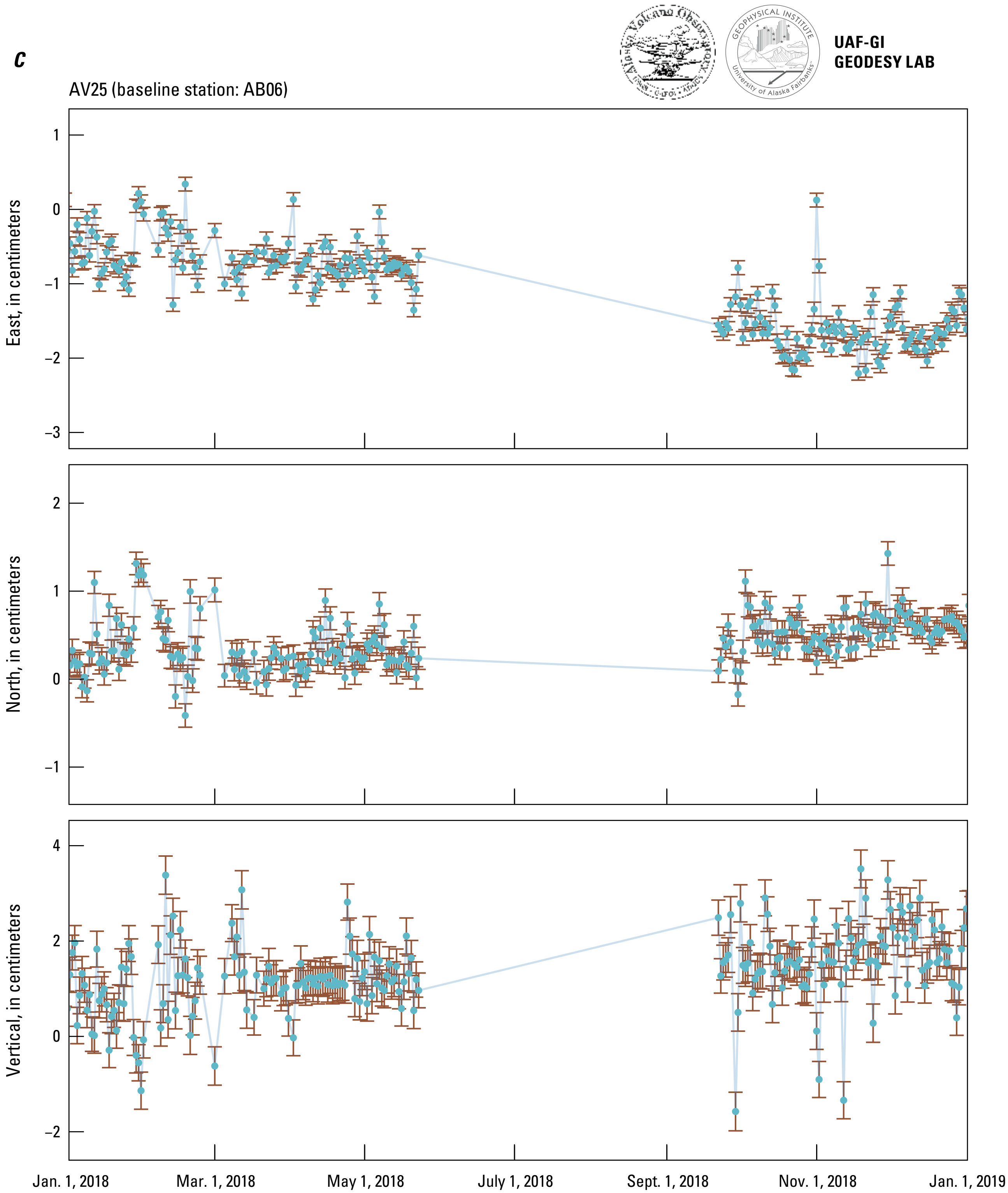


**Figure 16.** Global Positioning System velocity map (*A*) and displacement time series with 68 percent confidence levels showing movement of monitoring stations AV24 (*B*), AV25 (*C*), and AV26 (*D*) at Westdahl volcano (in the eastern Aleutian Islands, Alaska) from January 1 to December 31, 2018. Velocities and displacements are given with respect to station AB06, located away from any volcanoes on the east side of Unimak Island, near the community of False Pass, Alaska. Only AV24, AV25, and AV26 provided enough data during 2018 to reliably determine velocities, which are shown in centimeters per year (cm/year). Jan., January; Mar., March; Sept., September; Nov., November.—Continued

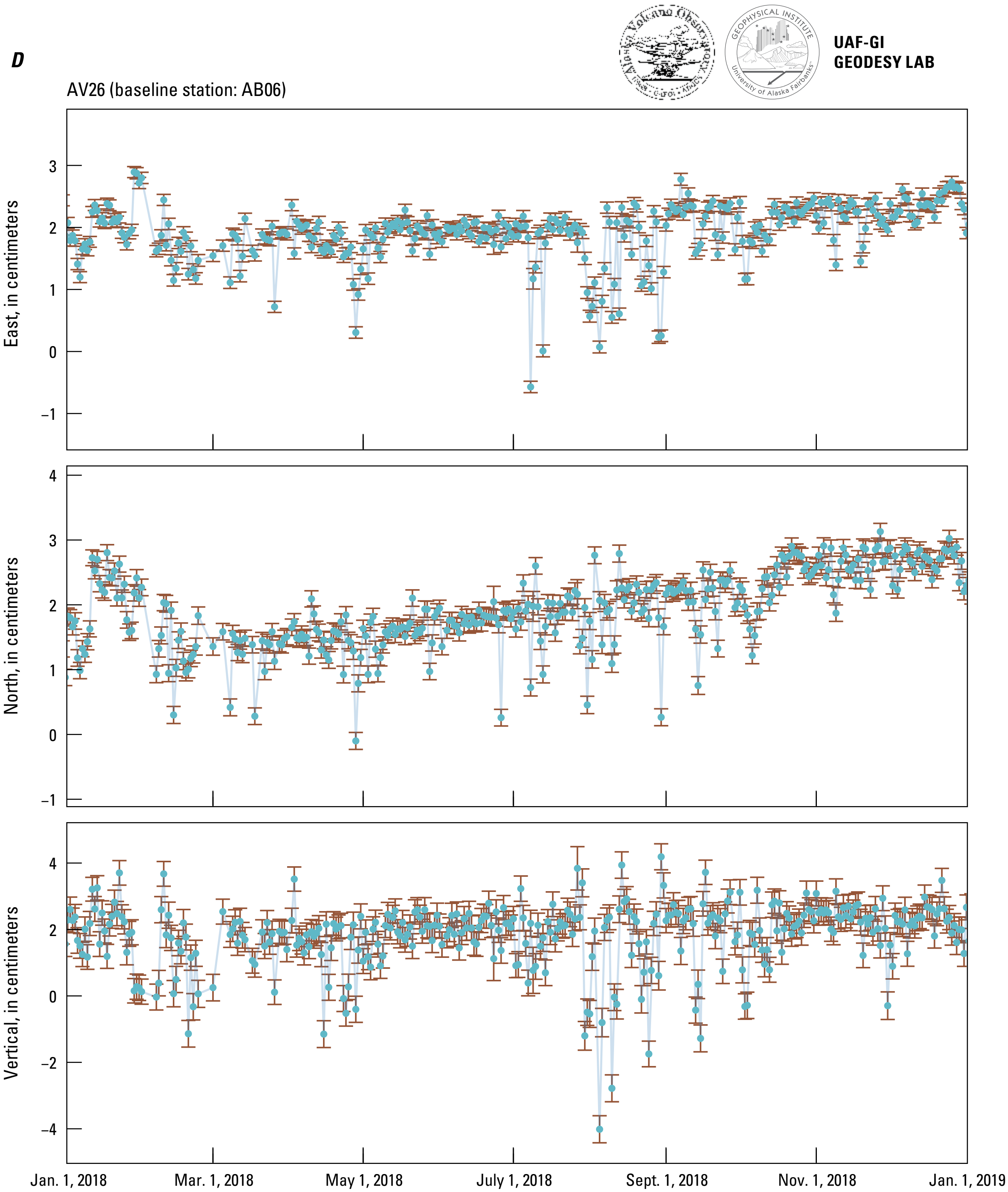


**Figure 16.** Global Positioning System velocity map (*A*) and displacement time series with 68 percent confidence levels showing movement of monitoring stations AV24 (*B*), AV25 (*C*), and AV26 (*D*) at Westdahl volcano (in the eastern Aleutian Islands, Alaska) from January 1 to December 31, 2018. Velocities and displacements are given with respect to station AB06, located away from any volcanoes on the east side of Unimak Island, near the community of False Pass, Alaska. Only AV24, AV25, and AV26 provided enough data during 2018 to reliably determine velocities, which are shown in centimeters per year (cm/year). Jan., January; Mar., March; Sept., September; Nov., November.—Continued

Westdahl volcano is a broad, gently sloping volcano on the west end of Unimak Island. An ice cap covering its summit is inferred to fill an older caldera (Calvert and others, 2005). Continued volcanism after this caldera's collapse produced several vents, the youngest of which are Faris and Westdahl Peaks. The satellite vent Pogromni Volcano, in contrast, likely predates the caldera (Calvert and others, 2005). Most known historical eruptions at Westdahl volcano have included an explosive phase involving the interaction of lava and ice, followed or accompanied by the production of blocky lava flows and lahars (McGimsey and others, 1995; Miller and others, 1998; Dean and others, 2002). The last notable unrest at the volcano took place in 2010 and was characterized by increased seismicity (Neal and others, 2014).

## Akutan Volcano

*GVP #311320*
54.133° N., 165.986° W.
1,303 m


Akutan Island, Fox Islands, Aleutian Islands

**LONG-TERM INFLATION**

In 2018, Akutan Volcano continued its long-term reinflation, which AVO has recorded since the installation of a GPS network at the volcano in 2005 (figs. 17, 18). The deformation was slightly

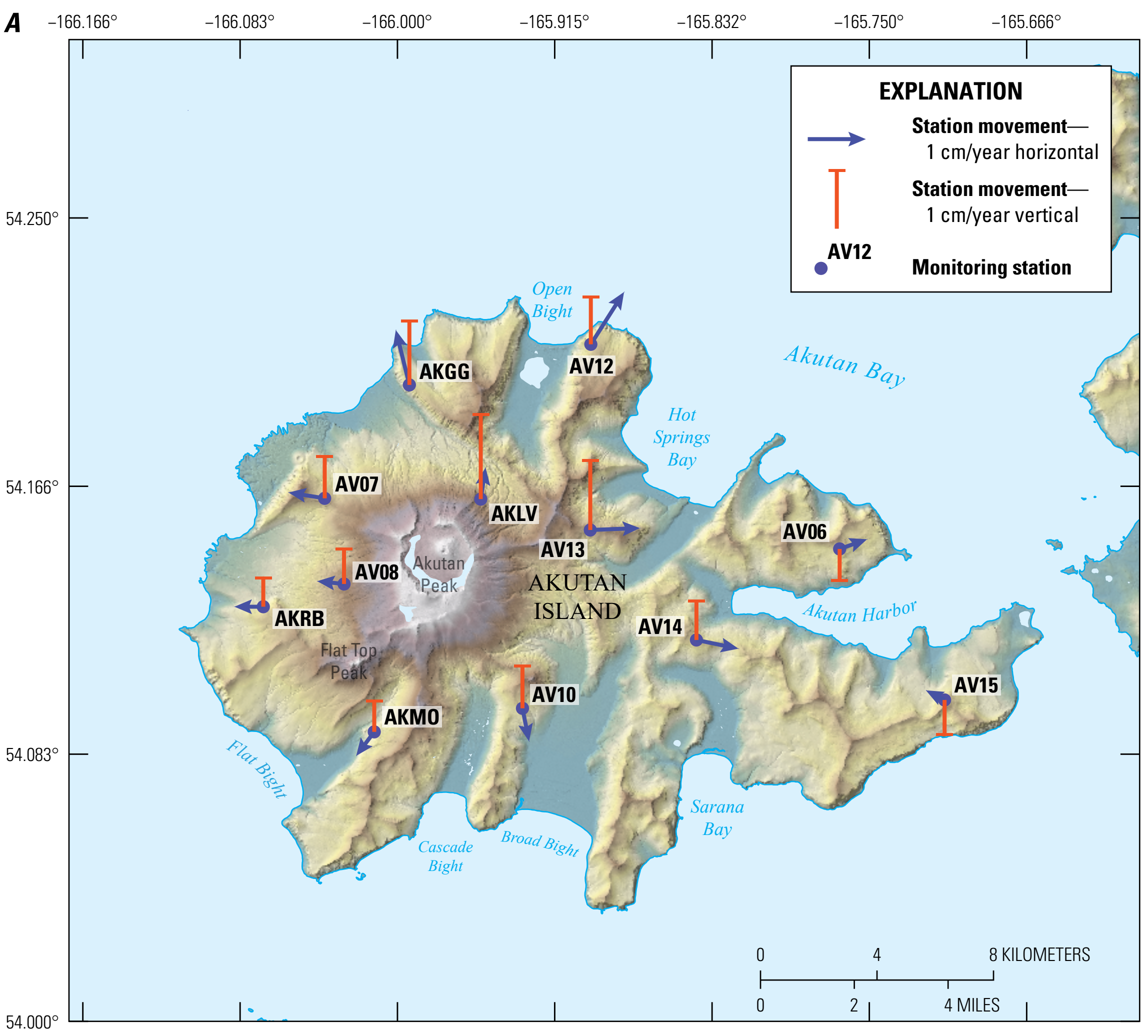


Base from National Map,
WGS 1984 Web Mercator

**Figure 17.** Global Positioning System velocity map (*A*) and displacement time series with 68 percent confidence levels showing movement of monitoring station AV10 (*B*) from June 2005 to June 2018 at Akutan Island, eastern Aleutian Islands, Alaska. The map shows long-term inflation as monitoring stations moved up and away from the volcano, and the displacement time series show this motion in the east, north, and vertical directions. Velocities and displacements are given relative to station AV09, located near the City of Unalaska, Alaska. The volcano inflates at an average rate of less than 1 centimeter per year (cm/year), though more rapid inflation steps are modulated onto this background rate. The deformation pattern seems consistent with a spherical source. Jan., January.

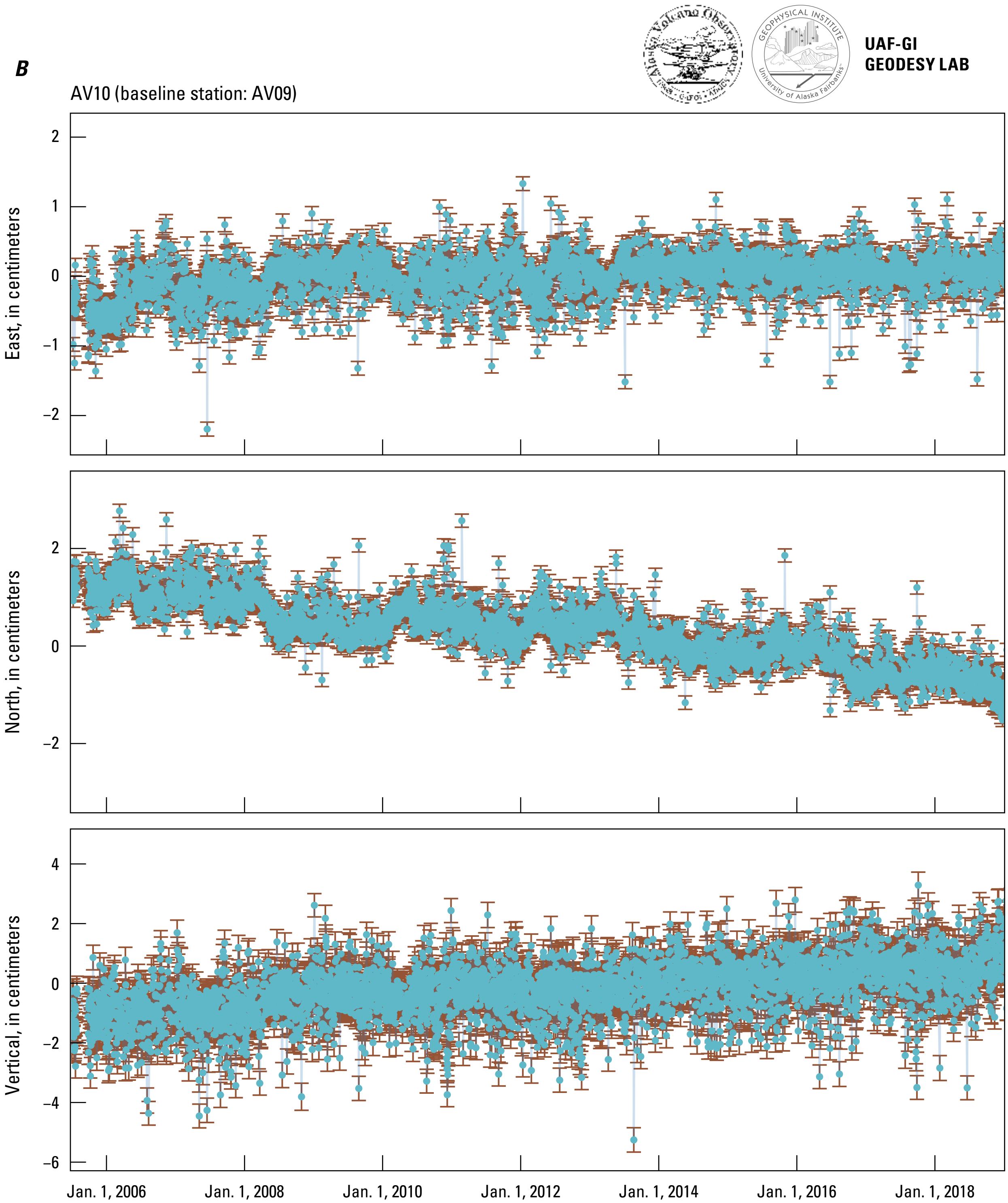


**Figure 17.** Global Positioning System velocity map (*A*) and displacement time series with 68 percent confidence levels showing movement of monitoring station AV10 (*B*) from June 2005 to June 2018 at Akutan Island, eastern Aleutian Islands, Alaska. The map shows long-term inflation as monitoring stations moved up and away from the volcano, and the displacement time series show this motion in the east, north, and vertical directions. Velocities and displacements are given relative to station AV09, located near the City of Unalaska, Alaska. The volcano inflates at an average rate of less than 1 centimeter per year (cm/year), though more rapid inflation steps are modulated onto this background rate. The deformation pattern seems consistent with a spherical source. Jan., January.—Continued

faster in 2018 compared to its long-term rate. DeGrandpre and others (2017) noted that inflation at Akutan Volcano is episodic and suggested a shallow magma reservoir resides 6–10 km beneath the volcano. Continued inflation of the volcano is consistent with an ongoing accumulation of magma at shallow levels. The Aviation Color Code and Volcano Alert Level for the volcano remained at **GREEN** and **NORMAL** throughout 2018.

Akutan Volcano is a symmetric stratocone that composes the western half of Akutan Island. It is one of the most active volcanoes of the Aleutian Arc, with at least 31 eruptions since 1790 and its most recent in 1992 (McGimsey and others, 1995). Its circular caldera, which is breached to the northwest, is 2 km in diameter and is ringed by several satellite vents ranging from the Pleistocene to late Holocene (Coombs and Jicha, 2021). All historical eruptive activity has taken place at an intracaldera cinder cone that measures about 200 m high (Richter and others, 1998b; Waythomas and others, 1998). The City of Akutan, Alaska, lies only 12 km east of the caldera rim, and one of the region's largest seafood processing plants is 1 km west of the city. In March 1996, two strong earthquake swarms took place on the island, causing minor damage and prompting some residents and plant workers to leave (Lu and others, 2000). A permanent seismic network was installed in the summer of 1996.

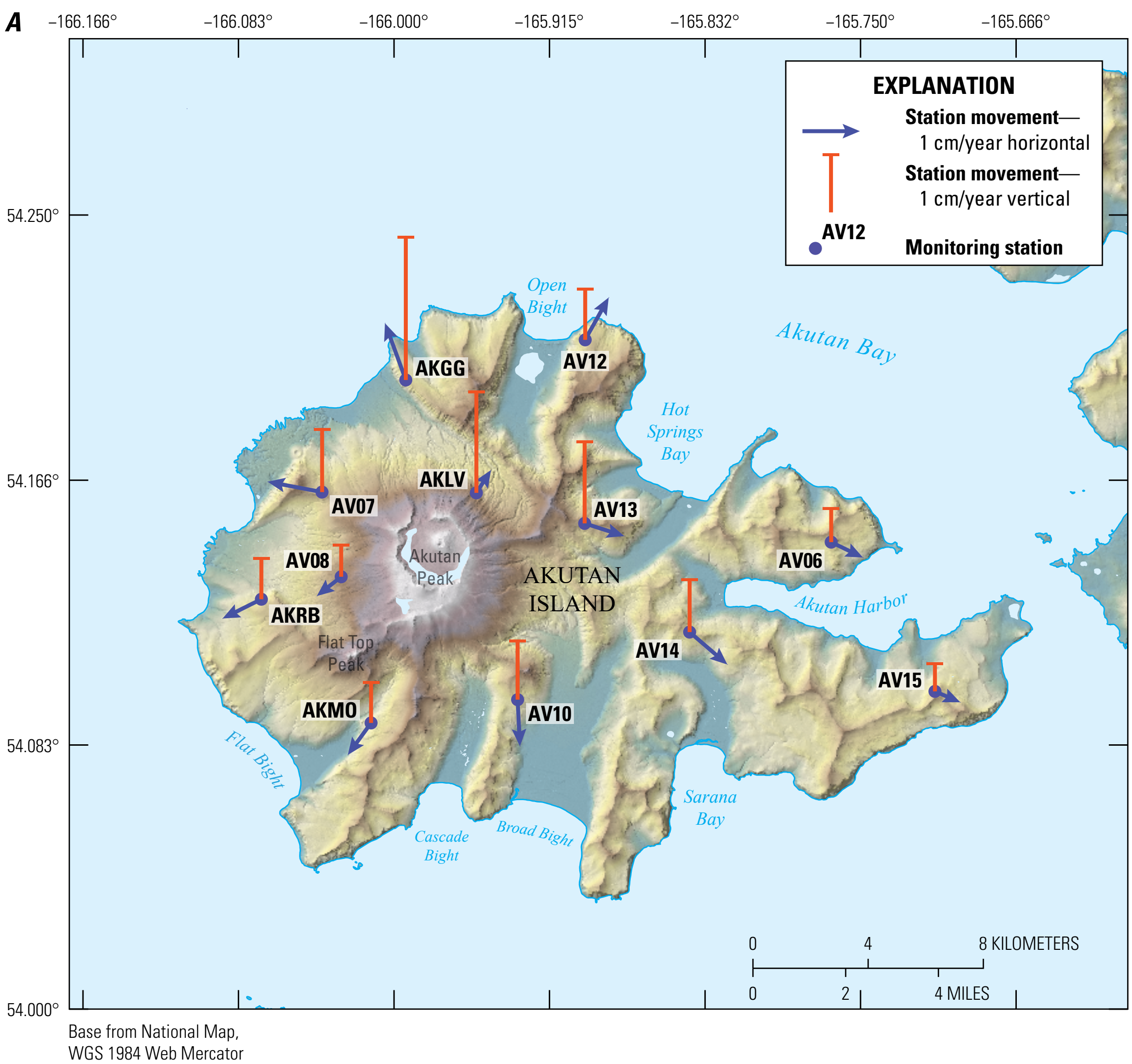


**Figure 18.** Global Positioning System velocity map (*A*) and displacement time series with 68 percent confidence levels showing movement of monitoring station AV10 (*B*) from January 1 to December 31, 2018, at Akutan Island, eastern Aleutian Islands, Alaska. Velocities and displacements are given relative to station AV09, located near the City of Unalaska, Alaska. Deformation rates, shown in centimeters per year (cm/year), appear higher in 2018 than the long-term rate shown in figure 17. Jan., January; Mar., March; Sept., September; Nov., November.

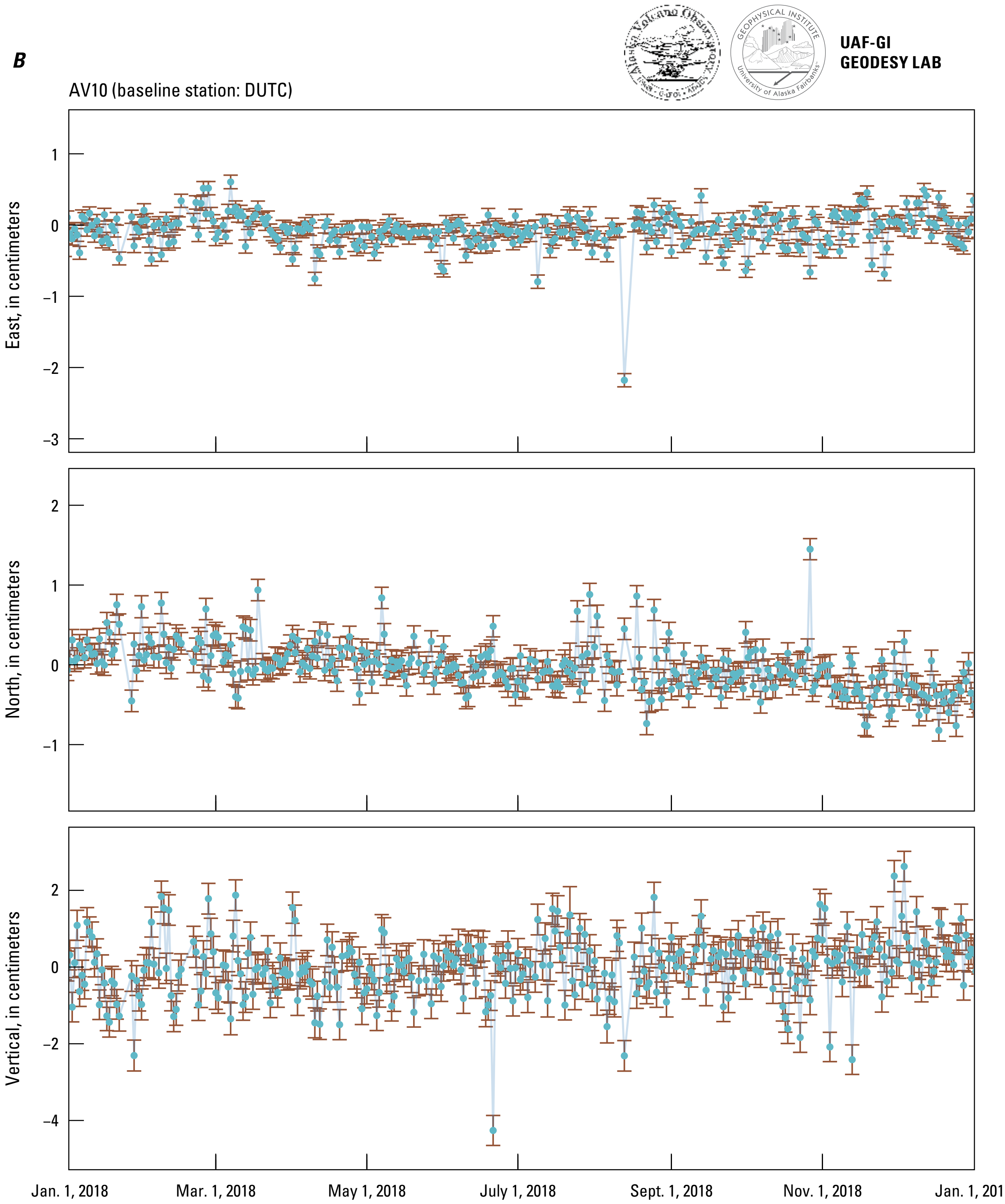


**Figure 18.** Global Positioning System velocity map (*A*) and displacement time series with 68 percent confidence levels showing movement of monitoring station AV10 (*B*) from January 1 to December 31, 2018, at Akutan Island, eastern Aleutian Islands, Alaska. Velocities and displacements are given relative to station AV09, located near the City of Unalaska, Alaska. Deformation rates, shown in centimeters per year (cm/year), appear higher in 2018 than the long-term rate shown in figure 17. Jan., January; Mar., March; Sept., September; Nov., November.—Continued

## Makushin Volcano


GVP #311310
53.887° N., 166.932° W.
1,800 m

Unalaska Island, Fox Islands, Aleutian Islands

**EARTHQUAKE SWARMS, GAS PLUMES**

Makushin Volcano continued showing signs of unrest in 2018. After the eruption of nearby Bogoslof volcano in 2016–2017, reports of steaming from the summit of Makushin Volcano increased in frequency. The number of located earthquakes near Makushin Volcano has also increased since 2012. Despite these mild signs of unrest, no observations were enough to raise the Aviation Color Code or Volcano Alert Level, which remained at **GREEN** and **NORMAL** throughout the year.

Steam emissions from Makushin Volcano were noted multiple times in the summer of 2018, both through webcam images seen by observatory personnel and in reports sent to AVO by residents of the City of Unalaska, Alaska (fig. 19). None of these reports differ in content from previous reports archived at AVO, which go back more than a decade. The increase in reports may be due in part to the activity at Bogoslof volcano, which could have prompted residents to forward more observations to AVO.

Independent of the increased frequency of reports of steaming, AVO performed its first aerial summit gas survey at Makushin Volcano in the summer of 2018. Gas observations from the volcano's gas plume yielded $SO_2$ fluxes of ~100 t/d along with low $CO_2/S_{total}$ (~1.5–2.5) and $SO_2/H_2S$ ratios (~1.1–1.7). These observations are consistent with degassing from a hot, mixed magmatic-hydrothermal system. The presence of $SO_2$, a magmatic gas, has not previously been detected from ground-based measurements at Makushin Volcano, although it was also detected at the volcano by a new instrument, the TROPOspheric Monitoring Instrument on the Copernicus Sentinel-5 Precursor satellite, which launched in the fall of 2017. Until repeat surveys establish baseline data, however, the significance of this $SO_2$ is unknown.

The increase in seismicity that began in 2012 continued in 2018, with more than 1,000 earthquakes located by AVO near Makushin Volcano during the year. As is typical for Makushin Volcano seismicity, several short earthquake swarms were noted. Four of these clusters, which took place in the months of January, July, September, and November, were located 5–10 km southeast of the summit, making this area the most seismically active on the volcano. Three more swarms took place in January, March, and June, about 20 km to the northeast, southwest, and southeast of the summit, respectively.

Makushin Volcano is on the eastern Aleutian island of Unalaska, about 25 km west of the City of Unalaska, the latter of which is an active seafood port (fig. 20). Makushin Volcano is a broad, truncated, deeply glaciated stratovolcano with a summit crater 3 km in diameter. Its summit is capped by a 40-$km^2$ icefield, but as ice cover has retreated, a small intracaldera cinder cone containing a turquoise-colored lake and abundant fumaroles has become a prominent feature. Makushin Volcano has produced 18 historical eruptions, the most recent of which took place on January 30, 1995, producing a small summit explosion and an ash plume that rose to an altitude as high as 10,000 ft (3,000 m) ASL (McGimsey and Neal, 1996; McConnell and others, 1998; Begét and others, 2000).

**Figure 19.** Photograph of steam rising from the summit area of Makushin Volcano (eastern Aleutian Islands, Alaska), taken by the webcam at seismograph station MREP on May 10, 2018. Direction of view is approximately northwest.

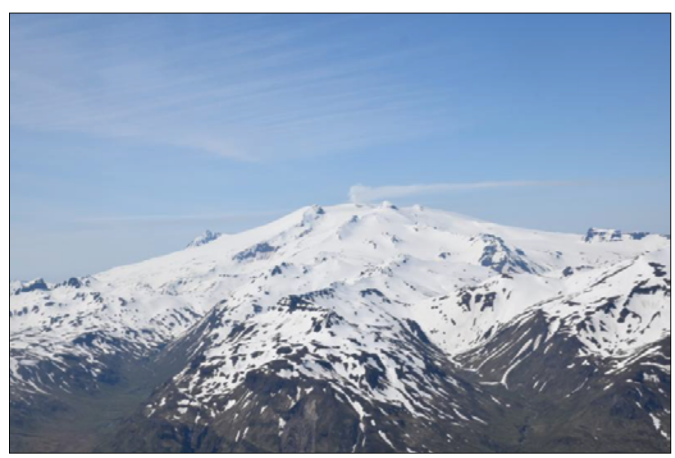

**Figure 20.** Oblique aerial photograph of Makushin Volcano (eastern Aleutian Islands, Alaska), viewed from the southeast, taken June 12, 2018. Photograph by Vlad Karpayev.

## Mount Okmok

*GVP #311290*
53.419° N., 168.132° W.
1,073 m


Umnak Island, Fox Islands, Aleutian Islands

**INFLATION**

In 2018, Mount Okmok (a name which herein includes associated volcanic features outside Okmok Caldera, such as Jag Peak and Tulik Volcano) continued the long-term reinflation that began immediately after its last eruption in 2008. This deformation takes place in discrete pulses that appear modulated onto a lower-rate, steady background deformation pattern. In 2018, monitoring stations OKCE and OKNC recorded a complete pulse (figs. 21, 22), with a total horizontal displacement of about 10 centimeters (cm) and a vertical displacement of as much as 12 cm. Past analyses of geodetic data (GPS and InSAR) indicate a shallow magma reservoir exists underneath the caldera floor (for example, see Freymueller and Kaufman, 2010; Lu and Dzurisin, 2014), and the continued volcanic inflation is consistent with an ongoing accumulation of shallow melt. Mount Okmok's Aviation Color Code and Volcano Alert Level remained at **GREEN** and **NORMAL** throughout 2018.

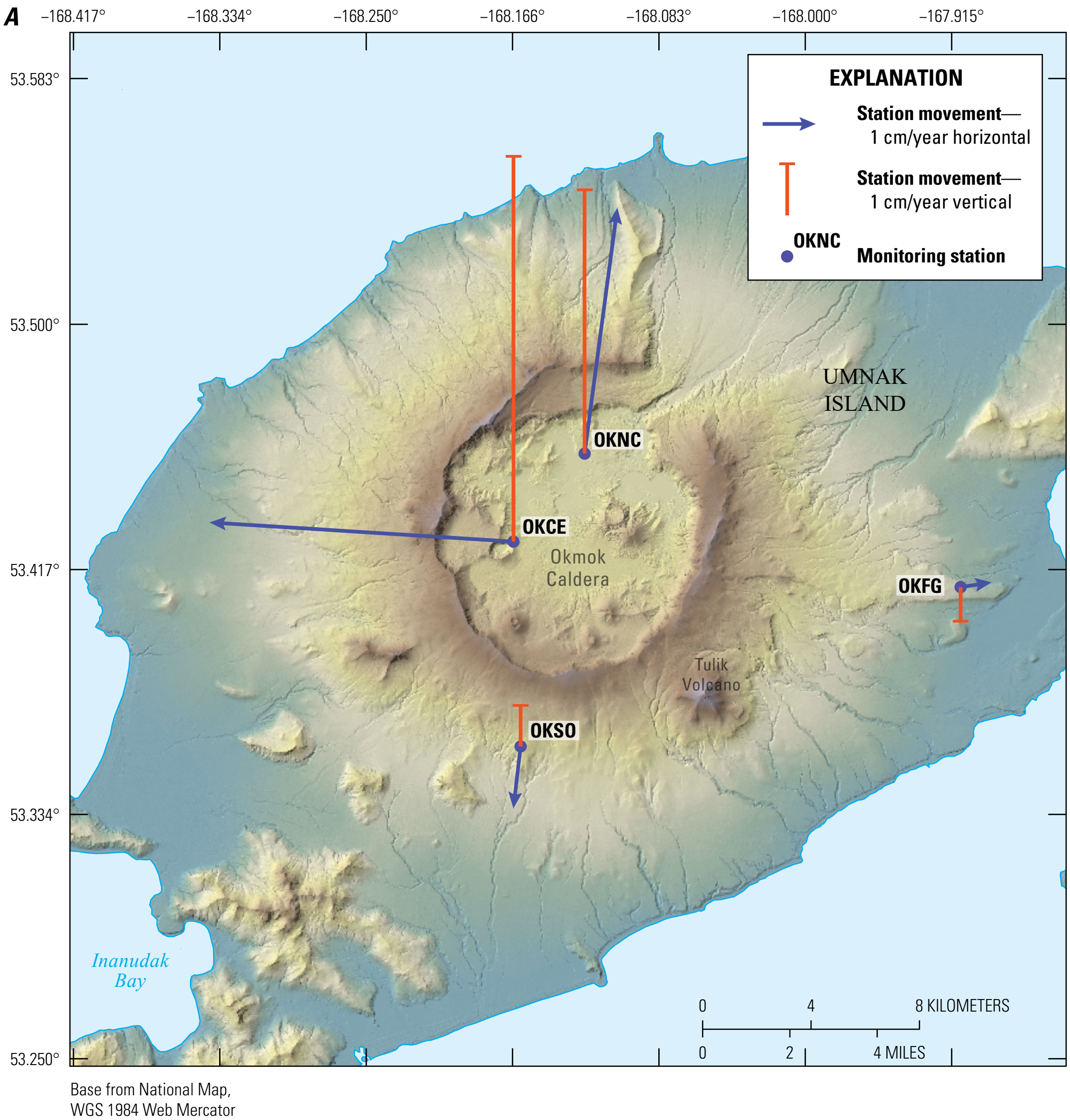


**Figure 21.** Global Positioning System velocity map (*A*) and displacement time series with 68 percent confidence levels showing movement of monitoring station OKCE (*B*) from September 2008 to September 2018 at Mount Okmok and in the surrounding area, eastern Aleutian Islands, Alaska. The map shows long-term inflation in centimeters per year (cm/year) as monitoring stations moved up and away from the volcano, and the displacement time series show this motion in the east, north, and vertical directions. Velocities and displacements are given relative to site AV09, located near the City of Unalaska, Alaska. Note that the time series begins after the 2008 eruption. Jan., January.

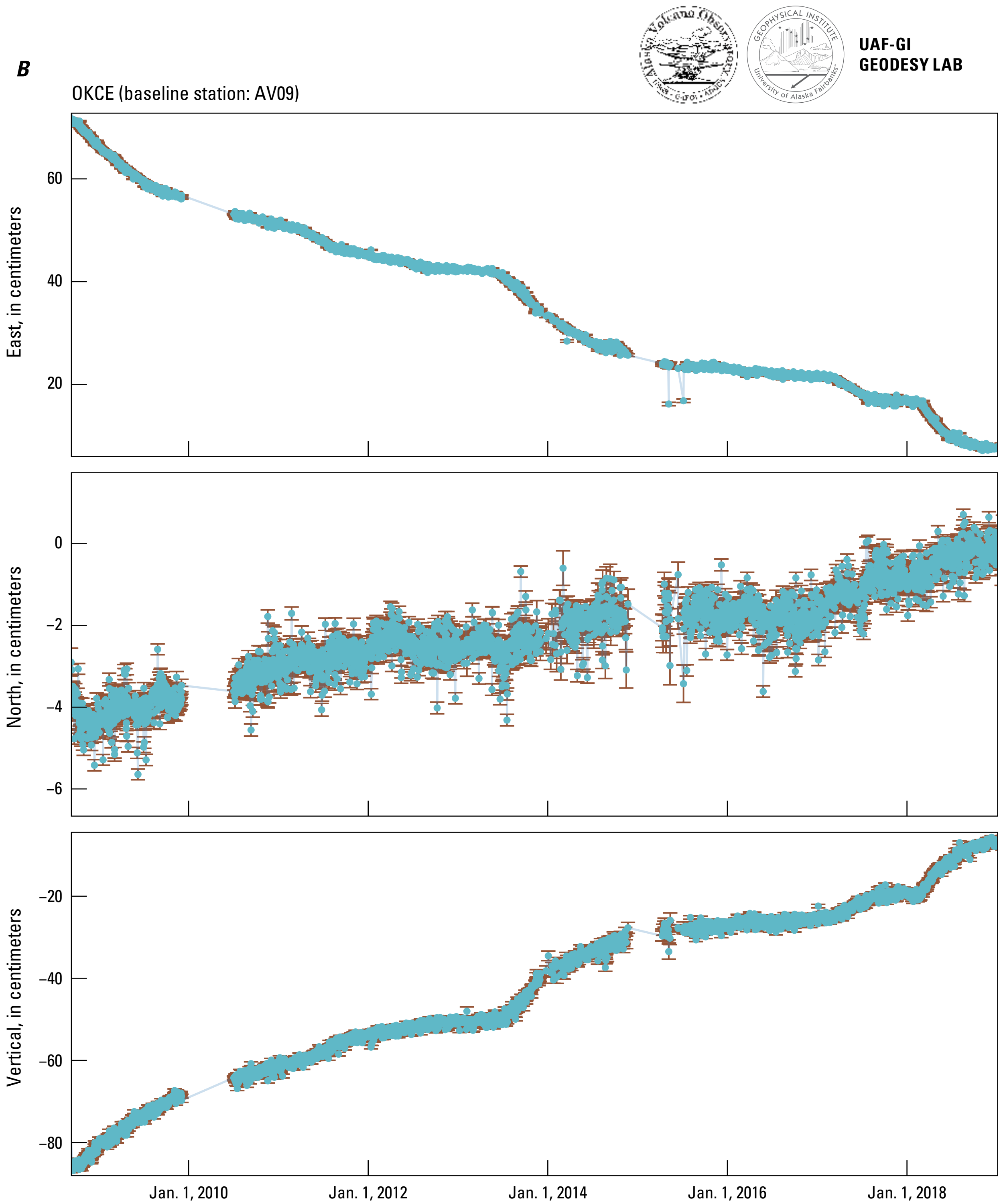


**Figure 21.** Global Positioning System velocity map (*A*) and displacement time series with 68 percent confidence levels showing movement of monitoring station OKCE (*B*) from September 2008 to September 2018 at Mount Okmok and in the surrounding area, eastern Aleutian Islands, Alaska. The map shows long-term inflation in centimeters per year (cm/year) as monitoring stations moved up and away from the volcano, and the displacement time series show this motion in the east, north, and vertical directions. Velocities and displacements are given relative to site AV09, located near the City of Unalaska, Alaska. Note that the time series begins after the 2008 eruption. Jan., January.—Continued

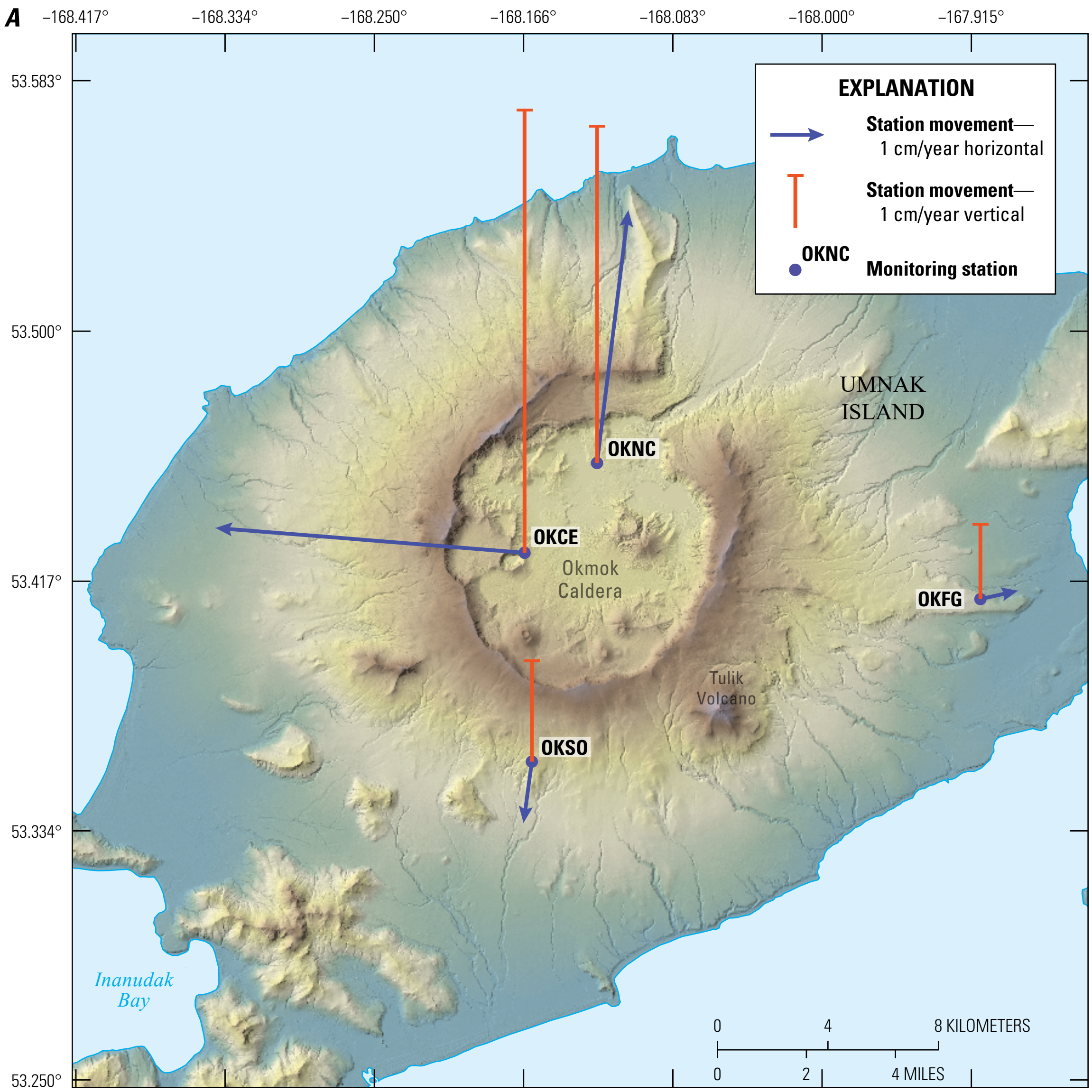


**Figure 22.** Global Positioning System velocity map (*A*) and displacement time series with 68 percent confidence levels showing movement of monitoring stations OKCE (*B*), OKNC (*C*), and OKSO (*D*) from January 1 to December 31, 2018, at Mount Okmok and in the surrounding area, eastern Aleutian Islands, Alaska. Note the change of scale vector length compared to figure 21. Velocities and displacements are given relative to site AV09, located near the City of Unalaska, Alaska. cm/year, centimeter per year; Jan., January; Mar., March; Sept., September; Nov., November.

Mount Okmok features a 10-kilometer-wide caldera with intra-and extra-caldera cones and lava flows. Occupying most of the east end of Umnak Island in the eastern Aleutian Islands, the volcano is 120 km southwest of the City of Unalaska. Built on a base of Tertiary volcanic rocks, it consists of three rock series: (1) older flows and pyroclastic beds of a pre-caldera shield complex, (2) pyroclastic deposits of two major, caldera-forming eruptions, and (3) a post-caldera field of small cones and lava flows that contains the historically active vents of the caldera (Byers, 1959; Larsen and others, 2007). Mount Okmok has erupted several times historically, mostly producing ash emissions that occasionally reached altitudes higher than 30,000 ft (9,100 m) ASL but were generally much lower. Mount Okmok has a history of lava flows, with recent flows emplaced on its caldera floor in 1945, 1958, and 1997 (Begét and others, 2005). The latest eruption of the volcano was a phreatomagmatic event during the summer of 2008 that built a new cone, informally called Ahmanilix, whereas other recent eruptions took place at a vent within the caldera referred to as cone A (Neal and others, 2011). Thermal springs and fumaroles occur in both Okmok Caldera and at Hot Springs Cove, 20 km to the southwest.

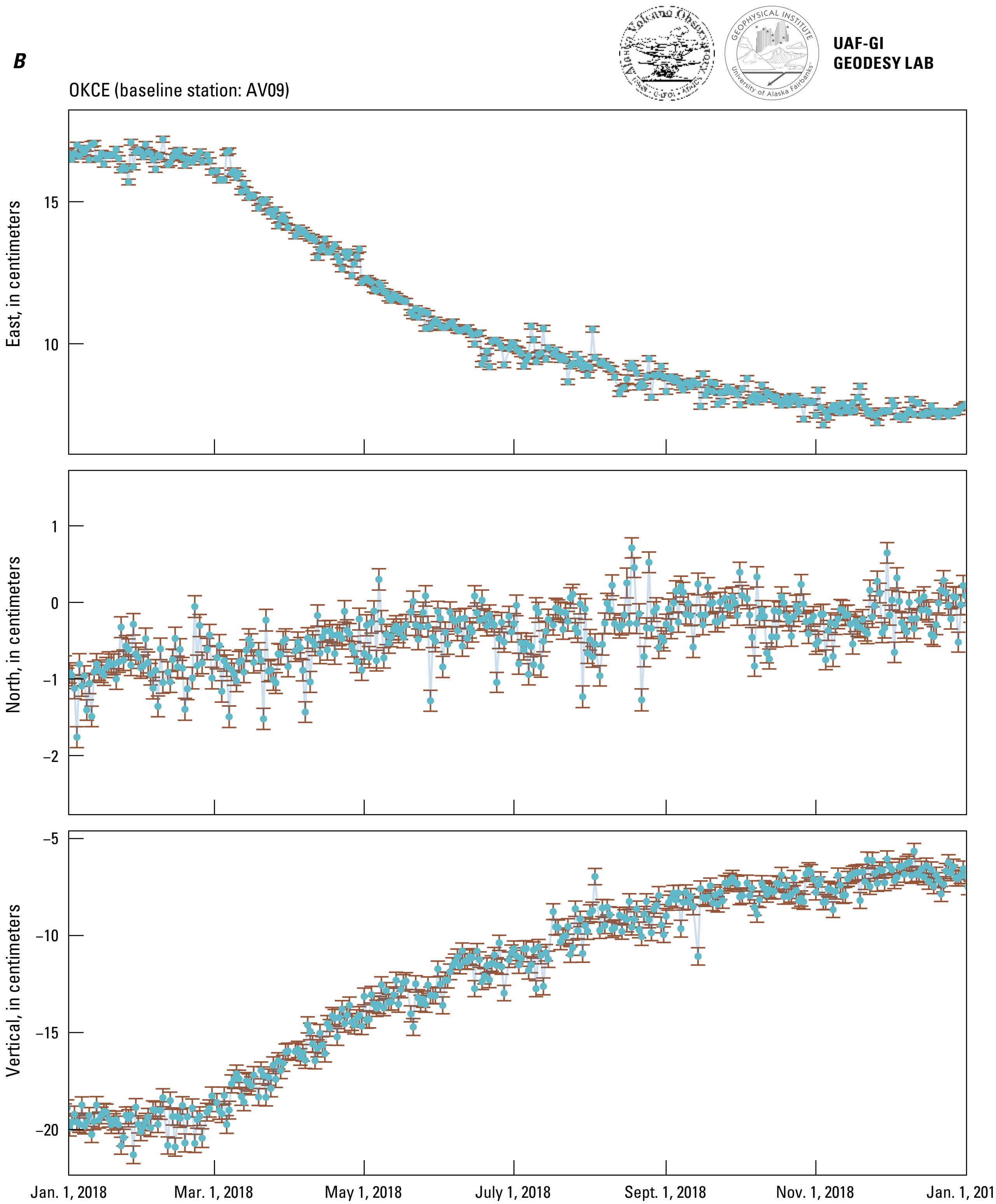


**Figure 22.** Global Positioning System velocity map (*A*) and displacement time series with 68 percent confidence levels showing movement of monitoring stations OKCE (*B*), OKNC (*C*), and OKSO (*D*) from January 1 to December 31, 2018, at Mount Okmok and in the surrounding area, eastern Aleutian Islands, Alaska. Note the change of scale vector length compared to figure 21. Velocities and displacements are given relative to site AV09, located near the City of Unalaska, Alaska. cm/year, centimeter per year; Jan., January; Mar., March; Sept., September; Nov., November.—Continued

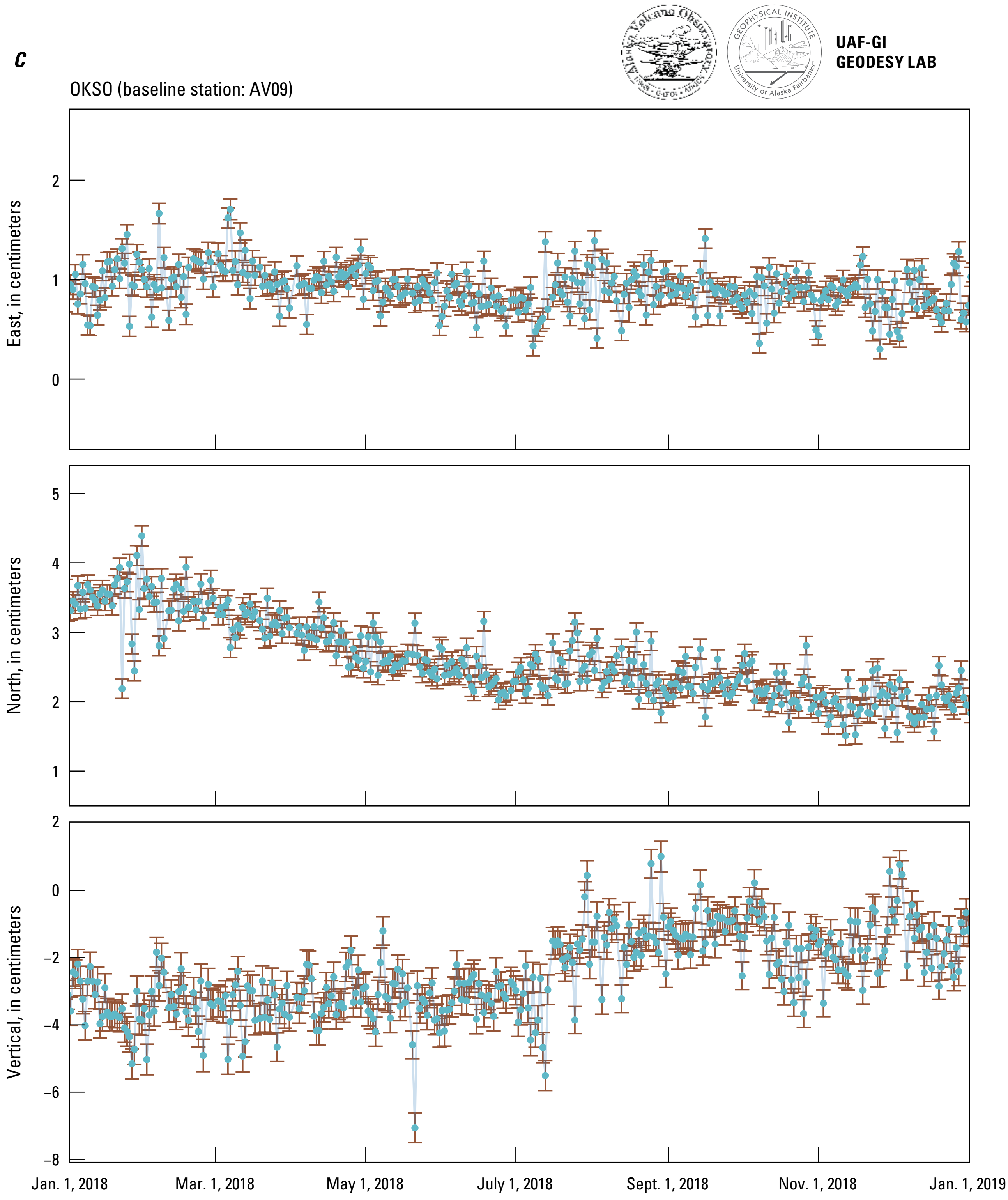


**Figure 22.** Global Positioning System velocity map (*A*) and displacement time series with 68 percent confidence levels showing movement of monitoring stations OKCE (*B*), OKNC (*C*), and OKSO (*D*) from January 1 to December 31, 2018, at Mount Okmok and in the surrounding area, eastern Aleutian Islands, Alaska. Note the change of scale vector length compared to figure 21. Velocities and displacements are given relative to site AV09, located near the City of Unalaska, Alaska. cm/year, centimeter per year; Jan., January; Mar., March; Sept., September; Nov., November.—Continued

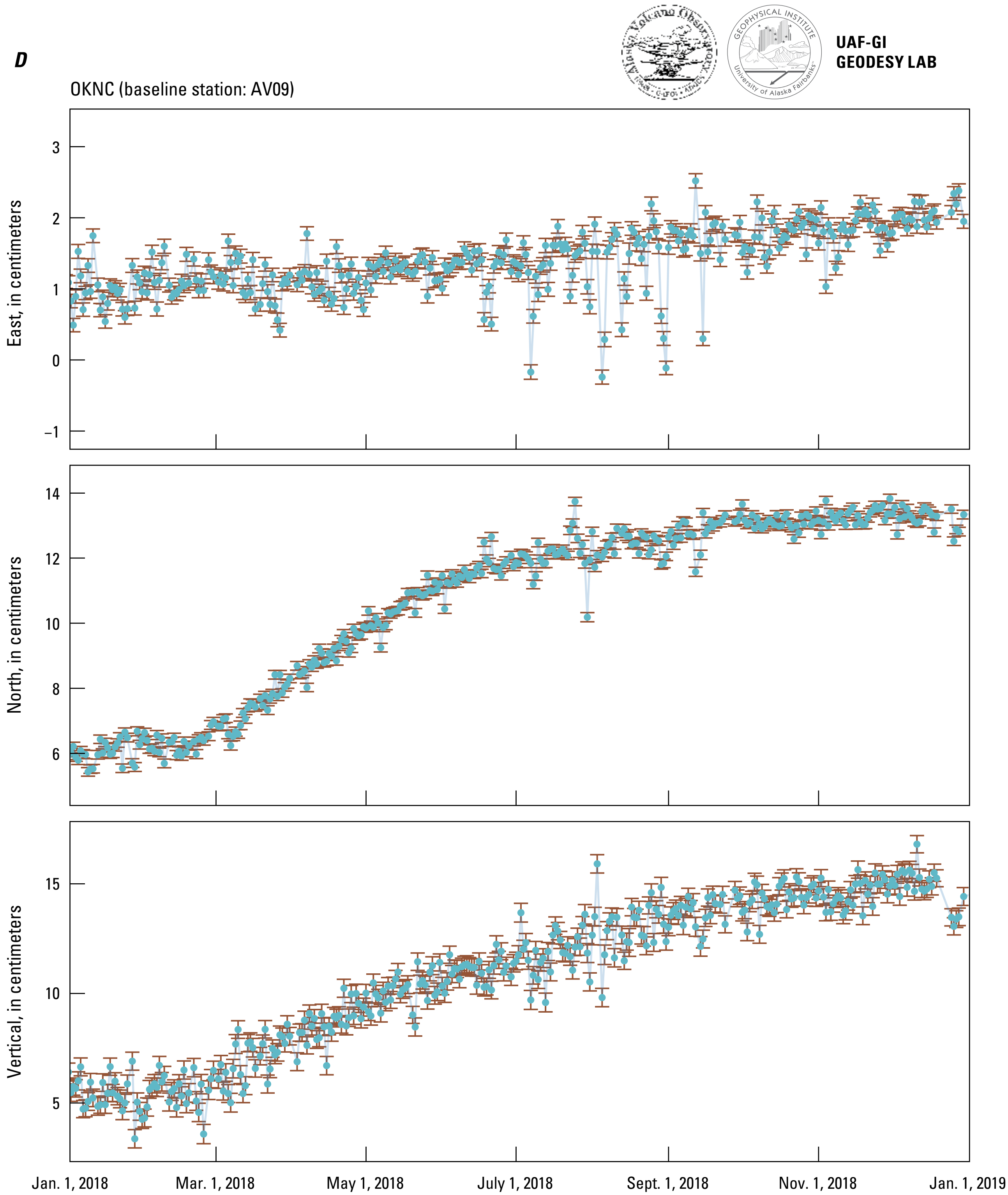


**Figure 22.** Global Positioning System velocity map (*A*) and displacement time series with 68 percent confidence levels showing movement of monitoring stations OKCE (*B*), OKNC (*C*), and OKSO (*D*) from January 1 to December 31, 2018, at Mount Okmok and in the surrounding area, eastern Aleutian Islands, Alaska. Note the change of scale vector length compared to figure 21. Velocities and displacements are given relative to site AV09, located near the City of Unalaska, Alaska. cm/year, centimeter per year; Jan., January; Mar., March; Sept., September; Nov., November.—Continued

## Mount Cleveland


*GVP #311240*
52.822° N., 169.945° W.
1,730 m

Chuginadak Island, Islands of Four Mountains, Aleutian Islands

**INTERMITTENT EXPLOSIONS AND DOME GROWTH**

Activity at Mount Cleveland during 2018 was similar to that of previous years, featuring nearly continuous degassing, elevated surface temperatures, and the growth of small lava domes that were subsequently destroyed by short-lived, ash-rich explosions. Nine explosions, grouped into two clusters, took place during 2018; one cluster spanned March through May and the other took place at the end of December (table 4). Mount Cleveland is currently monitored via seismic instruments, an infrasound array, a webcam, and satellite remote sensing. Seismograph station CLCO is located on Concord Point, 15.4 km from the edifice, and contains an infrasound array, a webcam, a broadband (three-component) seismometer, and a short-period (one-component) seismometer. A second station, CLES, is installed low on the east flank of Mount Cleveland, 3.5 km from the summit. This station contains two infrasound sensors and both a broadband and a short-period seismometer. The combination of these geophysical monitoring techniques allows AVO to characterize the ongoing activity at Mount Cleveland, which poses a hazard to aircraft despite its remote location.

In addition to the preexisting volcanic activity alarms at Mount Cleveland, AVO implemented two new alarms in 2018 to help detect sudden explosions. One alarm uses the co-located seismic and infrasound sensors at station CLES to quickly detect smaller explosions, and the other uses seismic data in the very-long-period band from station CLCO. This second alarm became especially useful after CLES had an extended data outage starting in September 2018; for the latter part of the year, AVO had only CLCO to supplement the usual remote sensing techniques used to monitor Mount Cleveland.

Mount Cleveland began 2018 at Aviation Color Code **ORANGE** and Volcano Alert Level **WATCH**, a response to its previous explosion on December 18, 2017, at 03:17 UTC (December 17 at 17:17 HAST). After several months without explosive activity, on February 9, 2018, AVO downgraded the Aviation Color Code and Volcano Alert Level to **YELLOW** and **ADVISORY**. The first explosion of 2018 took place on March 2 at 14:57 UTC (04:57 HAST) and was detected by AVO's automated infrasound alarms. The acoustic amplitude of the explosion was similar to that of the previous explosion, and ground-coupled airwaves were detected as far as the Pavlof Volcano and Korovin Volcano seismic networks (747 km and 1,025 km away, respectively). A small volcanic cloud was observed in satellite data moving east-northeast shortly after the explosion. The event prompted AVO to raise the Aviation Color Code and Volcano Alert Level again to **ORANGE** and **WATCH**. After a few days with no substantial eruptive activity, on March 5, AVO downgraded the Aviation Color Code and Volcano Alert Level to **YELLOW** and **ADVISORY**.

The next explosion took place on March 15 at 06:19 UTC (March 14 at 21:19 HADT) and was detected by the Mount Okmok infrasound array. The ground-coupled airwaves from this event were also detected by the Mount Okmok seismic network. Mount Cleveland produced another short-lived explosion on April 4 at 11:55 UTC (02:55 HADT), and possible jetting took place about 40 minutes later. In contrast to other explosions on Mount Cleveland, which typically have no notable precursory activity, a low-frequency seismic event preceded the April 4 explosion by about 19 hours. Satellite imagery taken after the explosion indicated the presence of hot material on the west flank from the summit down to the coast (fig. 23) and a small volcanic cloud drifting at an altitude of about 19,000 ft (5,800 m) ASL. AVO upgraded the Aviation Color Code and Volcano Alert Level to **ORANGE** and **WATCH** in response to this explosion. Activity on the volcano declined after April 4, and on April 6, AVO downgraded the Aviation Color Code and Volcano Alert Level back to **YELLOW** and **ADVISORY**. Another small explosion took place on April 13 at 15:59 UTC (06:59 HADT).

The next explosion at Mount Cleveland took place on May 5 at 06:08 UTC (May 4 at 21:08 HADT) and was detected by both the newly implemented seismic and acoustic alarms at CLES and by the previously running alarms on the CLCO infrasound array. A small volcanic cloud from the explosion, visible in satellite imagery, drifted southeast at an altitude of about 22,000 ft (6,700 m) ASL. In response to the event, AVO raised the Aviation Color Code and Volcano Alert Level to **ORANGE** and **WATCH**. After no new explosive activity, on May 6, AVO downgraded the Aviation Color Code and Volcano Alert Level back to **YELLOW** and **ADVISORY**. The event on May 5 was the last in Mount Cleveland's first cluster of explosions in 2018.

On June 3 and 9, two small swarms of local earthquakes took place near Mount Cleveland but did not appear to be associated with any explosive activity. A few earthquakes from the June 3 seismic swarm are shown in figure 24, as recorded by stations CLES and CLCO. Satellite imagery indicated that between June 19 and 25, a new lava dome measuring 80 m in diameter grew within the crater (fig. 25). The appearance of the dome prompted AVO to upgrade the Aviation Color Code and Volcano Alert Level to **ORANGE** and **WATCH** because the presence of lava over the active vent increased the possibility of a vent-clearing explosion. After a few months without explosive activity, on August 22, AVO downgraded the Aviation Color Code and Volcano Alert Level to **YELLOW** and **ADVISORY**.

A data outage took place at the local monitoring station (CLES) on September 23 and persisted for the rest of the year, leaving the seismometer at the distal station (CLCO) as the only local instrumentation to supplement AVO's remote sensing techniques.

The second cluster of explosions to affect Mount Cleveland in 2018 began on December 10 at 08:55 UTC (December 9 at 22:55 HAST). The seismic amplitude of this first explosion, which was similar to that of previous explosions in 2018, triggered the seismic alarm at station CLCO. The seismic stations in the town of

**Table 4.** Summary of activity and observations in 2018 at Mount Cleveland, in the eastern Aleutian Islands, Alaska.

[Entries without elevated temperatures may simply mean clouds obscured the ground. Dates shown as month/day/year; UTC, coordinated universal time; AVO, Alaska Volcano Observatory; ASL, above sea level; ft, foot; m, meter; VT, volcano-tectonic]

| Aviation Color Code/ Volcano Alert Level | Date (UTC) | Observation description |
|---|---|---|
| ORANGE/WATCH | 01/05/2018 | Moderately elevated surface temperatures |
| ORANGE/WATCH | 01/14/2018 | New dome growth |
| ORANGE/WATCH | 01/20/2018 | Weakly elevated surface temperatures |
| ORANGE/WATCH | 01/21/2018 | Moderately elevated surface temperatures |
| ORANGE/WATCH | 01/29/2018 | Moderately elevated surface temperatures |
| ORANGE/WATCH | 01/30/2018 | Moderately elevated surface temperatures |
| YELLOW/ADVISORY | 02/09/2018 | No considerable activity since the explosion on December 18, 2017; AVO lowered the Aviation Color Code and Volcano Alert Level |
| YELLOW/ADVISORY | 02/14/2018 | Weakly elevated surface temperatures |
| YELLOW/ADVISORY | 02/16/2018 | Moderately elevated surface temperatures |
| YELLOW/ADVISORY | 02/28/2018 | Weakly elevated surface temperatures |
| ORANGE/WATCH | 03/02/2018 | Explosion detected by automated infrasound alarms; plume reaching an altitude of 15,000 ft (4,600 m) ASL, heading east-northeast; AVO raised the Aviation Color Code and Volcano Alert Level |
| ORANGE/WATCH | 03/03/2018 | Weakly elevated surface temperatures |
| YELLOW/ADVISORY | 03/05/2018 | AVO lowered the Aviation Color Code and Volcano Alert Level; deeper crater and ballistic impact pits seen in satellite data |
| YELLOW/ADVISORY | 03/08/2018 | Small swarm of VT earthquakes |
| YELLOW/ADVISORY | 03/15/2018 | Explosion (smaller than the March 2 explosion) |
| YELLOW/ADVISORY | 03/20/2018 | Moderately elevated surface temperatures |
| ORANGE/WATCH | 04/04/2018 | Explosion with similar seismic energy and more acoustic energy than the March 15 explosion, followed by a short tremor signal; highly elevated surface temperatures; hot material reaching the coast and possible ash cloud seen in satellite data; AVO raised the Aviation Color Code and Volcano Alert Level |
| YELLOW/ADVISORY | 04/06/2018 | AVO lowered the Aviation Color Code and Volcano Alert Level |
| YELLOW/ADVISORY | 04/13/2018 | Explosion seen in seismic and acoustic data |
| YELLOW/ADVISORY | 04/19/2018 | Satellite data showed ballistics as large as 10 m in diameter scattered near a new crater formed by the April 13 explosion |
| ORANGE/WATCH | 05/05/2018 | Explosion detected by automated infrasound alarms and new seismic and acoustic alarms; satellite data showed an ash plume drifting southeast at an altitude of 22,000 ft (6,700 m) ASL; AVO raised the Aviation Color Code and Volcano Alert Level |
| YELLOW/ADVISORY | 05/06/2018 | AVO lowered the Aviation Color Code and Volcano Alert Level |
| YELLOW/ADVISORY | 05/11/2018 | Satellite data showed minor changes to the summit crater, including a layer of new tephra, after the May 5 explosion |
| YELLOW/ADVISORY | 05/12/2018 | Possible ash plume observed in satellite data |
| YELLOW/ADVISORY | 05/14/2018 | Steam plume observed in remote sensing data |
| YELLOW/ADVISORY | 05/15/2018 | Moderately elevated surface temperatures |
| YELLOW/ADVISORY | 05/16/2018 | Weakly elevated surface temperatures |
| YELLOW/ADVISORY | 05/22/2018 | Weakly elevated surface temperatures |
| YELLOW/ADVISORY | 05/27/2018 | Highly elevated surface temperatures |
| YELLOW/ADVISORY | 06/03/2018 | Weakly elevated surface temperatures; small earthquake swarm |
| YELLOW/ADVISORY | 06/09/2018 | Small earthquake swarm |
| YELLOW/ADVISORY | 06/12/2018 | Minor steaming |
| YELLOW/ADVISORY | 06/14/2018 | Weakly elevated surface temperatures |
| YELLOW/ADVISORY | 06/18/2018 | Moderately elevated surface temperatures |
| YELLOW/ADVISORY | 06/23/2018 | Possible tremor |
| ORANGE/WATCH | 06/26/2018 | New dome growth observed in satellite data; 20-meter-diameter smaller dome observed on top of the central vent; AVO raised the Aviation Color Code and Volcano Alert Level |
| ORANGE/WATCH | 07/07/2018 | Weakly elevated surface temperatures; minor steaming |
| ORANGE/WATCH | 07/10/2018 | Weakly elevated surface temperatures; minor steaming |
| ORANGE/WATCH | 07/11/2018 | Weakly elevated surface temperatures |

**Table 4.**—Continued

| Aviation Color Code/ Volcano Alert Level | Date (UTC) | Observation description |
|---|---|---|
| ORANGE/WATCH | 07/19/2018 | Weakly elevated surface temperatures |
| ORANGE/WATCH | 07/24/2018 | Weakly elevated surface temperatures; possible ballistic blocks in summit crater |
| ORANGE/WATCH | 07/25/2018 | Minor steaming |
| ORANGE/WATCH | 07/26/2018 | Steam plume observed in remote sensing data |
| ORANGE/WATCH | 07/27/2018 | Steam plume observed in remote sensing data |
| ORANGE/WATCH | 08/07/2018 | Moderately elevated surface temperatures; minor steaming |
| ORANGE/WATCH | 08/11/2018 | Weakly elevated surface temperatures |
| ORANGE/WATCH | 08/13/2018 | Moderately elevated surface temperatures; minor steaming |
| ORANGE/WATCH | 08/15/2018 | Weakly elevated surface temperatures |
| YELLOW/ADVISORY | 08/22/2018 | Moderately elevated surface temperatures; AVO lowered the Aviation Color Code and Volcano Alert Level |
| YELLOW/ADVISORY | 08/26/2018 | Weakly elevated surface temperatures |
| YELLOW/ADVISORY | 08/27/2018 | Weakly elevated surface temperatures |
| YELLOW/ADVISORY | 08/28/2018 | Weakly elevated surface temperatures; minor steaming |
| YELLOW/ADVISORY | 08/30/2018 | Weakly elevated surface temperatures; minor steaming |
| YELLOW/ADVISORY | 08/31/2018 | Weakly elevated surface temperatures |
| YELLOW/ADVISORY | 09/01/2018 | Weakly elevated surface temperatures |
| YELLOW/ADVISORY | 09/02/2018 | Weakly elevated surface temperatures |
| YELLOW/ADVISORY | 09/03/2018 | Moderately elevated surface temperatures; steam plume |
| YELLOW/ADVISORY | 09/07/2018 | Weakly elevated surface temperatures |
| YELLOW/ADVISORY | 09/08/2018 | Moderately elevated surface temperatures |
| YELLOW/ADVISORY | 09/09/2018 | Moderately elevated surface temperatures; minor steaming |
| YELLOW/ADVISORY | 09/11/2018 | Weakly elevated surface temperatures |
| YELLOW/ADVISORY | 09/18/2018 | Moderately elevated surface temperatures; steam plume |
| YELLOW/ADVISORY | 09/19/2018 | Moderately elevated surface temperatures |
| YELLOW/ADVISORY | 09/20/2018 | Moderately elevated surface temperatures; possible recent dome growth |
| YELLOW/ADVISORY | 09/22/2018 | Weakly elevated surface temperatures; steam plume |
| YELLOW/ADVISORY | 09/26/2018 | Moderately elevated surface temperatures; steam plume |
| YELLOW/ADVISORY | 09/29/2018 | Moderately elevated surface temperatures |
| YELLOW/ADVISORY | 09/30/2018 | Subtle dome subsidence observed in satellite data |
| YELLOW/ADVISORY | 10/29/2018 | Moderately elevated surface temperatures |
| YELLOW/ADVISORY | 10/30/2018 | Moderately elevated surface temperatures |
| YELLOW/ADVISORY | 10/31/2018 | Moderately elevated surface temperatures |
| YELLOW/ADVISORY | 11/09/2018 | Moderately elevated surface temperatures |
| YELLOW/ADVISORY | 11/13/2018 | Weakly elevated surface temperatures |
| YELLOW/ADVISORY | 11/17/2018 | Weakly elevated surface temperatures; possible tremor-like signal |
| YELLOW/ADVISORY | 12/04/2018 | Possible tremor-like signal |
| YELLOW/ADVISORY | 12/05/2018 | Weakly elevated surface temperatures |
| YELLOW/ADVISORY | 12/08/2018 | Weakly elevated surface temperatures |
| YELLOW/ADVISORY | 12/09/2018 | Explosion detected seismically; satellite data showed most of lava dome destroyed and formation of narrow debris flow |
| YELLOW/ADVISORY | 12/11/2018 | Moderately elevated surface temperatures |
| ORANGE/WATCH | 12/12/2018 | Explosion 1.5 times larger than previous explosion, detected by a seismic-only alarm; $SO_2$ detected in satellite data; AVO raised the Aviation Color Code and Volcano Alert Level |
| ORANGE/WATCH | 12/15/2018 | Steam plume observed in remote sensing data |
| ORANGE/WATCH | 12/16/2018 | Explosion larger than December 12 explosion, detected by a seismic-only alarm; one lighting stroke recorded with explosion; ash cloud observed in satellite data at 25,000–30,000 ft (7,600–9,100 m) ASL, heading northeast; satellite data also showed a deeper crater with ballistics after the explosion |
| ORANGE/WATCH | 12/29/2018 | Small explosion detected by local seismometers; satellite data showed an ash cloud to 17,000 ft (5,200 m) ASL; $SO_2$ detected |

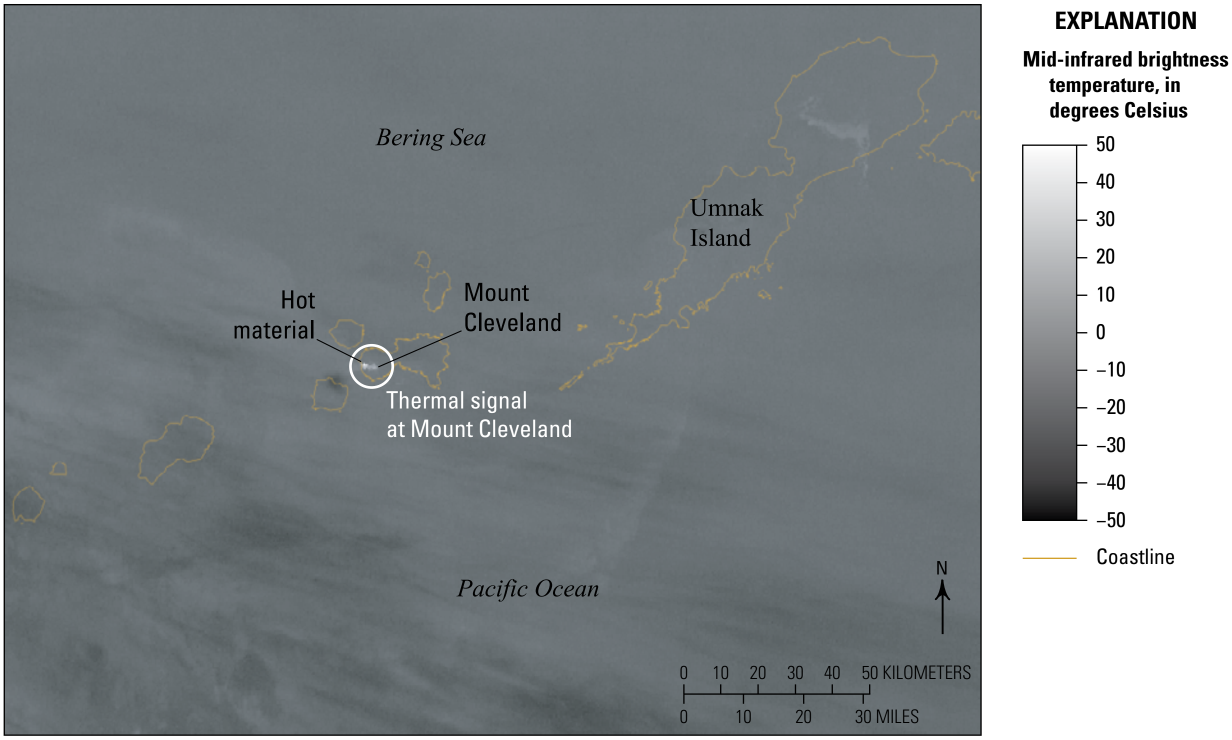


**Figure 23.** Annotated mid-infrared satellite image showing hot material on the west flank of Mount Cleveland (eastern Aleutian Islands, Alaska) reaching to the coast after the explosion of April 4, 2018. Image taken at 12:16 coordinated universal time by a Visible Infrared Imaging Radiometer Suite (VIIRS) instrument on the National Oceanic and Atmospheric Administration's NOAA-20 satellite.

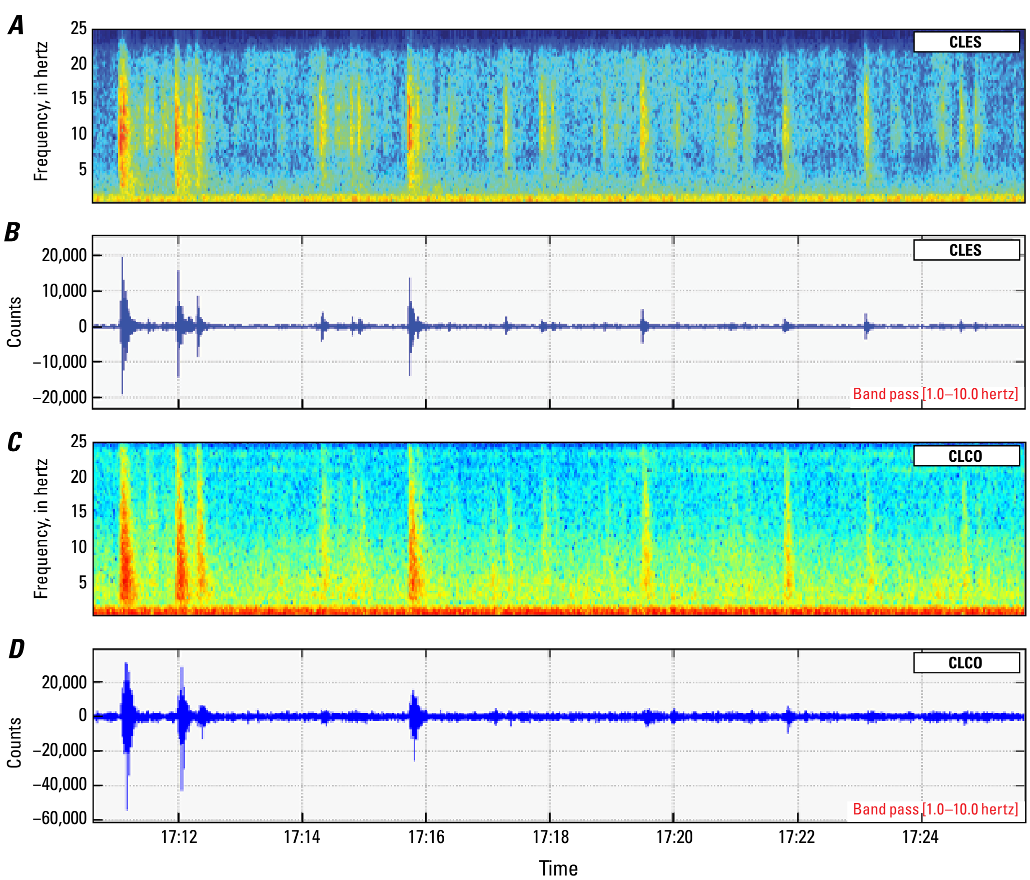


**Figure 24.** Spectrogram graphs (*A* and *C*) and broadband vertical seismogram graphs (*B* and *D*) showing a small swarm of earthquakes at Mount Cleveland (eastern Aleutian Islands, Alaska) on June 3, 2018. A 1.0–10.0-hertz band-pass filter is applied to both seismograms. The horizontal (time) axes of all four charts span from 17:11 to shortly before 17:26 coordinated universal time (8:11 to shortly before 8:26 Hawaii-Aleutian standard time). Station CLES, located on the east flank of Mount Cleveland, is closer to the summit than station CLCO, located on the other side of the island at Concord Point.

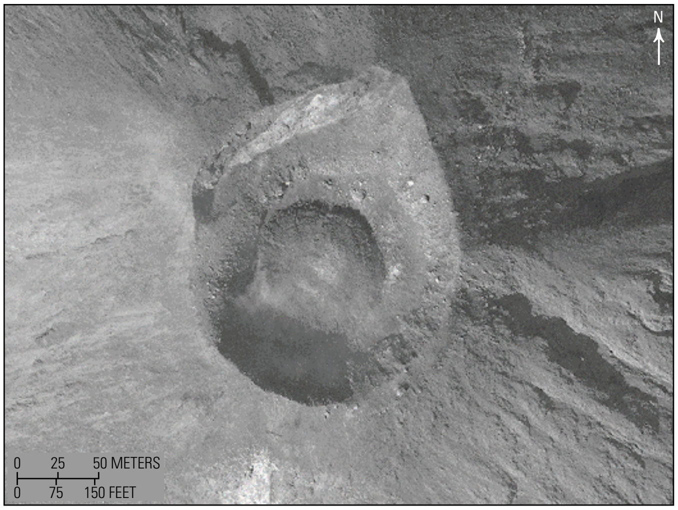




**Figure 25.** Satellite image from September 4, 2018, showing the lava dome that formed between June 19 and 25 in the summit crater of Mount Cleveland, eastern Aleutian Islands, Alaska. The dome was approximately 80–90 meters in diameter at the time. Image taken by the Worldview-1 satellite, courtesy of Matthew Loewen (U.S. Geological Survey/Alaska Volcano Observatory) via the DigitalGlobe NextView license.

Nikolski, Alaska, and at Mount Okmok recorded ground-coupled airwaves. Satellite imagery taken after the explosion indicated that most of the summit lava dome was removed and that new debris flow deposits extended 2.6 km east-northeast of the summit. Another explosion took place on December 12 at 20:52 UTC (10:52 HAST), with an amplitude about 1.5 times larger than the previous explosion. The same day, AVO upgraded the Aviation Color Code and Volcano Alert Level to **ORANGE** and **WATCH**.

The next explosion in the cluster took place on December 16 at 16:37 UTC (06:37 HAST). It triggered the seismic alarm and was also detected by the Mount Okmok seismic network in the form of weak, ground-coupled airwaves. This explosion was slightly larger than the previous one, producing a small ash cloud that reached an altitude of about 25,000–30,000 ft (7,600–9,100 m) ASL, possible $SO_2$ gas emissions, and a single stroke of lightning (detected by the World Wide Lightning Location Network). Mount Cleveland produces volcanic lighting infrequently; its only other known occurrences took place in 2009 and 2014.

The final explosion of Mount Cleveland in 2018 took place on December 29 at 03:17 UTC (December 28 at 17:17 HAST). A pilot weather report from after the explosion described an ash cloud reaching an altitude as high as 17,000 ft (5,200 m) ASL. Mount Cleveland remained at Aviation Color Code and Volcano Alert Level **ORANGE** and **WATCH** for the remainder of 2018.

Mount Cleveland forms the western part of Chuginadak Island, an uninhabited island in the Islands of Four Mountains group of the east-central Aleutian Islands. The volcano is about 75 km west of the community of Nikolski and 1,500 km southwest of Anchorage. Short-lived ash explosions, lava fountaining, lava flows, and lahars have characterized its historical eruptions. In February 2001, after 6 years of quiescence, Mount Cleveland had three explosive events that produced a rubbly lava flow, a hot avalanche that reached the sea, and ash clouds reaching altitudes as high as 39,000 ft (12,000 m) ASL (Dean and others, 2004). Intermittent explosive eruptions have taken place every year since 2001, with exceptional explosive activity in 2011–2012.

## Great Sitkin Volcano


*GVP #311120*
52.0765° N., 176.1109° W.
1,740 m

Great Sitkin Island, Andreanof Islands, Aleutian Islands

**EARTHQUAKE SWARM, EXPLOSIONS**

In late July 2016, Great Sitkin Volcano entered a period of unrest characterized by an elevated frequency of earthquakes, anomalous steaming from its crater, and small explosive events (Dixon and others, 2020). Volcanic activity continued throughout 2018 with additional small earthquakes, steaming from the summit crater, and several more small explosion events.

During 2018, AVO located more than 2,300 earthquakes at Great Sitkin Volcano, principally clustered in the shallow crust (extending from the summit to roughly 10 km below sea level). Additional earthquakes were also located between 15 and 35 km depth (fig. 26), with waveforms and frequency contents suggesting both VT and deep LP earthquakes. The magnitudes of these located events ranged from an $M_L$ of less than −1.0 to 2.48—the largest event took place on August 31, 2018 (fig. 27). Unfortunately, the Great Sitkin Volcano seismic network experienced several station failures in 2018, most importantly at stations GSTD and GSSP, which impaired AVO's ability to locate earthquakes and resulted in the data gaps seen in figure 27. The most notable of these failure periods spanned early November 2017 to mid-January 2018. Shorter-term failures of station GSSP also compromised AVO's earthquake locating capabilities during the winter of 2018–2019.

AVO identified several tremor bursts associated with this unrest during 2018, with most taking place between June and December. Interpreted as small explosion events, the tremor bursts contained a variety of waveforms with impulsive to emergent onsets, extended codas, and frequency between 1 and 15 hertz. The bursts were commonly associated with increased earthquake activity (fig. 28), but none produced infrasound signals identifiable by sensors in the nearby City of Adak, Alaska.

The explosion of June 10, 2018, proved especially noteworthy when a Sentinel-2 satellite image acquired on June 11 at 23:00 UTC (14:00 HADT) showed a 2-kilometer-long ash deposit extending southwest from the summit of Great Sitkin Volcano. Additional photographs of the summit area taken from a passing aircraft a week later showed an ash deposit on the snow (fig. 29). This deposit presumably came from the June 10 explosion.

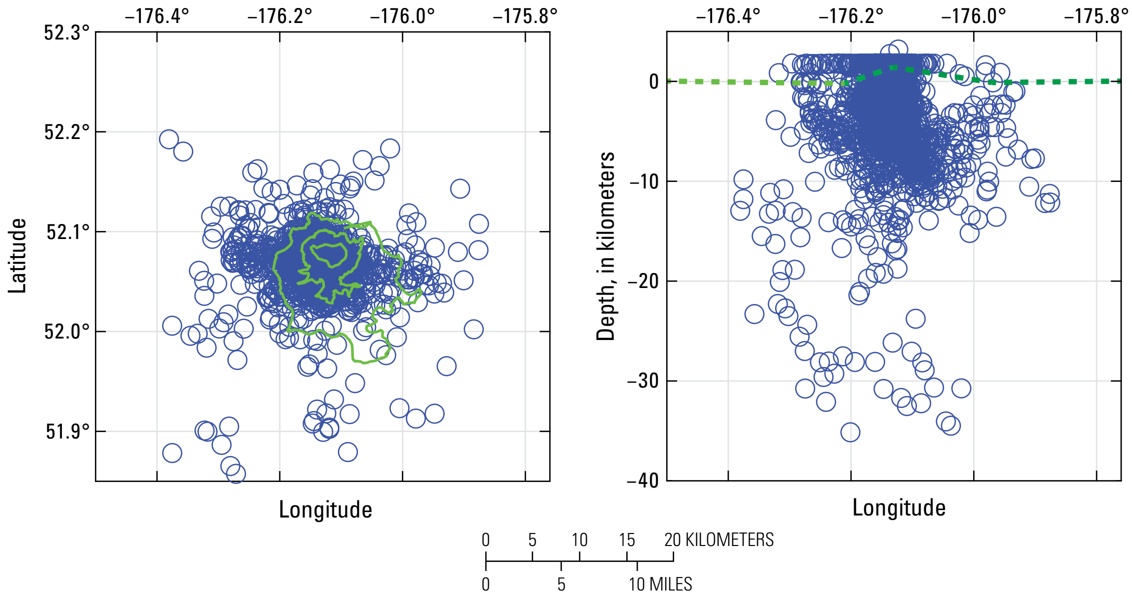


**Figure 26.** Map (*A*) and east-west cross section (*B*) showing earthquakes at Great Sitkin Volcano (in the central Aleutian Islands, Alaska) located by the Alaska Volcano Observatory in 2018. Solid lines represent 0-, 2000-, and 4000-foot topographic contours. The dashed line shows the approximate elevation profile of the island. Earthquake focal depths are calculated relative to sea level, with negative depths reflecting height above sea level.

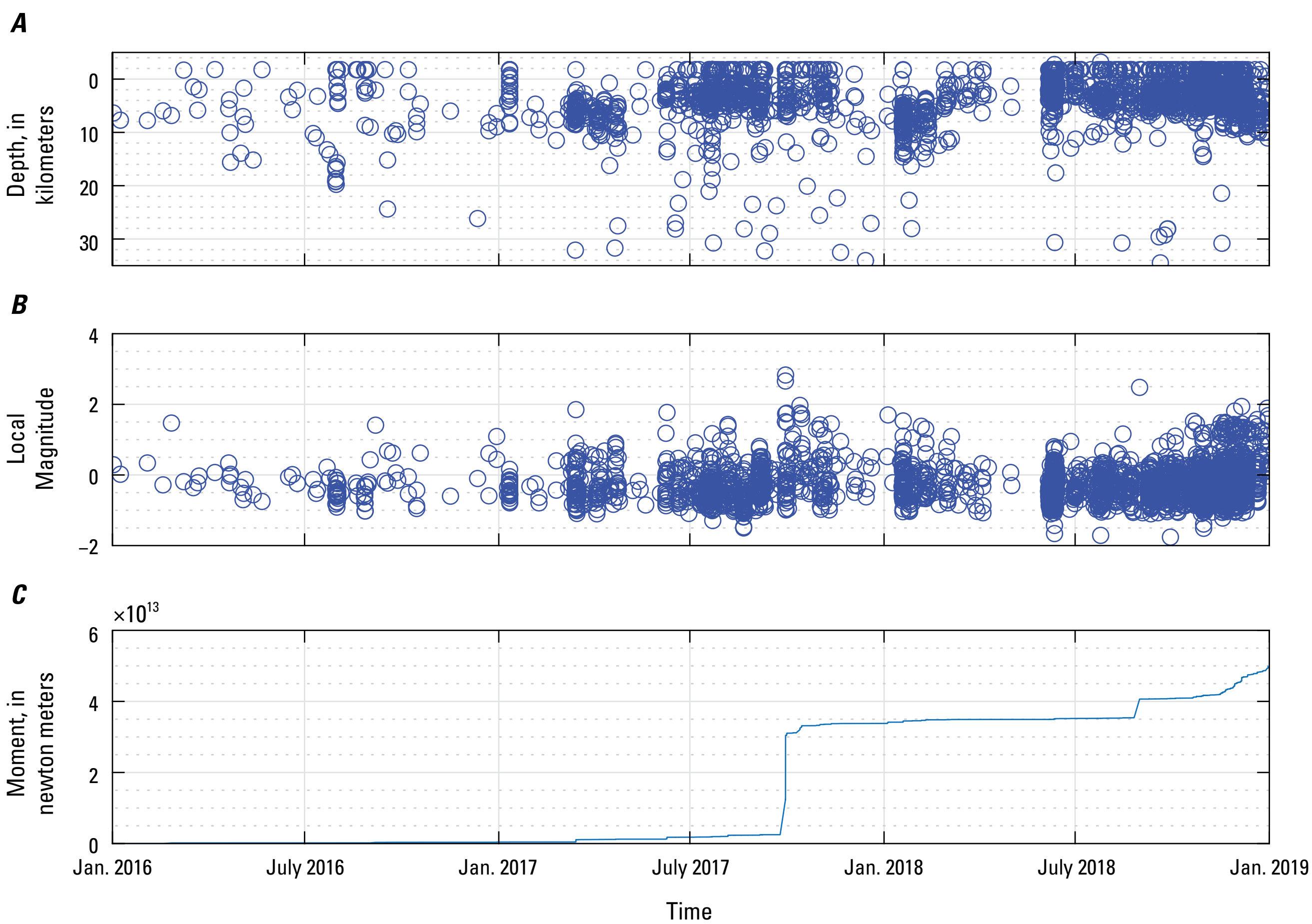


**Figure 27.** Graphs of depth (*A*), local magnitude (*B*), and cumulative seismic moment (*C*) of earthquakes at Great Sitkin Volcano (in the central Aleutian Islands, Alaska) from 2016 through 2018. Earthquake focal depths are calculated relative to sea level, with negative depths reflecting height above sea level. Jan., January.

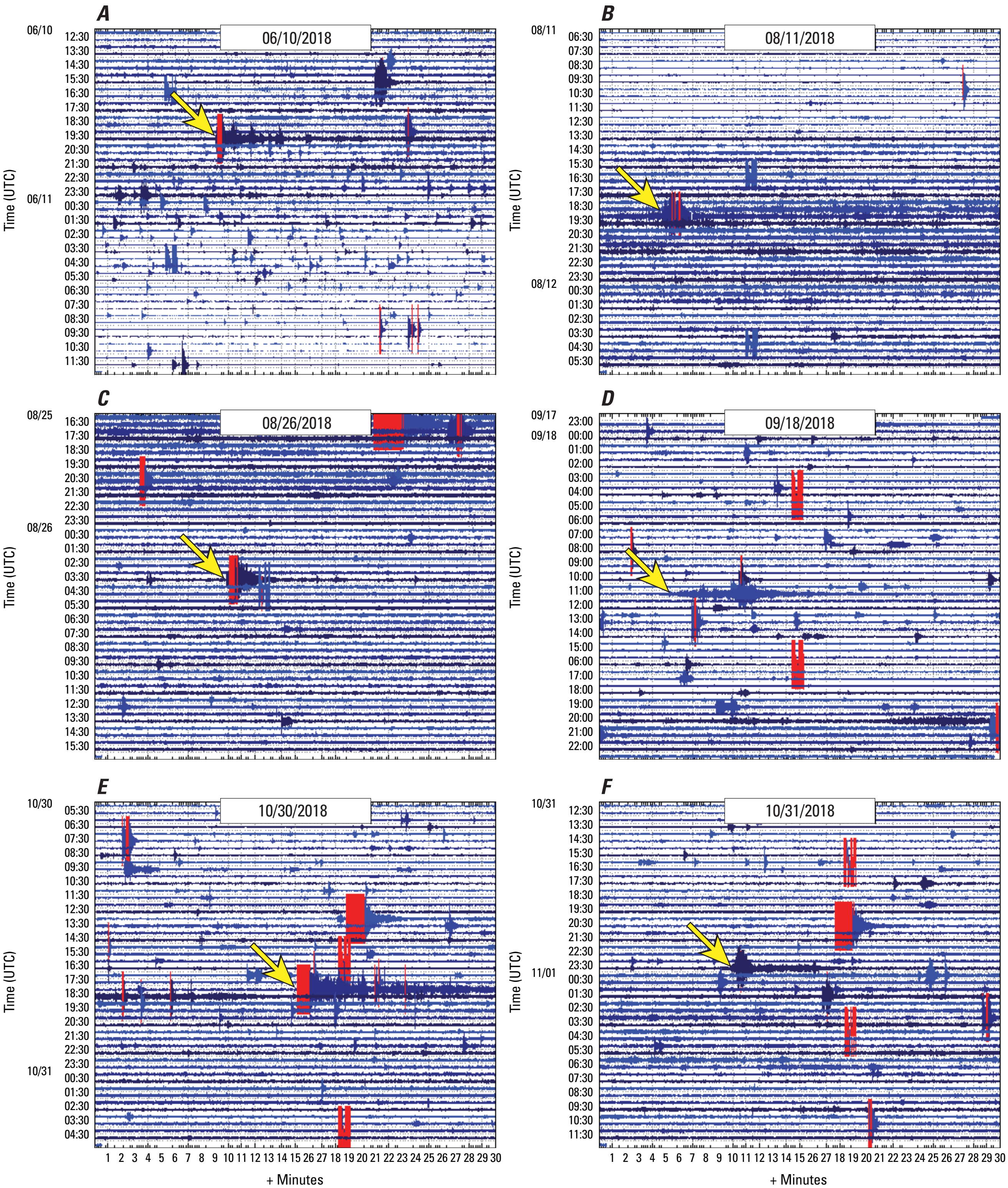


**Figure 28.** Twenty-four-hour helicorder-style seismograms of data from station GSSP, showing possible explosion signals from Great Sitkin Volcano (in the central Aleutian Islands, Alaska) in 2018. The plots show events taking place on June 10 (*A*), August 11 (*B*), August 26 (*C*), September 18 (*D*), October 30 (*E*), and October 31, 2018 (*F*). Red coloring indicates clipped signals. Arrows note the approximate onset time of each signal. Times provided in coordinated universal time (UTC). Dates shown as month/day/year and month/day (in 2018).

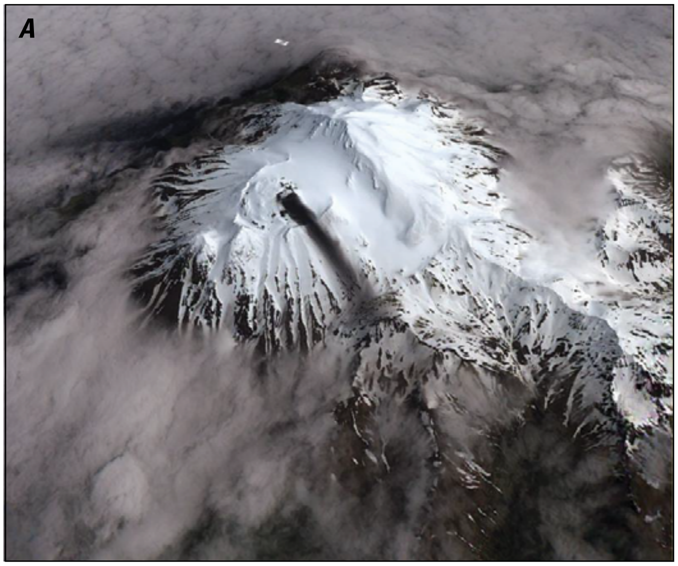


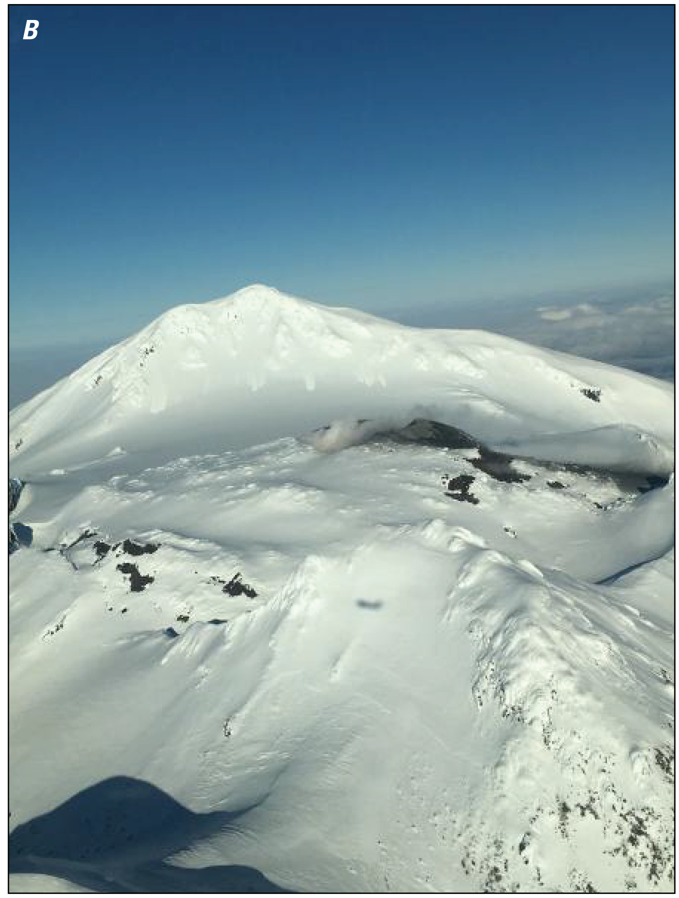


**Figure 29.** Photographs from June 2018 of Great Sitkin Volcano, located in the central Aleutian Islands, Alaska, showing evidence of volcanic activity. *A*, Satellite image of the volcano, acquired June 11, 2018, at 23:00 UTC, featuring an ash deposit extending about two kilometers southeast of the summit. The deposit is presumably associated with the seismic signal that began on June 10 at 19:38 UTC. Minor steaming from the Great Sitkin Volcano lava dome is also visible in the image. Image taken by Sentinel-2; view direction approximately to the east. *B*, Aerial photo from June 19, 2018, showing minor steaming from the summit lava dome and the new ash deposit extending from the summit vent. Photograph by Dave Clum; view direction approximately to the southeast.

To characterize the size and progression of the Great Sitkin Volcano explosions, AVO measured the durations of their signals using methodology described by Searcy and Power (2020) (fig. 30). Tremor events lasting less than 2 minutes were excluded, though several took place during the unrest. For many of the signals, some uncertainty remains on whether they reflect explosions, short volcanic tremor episodes, or more minor steam bursts. Except for the event on June 10, which produced an identifiable ash deposit, any of these events could have been produced by any of the previously listed mechanisms.

In response to the volcanic activity, AVO made four changes to Great Sitkin Volcano's Aviation Color Code and Volcano Alert Level during 2018. The volcano began the year at **YELLOW** and **ADVISORY**, but on January 18, after the number of earthquakes had fallen to background levels, AVO lowered the Aviation Color Code and Volcano Alert Level to **GREEN** and **NORMAL**. It raised them again to **YELLOW** and **ADVISORY** on June 10 in response to the explosion signal that took place that day. The Aviation Color Code and Volcano Alert Level were lowered back to **GREEN** and **NORMAL** on June 27 after declining earthquake activity, then raised to **YELLOW** and **ADVISORY** again on July 1 as earthquake activity increased. Great Sitkin Volcano remained at **YELLOW** and **ADVISORY** for the rest of 2018.

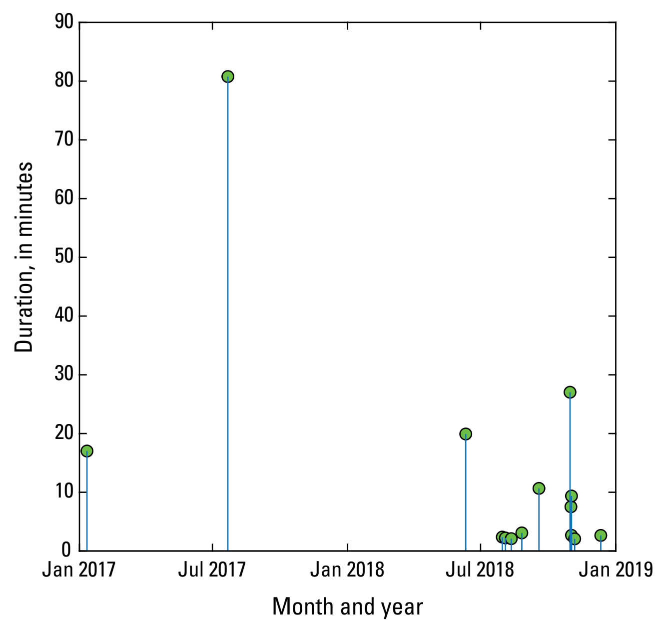


**Figure 30.** Graph of durations of seismic signals likely associated with explosions at Great Sitkin Volcano (central Aleutian Islands, Alaska) between January 2016 and January 2019.

Great Sitkin Volcano is a basaltic andesite volcano that composes most of the northern half of Great Sitkin Island, which is in the Andreanof Islands group of the central Aleutian Islands (Waythomas and others, 2003a, 2003b). The volcano consists of an older, partly collapsed volcano and a younger resurgent cone that has a summit crater 1.5 km across (Simons and Mathewson, 1955; Waythomas and others, 2003b). Great Sitkin Volcano erupted at least twice in the 20th century, prior to the ongoing activity described here. In 1974, a lava dome formed in the summit crater, accompanied by at least one ash cloud that reached an altitude as high as 10,000 ft (3,000 m) ASL (Associated Press, 1974). A poorly documented eruption in 1945 also produced a lava dome, which was then partly destroyed by the 1974 eruption. Additionally, at some point within the past 280 years, a large explosive eruption produced pyroclastic flows that partly filled a valley on the southwest flank of the volcano (Waythomas and others, 2003b).

## Mount Gareloi


*GVP #311070*
51.789° N., 178.794° W.
1,573 m

Gareloi Island, Andreanof Islands, Aleutian Islands

**INCREASED SEISMICITY, SMALL ASH EMISSION**

The typical seismicity of Mount Gareloi is characterized by many low-frequency earthquakes that are commonly too small to be located by its seismic network, which comprises six stations on Gareloi Island and nearby Kavalga Island. Although the frequency of located seismic events varied in the past, seismicity at Mount Gareloi was fairly constant in recent years: 265 earthquakes were located in 2016 and 269 were located in 2017. In the summer of 2018, however, AVO located an anomalously high number of earthquakes, with 190 located in June and 178 in July. AVO then located 80 earthquakes in August and 77 in September before the volcano returned to typical activity levels in the fall. This period of increased activity was dominated by low-frequency earthquakes at depths of 5–15 km, which is typical for seismicity at Mount Gareloi. AVO paid close attention to the elevated seismicity rates but kept the Aviation Color Code and Volcano Alert Level at **GREEN** and **NORMAL**.

In 2022, while retrospectively reviewing high-resolution satellite imagery of Mount Gareloi, AVO found a 2018 image showing an approximately 5-kilometer-long ash deposit extending north-northwest from the south fumarole field of the volcano (fig. 31). This image, taken by the WorldView-2 satellite on June 12, appears to record a previously unrecognized small ash emission (eruption). Satellite imagery acquired by Planet Labs PBC first shows the ash streak on June 6; the actual emission may have taken place on June 5.

Mount Gareloi, which makes up most of Gareloi Island, is a stratovolcano with a basal area of 10 by 8 km, featuring two summits separated by a narrow saddle (Miller and others, 1998). Both summits have been historically active (Coombs and others, 2012), and the south summit features several conspicuous, active fumaroles. An additional 13 craters, ranging from 80 to 1,600 m in diameter, occupy a south-southeast trending fissure that extends down from this south summit. The craters formed in 1929 during a major explosive eruption that also produced four blocky lava flows and a blanket of glassy andesitic tuff. The tuff now covers an area of roughly 2.5 by 5 km on the southeast flank of the volcano (Coats, 1959).

## Semisopochnoi Island (Mount Young)


*GVP #311060*
51.929° N., 179.598° W.
800 m

Semisopochnoi Island, Rat Islands, Aleutian Islands

**MINOR ERUPTION**

Activity at Semisopochnoi Island, in the Rat Islands, Alaska, began in September 2018 and continued through the fall. It was characterized by sporadic, weak eruptive activity from the north cone of Mount Young (fig. 32). Though seismic tremor and explosion signals captured most of this activity, AVO also made infrequent infrasound detections and satellite observations of steam emissions and small ash deposits. Retrospective analysis showed that activity continued through the end of the year, but real-time observations were limited by a prolonged data outage beginning November 1, 2018.

The first activity detected at Mount Young in 2018 included two minor seismic bursts on September 8 at 08:10 and 09:44 UTC (September 7 at 22:10 and 23:44 HADT) (table 5, fig. 33). This seismicity was preceded by weak tremor beginning on August 25, but AVO only recognized the tremor during retrospective analyses. Satellite imagery taken during the summer showed a seasonal lake within the crater of the north cone on Mount Young, but satellite imagery from September 4 showed the crater steaming, and satellite imagery from September 5 showed the lake to be three times larger than normal (fig. 34). On September 10, ash deposits extending about 1 km west of the north cone were visible in satellite imagery (fig. 32), and within the crater, AVO noted a new tephra cone about 75 m in diameter.

Seismicity increased on September 16; strong tremor beginning at 16:31 UTC (07:31 HADT) caused AVO to raise the Aviation Color Code and Volcano Alert Level from **GREEN** and **NORMAL** to **YELLOW** and **ADVISORY**. The lake in the crater dried up around the same time, and on September 15 and 17, AVO observed fumaroles and steam in satellite imagery (fig. 34). On September 17, an increase in seismicity and tremor strength, in addition to the recognition of the ash deposit in the September 10 satellite image, led AVO to increase the Aviation Color Code and Volcano Alert Level again to **ORANGE** and **WATCH**.

From September 16 to 29, seismicity alternated between continuous tremor and tremor bursts. At the same time,

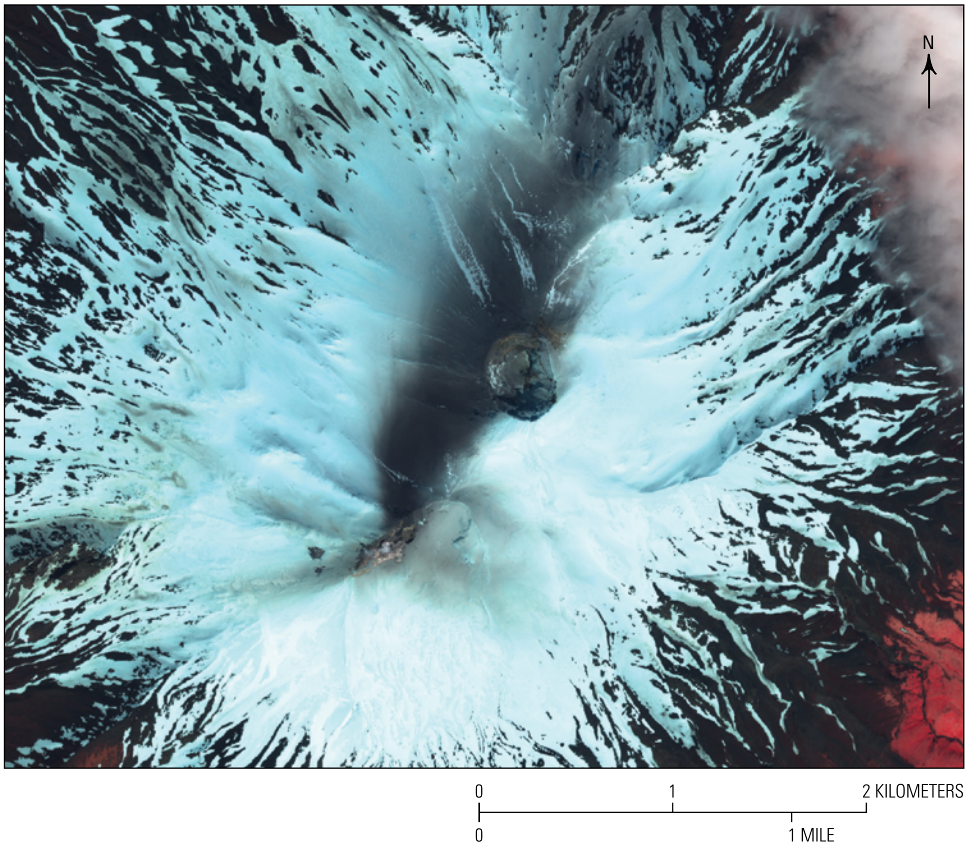


**Figure 31.** Near-infrared satellite image from June 12, 2022, showing an ash deposit extending approximately 5 kilometers north-northeast from a summit vent at Mount Gareloi, central Aleutian Islands, Alaska. Image taken by the Worldview-2 satellite.

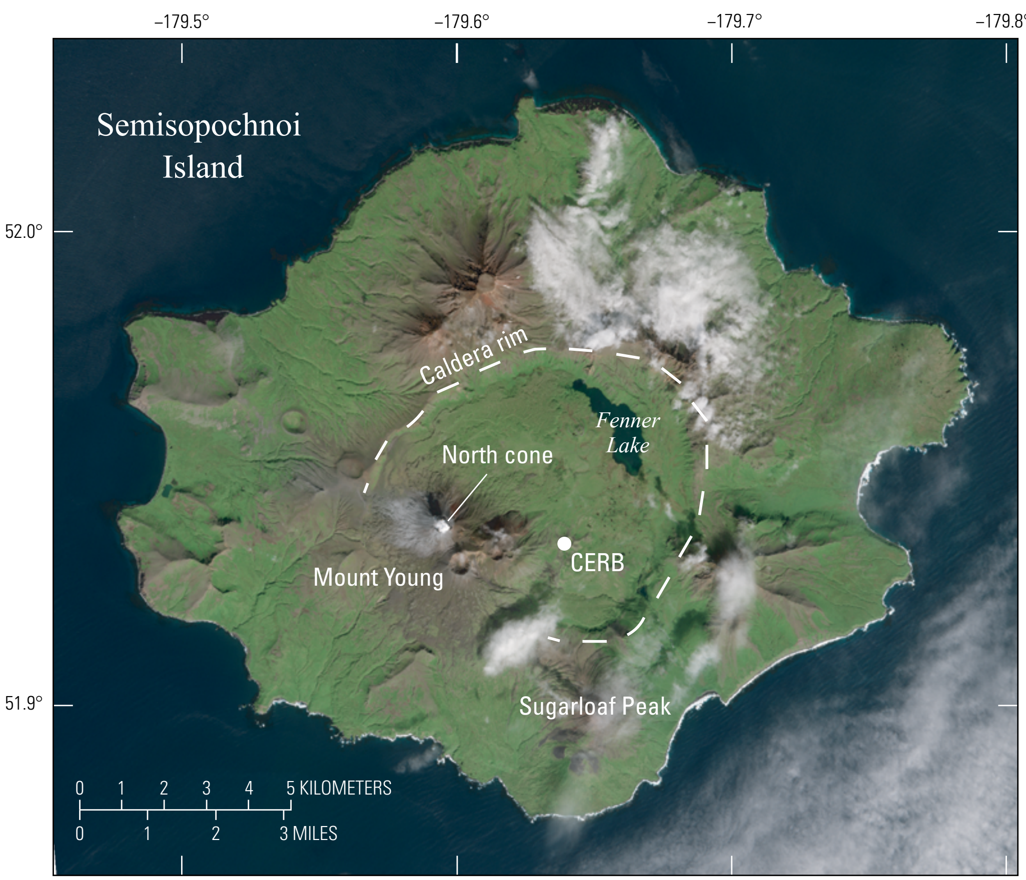


**Figure 32.** Satellite image of Semisopochnoi Island in the Rat Islands, Alaska, on September 10, 2018, showing active and recently active volcanic features. The north cone of Mount Young is steaming in this image, with a light dusting of gray ash visible on the west flank of the cone. Image taken by Sentinel-2.

**Table 5.** Summary of activity and observations at Mount Young during 2018.

[Dates shown as month/day/year. UTC, coordinated universal time; ASL, above sea level]

| Aviation Color Code/ Volcano Alert Level | Date (UTC) | Observation description |
|---|---|---|
| GREEN/NORMAL | 08/25/2018 | Weak tremor began |
| GREEN/NORMAL | 09/04/2018 | Steaming in crater |
| GREEN/NORMAL | 09/05/2018 | Crater lake three times normal size by this date; steam observed |
| GREEN/NORMAL | 09/10/2018 | Steaming in crater; new tephra cone and tephra deposit observed |
| GREEN/NORMAL | 09/15/2018 | Steam plume |
| GREEN/NORMAL | 09/16/2018 | Tremor and increasing seismicity |
| YELLOW/ADVISORY | 09/16/2018 | Increased seismicity; stronger tremor; steam plume; lake dried up; Aviation Color Code and Volcano Alert Level changed |
| ORANGE/WATCH | 09/17/2018 | Aviation Color Code and Volcano Alert Level changed |
| ORANGE/WATCH | 09/19/2018 | Weakly elevated surface temperatures |
| ORANGE/WATCH | 09/20/2018 | Steam plume |
| ORANGE/WATCH | 09/21/2018 | First infrasound detection |
| ORANGE/WATCH | 09/22/2018 | Possible tephra deposit seen in satellite |
| ORANGE/WATCH | 09/25/2018 | Steam plume and tephra deposits |
| ORANGE/WATCH | 09/27/2018 | Pit formed in crater; tephra deposits visible in satellite |
| ORANGE/WATCH | 09/29/2018 | Tephra cone grows within crater through October 1 |
| ORANGE/WATCH | 10/06/2018 | $SO_2$ detected |
| ORANGE/WATCH | 10/11/2018 | Crater lake returned |
| YELLOW/ADVISORY | 10/12/2018 | Aviation Color Code and Volcano Alert Level changed |
| YELLOW/ADVISORY | 10/26/2018 | Eruption with strong tremor and ash plume to 12,000 feet (3,700 meters) ASL |
| ORANGE/WATCH | 10/26/2018 | Aviation Color Code and Volcano Alert Level changed |
| ORANGE/WATCH | 10/30/2018 | $SO_2$ detected |
| ORANGE/WATCH | 11/01/2018 | Real-time seismic data lost |
| ORANGE/WATCH | 11/11/2018 | End of strong tremor (identified retrospectively) |
| YELLOW/ADVISORY | 11/21/2018 | Aviation Color Code and Volcano Alert Level changed |
| YELLOW/ADVISORY | 12/01/2018 | Steaming in crater |
| YELLOW/ADVISORY | 12/05/2018 | Crater lake refilled |
| YELLOW/ADVISORY | 12/10/2018 | Steaming in crater |
| YELLOW/ADVISORY | 12/19/2018 | Steaming in crater |
| UNASSIGNED | 12/19/2018 | Aviation Color Code and Volcano Alert Level changed |

atmospheric propagation conditions improved between Semisopochnoi Island and the infrasound array on Adak Island (a 13-minute delay), leading to the first infrasound explosion detection on September 21 (fig. 33). Satellite imagery indicated weakly elevated surface temperatures on September 19 and the presence of steam on September 20. Tephra deposits were seen east and southeast of the north cone of Mount Young in satellite imagery the following week (fig. 34). A small pit formed in the cone's crater by September 27, and between September 29 and October 1, a new tephra cone grew around the pit and thick tephra deposits accumulated on the adjacent crater floor.

Weak tremor was reported on October 2–4, 8, and 10, and a small $SO_2$ plume was detected in OMPS satellite data on October 6, but no infrasound was detected in early October (fig. 33). AVO saw no evidence of eruptive activity in satellite images during this period and the crater lake returned by October 11. This lull in activity led AVO to lower the Aviation Color Code and Volcano Alert Level to **YELLOW** and **ADVISORY** on October 12.

Strong seismic tremor began again on October 26 at 04:47 UTC (October 25 at 19:47 HADT), accompanied by a small ash plume reaching an altitude of 12,000 ft (3,700 m) ASL (fig. 35) and infrasonic tremor detections at the array on Adak Island. This activity triggered an increase in the Aviation Color Code and Volcano Alert Level again to **ORANGE** and **WATCH**. Small explosions, accompanied by ground-coupled

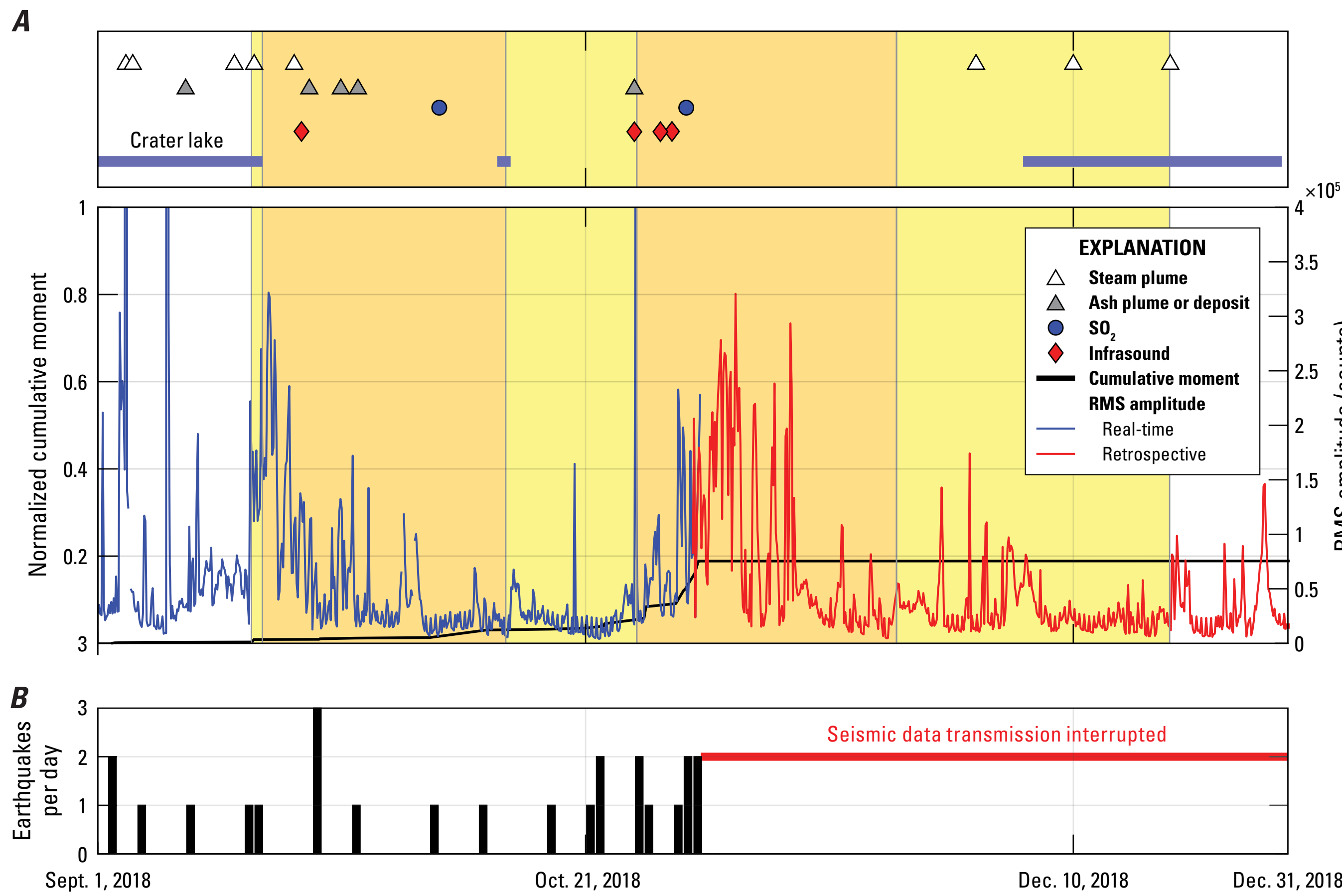


**Figure 33.** Chronology of volcanic activity from September through December 2018 at Mount Young. *A*, Time series graph of normalized cumulative moment of earthquakes and root mean squared (RMS) seismic amplitude from station CERB. An instrument failure on November 1 prevented the Alaska Volcano Observatory from processing seismic data in real time during November and December, so these data were processed retrospectively in 2019. Lines above the graph indicate periods when a crater lake was observed in the north cone of Mount Young; symbols at the top of the graph indicate detections of steam plumes, ash, sulfur dioxide ($SO_2$), and infrasound. *B*, Time series graph of the number of earthquakes recorded daily prior to the data outage on November 1. Sept., September; Oct., October; Dec., December.

airwaves and some infrasound detections, continued until November 1. Clouds obscured all satellite views during this time, but a possible $SO_2$ signal was detected in OMPS satellite data on October 30.

Unfortunately, the satellite connection to the real-time seismic data receive facility (on Amchitka Island) failed on November 1 and was not recovered until June 2019. During the outage, AVO observed no changes in satellite imagery and detected no explosions from the nearby Adak Island infrasound array. Owing to a lack of evidence of ongoing eruptive activity, AVO lowered the Aviation Color Code and Volcano Alert Level to **YELLOW** and **ADVISORY** on November 21. With continued apparent quiescence, AVO changed the Aviation Color Code and Volcano Alert Level to **UNASSIGNED** on December 19. After the missing seismic data were recovered in 2019, a retrospective analysis (fig. 33) found that strong tremor and likely eruptive activity continued through at least November 11, 2018. Satellite imagery showed steam in the crater on December 1, 10, and 19, 2018.

Although the unrest in 2014–2015 was associated with considerable deformation, InSAR measurements have shown little to no deformation since then (fig. 36), and even the 2018 activity lacked associated surface displacement. In a preliminary analysis of Sentinel-1 interferograms, a small signal occasionally appeared on the west flank of Mount Young's north cone (fig. 37), but this signal could simply reflect surface deformation,

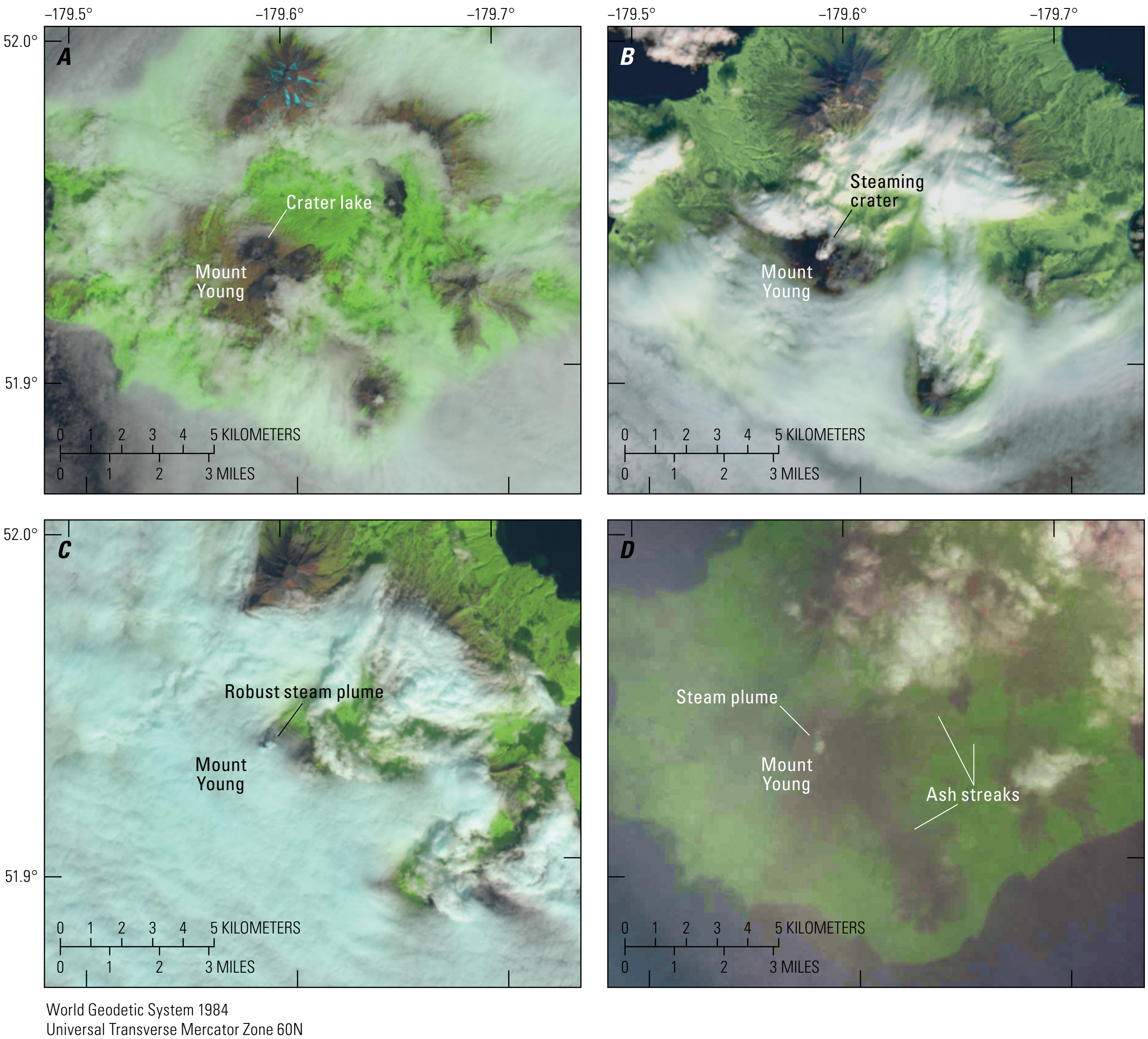


**Figure 34.** "Natural Color" multispectral satellite images of Semisopochnoi Island, in the Rat Islands, Alaska. *A*, Sentinel-2 image from July 27, 2018, showing a small lake within the crater of the north cone of Mount Young. *B*, Landsat-8 image from September 4, 2018, showing steaming from the crater. *C*, Sentinel-2 image from September 15, 2018, showing a small but robust steam plume from the crater. *D*, Sentinel-2 image from September 25, 2018, showing a steam plume from the crater and small, dark ash streaks extending as far as 6 kilometers to the east and southeast.

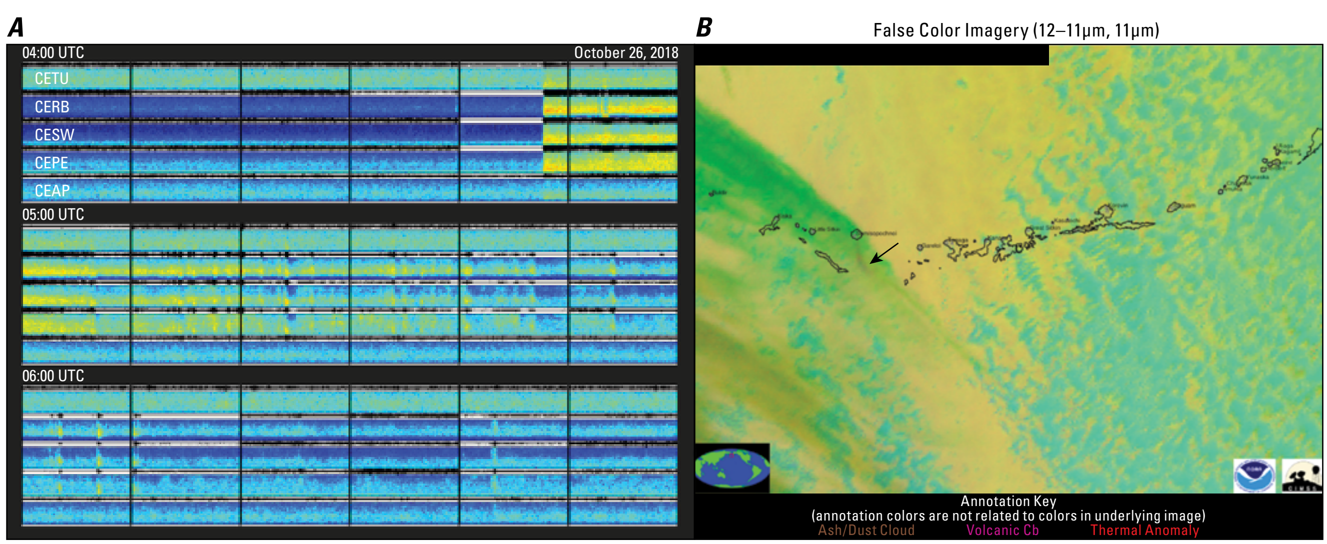

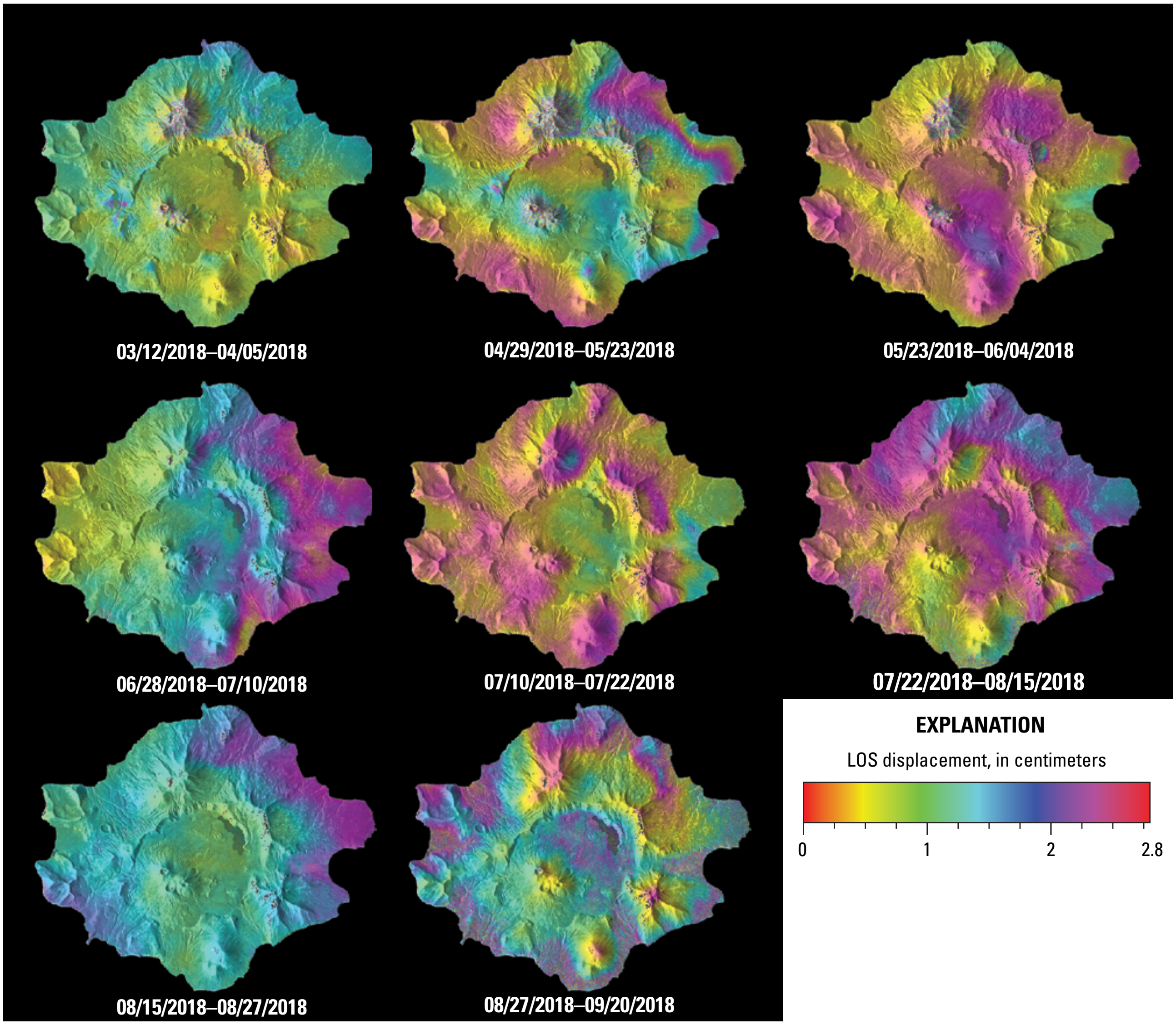


**Figure 36.** Satellite interferograms of Semisopochnoi Island, in the Rat Islands, Alaska, over eight separate periods from mid-March to late September 2018. The interferograms indicate the island had little to no deformation for most of the year. Topographic corrections for atmosphere have been applied but artifacts of turbulent atmospheric noise are occasionally present, particularly on the east flanks of elevated features. Imagery acquired by Sentinel-1 on path 81 (descending). Line-of-sight (LOS) displacement shown in centimeters (cm). Dates shown as month/day/year.

**Figure 35.** Seismic data spectrograms from, and satellite imagery of, Semisopochnoi Island in the Rat Islands, Alaska, during the eruption on October 26, 2018. *A*, Seismic spectrograms from 04:00 to 06:00 coordinated universal time (UTC), showing that the eruption started at 04:47 UTC. Spectrograms are taken from five stations: CETU, CERB, CESW, CEPE, and CEAP. *B*, False color composite satellite image of the eastern Aleutian Islands showing an ash cloud trailing from Semisopochnoi Island. Image taken at 06:20 UTC by the Advanced Himawari Imager (AHI) on Himawari-8. False color bands comprise 12–11 micrometers (µm), 8–8.5 µm, and 11 µm.

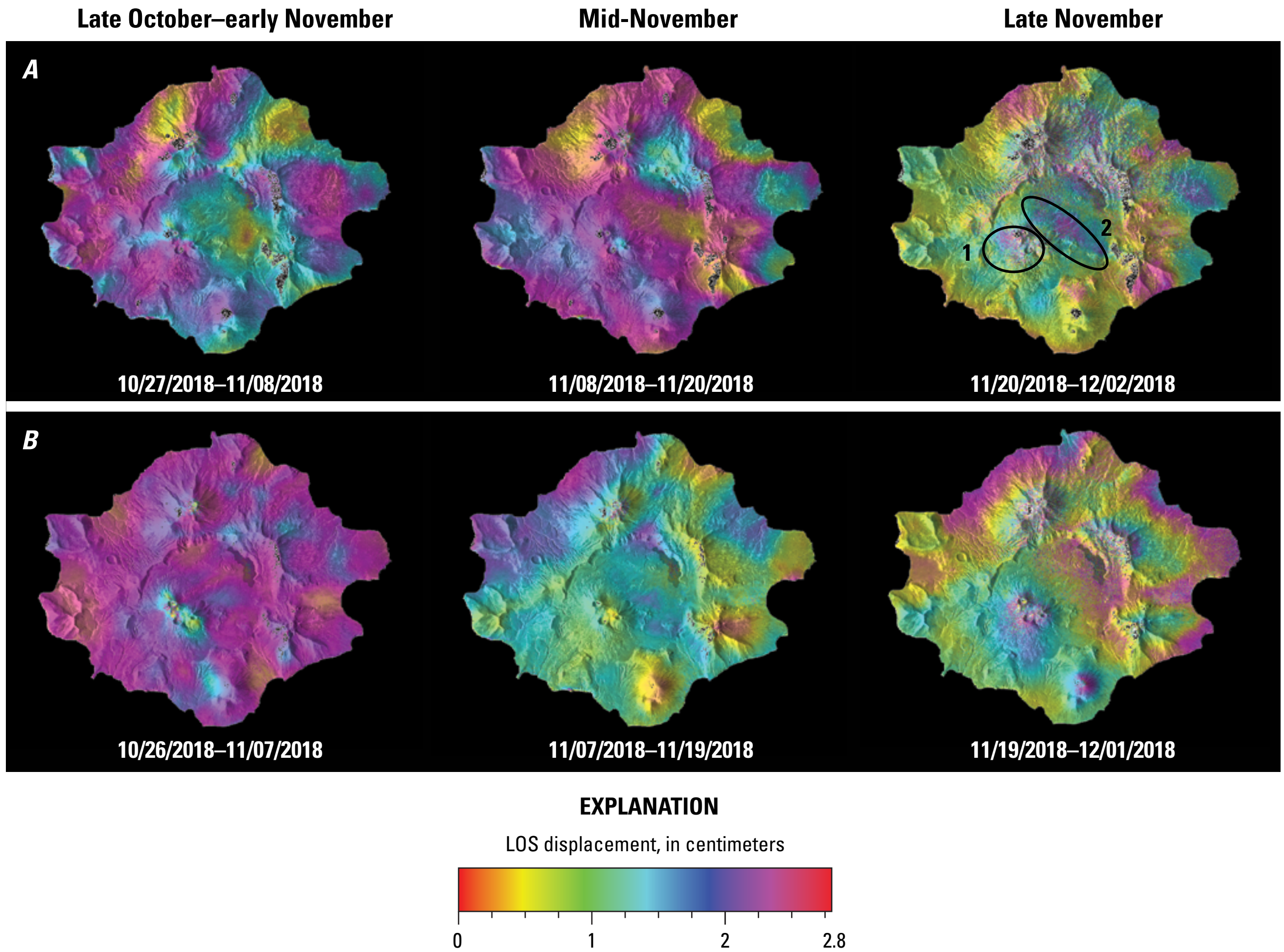


**Figure 37.** Satellite interferograms of Semisopochnoi Island, in the Rat Islands, Alaska, taken from two paths during the height of the fall 2018 eruptive activity. *A*, Images from path 8, an ascending track. The path 8 interferogram spanning late October–early November shows short-term variation in atmospheric turbulence. A small deformation signal, occasionally visible on the southwest flank of Mount Young's north cone, is highlighted by circle 1 in the late November interferogram. This signal is suspected to be related to recent eruptive events and is potentially linked to a deeper source (circle 2) located near the modeled source of the 2014–2015 deformation (DeGrandpre and others, 2019). *B*, Images from path 81, a descending track. Like the corresponding interferogram from path 8, the path 81 interferogram spanning late October–early November also shows short-term atmospheric turbulence variation. Imagery acquired by Sentinel-1. Line-of-sight (LOS) displacement shown in centimeters (cm). Dates shown as month/day/year.

atmospheric noise, or a change in spectral properties due to freshly deposited ash. A more spatially extensive signal might exist in the center of the caldera near the modeled deformation source of the 2014–2015 inflationary episodes (fig. 37) (DeGrandpre and others, 2019). This signal could represent deformation from a deeper source, but the magnitude of surface displacement is so small (less than 1 millimeter) that the mechanisms producing the signal would be more likely related to processes like gas exsolution or crystallization rather than magma volume flux. Additional analysis is required to eliminate atmospheric noise as a possible source of the apparent displacement.

Semisopochnoi Island is a young, uninhabited volcanic island in the west Aleutian Islands. Though its largest feature is a caldera 7 kilometers in diameter that formed 6,900–5,000 years ago, it also has many post-caldera cones (fig. 32) (Coombs and others, 2018). The last recorded eruption before 2018 took place in 1987 from Sugarloaf Peak on the south end of the island. This event produced a 90-kilometer-long plume that was visible in satellite images and that deposited ash on the flanks of the volcano; these ash deposits were later observed by pilots (Reeder, 1990). Mount Young, a cluster of three cones within the larger caldera, has also erupted repeatedly in the Holocene, producing crystal-rich basaltic andesite lava and tephra from all three cones. Most fall deposits associated with the cones are consistent with small- to moderate-sized ash clouds, but some lapilli-size units suggest eruption intensities with a Volcanic Explosivity Index as high as 3 (Coombs and others, 2018). The most recent unrest at Semisopochnoi Island prior to 2018 was a pair of seismicity and deformation episodes in 2014–2015. These episodes have been modeled as the result of two rapid magma intrusions, which inserted 0.072 $km^3$ of magma into a spheroidal storage zone about 8 km beneath the caldera (DeGrandpre and others, 2019).

## References Cited


Allstadt, K., and Malone, S.D., 2014, Swarms of repeating stick-slip icequakes triggered by snow loading at Mount Rainier volcano: Journal of Geophysical Research, Earth Surface, v. 119, no. 5, p. 1180–1203, https://doi.org/10.1002/2014JF003086.

Associated Press, 1974, Sitkin Island volcano puts on bright show: Fairbanks Daily News-Miner, February 21, 1974, p. 1.

Bacon, C.R., Sisson, T.W., Calvert, A.T., and Nye, C.J., 2009, Geologic map of the 350 km3 basalt-to-dacite Veniaminof Volcano, Aleutian Arc [abs.]: Geological Society of America Abstracts with Programs, v. 41, no. 7, p. 660–661, accessed October 24, 2022, at https://gsa.confex.com/gsa/2009AM/webprogram/Paper164030.html.

Begét, J.E., Larsen, J.F., Neal, C.A., Nye, C.J., and Schaefer, J.R., 2005, Preliminary volcano-hazard assessment for Okmok Volcano, Umnak Island, Alaska: Alaska Division of Geological & Geophysical Surveys Report of Investigations 2004-3, 1 sheet, scale 1:150,000, 32-p. pamphlet, https://doi.org/10.14509/7042.

Begét, J.E., Nye, C.J., and Bean, K.W., 2000, Preliminary volcano-hazard assessment for Makushin Volcano, Alaska: Alaska Division of Geological & Geophysical Surveys Report of Investigations 2000-4, 1 sheet, scale 1:100,000, 22-p. pamphlet, https://doi.org/10.14509/2679.

Byers, F.M., Jr., 1959, Geology of Umnak and Bogoslof Islands, Aleutian Islands, Alaska, *in* Investigations of Alaskan volcanoes: U.S. Geological Survey Bulletin 1028-L, p. 267–369, https://doi.org/10.3133/b1028L.

Calvert, A.T., Moore, R.B., and McGimsey, R.G., 2005, Argon geochronology of Late Pleistocene to Holocene Westdahl Volcano, Unimak Island, Alaska, *in* Haeussler, P.J., and Galloway, J.P., eds., Studies by the U.S. Geological Survey in Alaska, 2004: U.S. Geological Survey Professional Paper 1709-D, 16 p., https://doi.org/10.3133/pp1709D.

Cameron, C.E., Dixon, J.P., Neal, C.A., Waythomas, C.F., Schaefer, J.R., and McGimsey, R.G., 2017, 2014 Volcanic activity in Alaska—Summary of events and response of the Alaska Volcano Observatory: U.S. Geological Survey Scientific Investigations Report 2017–5077, 81 p., https://doi.org/10.3133/sir20175077.

Cameron, C.E., Schaefer, J.R., and Mulliken, K.M., 2018, Historically active volcanoes of Alaska: Alaska Division of Geological & Geophysical Surveys Miscellaneous Publication 133, v. 3, 2 sheets, https://doi.org/10.14509/30142.

Cameron, C.E., Dixon, J.P., Waythomas, C.F., Iezzi, A.M., Wallace, K.L., McGimsey, R.G., and Bull, K.F., 2020, 2016 Volcanic activity in Alaska—Summary of events and response of the Alaska Volcano Observatory: U.S. Geological Survey Scientific Investigations Report 2020–5125, 63 p., https://doi.org/10.3133/sir20205125.

Cameron, C.E., Crass, S.W., and AVO Staff, eds., 2022, Geologic Database of Information on Volcanoes in Alaska (GeoDIVA): Alaska Division of Geological & Geophysical Surveys Digital Data Series 20, https://doi.org/10.14509/30901.

Coats, R.R., 1959, Geologic reconnaissance of Gareloi Island, Aleutian Islands, Alaska, *in* Investigations of Alaskan volcanoes: U.S. Geological Survey Bulletin 1928-J, p. 249–256, 1 sheet, https://doi.org/10.3133/b1028J.

Coombs, M.L., and Jicha, B.R., 2021, The eruptive history, magmatic evolution, and influence of glacial ice at long-lived Akutan volcano, eastern Aleutian Islands, Alaska, USA: Geological Society of America Bulletin, v. 133, no. 5–6, p. 963–991, https://doi.org/10.1130/B35667.1.

Coombs, M.L., Larsen, J.F., and Neal, C.A., 2018, Postglacial eruptive history and geochemistry of Semisopochnoi volcano, western Aleutian Islands, Alaska: U.S. Geological Survey Scientific Investigations Report 2017–5150, 33 p., https://doi.org/10.3133/sir20175150.

Coombs, M.L., McGimsey, R.G., and Browne, B.L., 2012, Geologic map of Mount Gareloi, Gareloi Island, Alaska: U.S. Geological Survey Scientific Investigations Map 3145, 1 sheet, scale 1:24,000, 18-p. pamphlet, https://doi.org/10.3133/sim3145.

Dean, K.G., Dehn, J., Engle, K., Izbekov, P., and Papp, K., 2002, Operational satellite monitoring of volcanoes at the Alaska Volcano Observatory, *in* Harris, A.J.H., Wooster, M., and Rothery, D.A., eds., Monitoring volcanic hotspots using thermal remote sensing: Advances in Environmental Monitoring and Modelling, v. 1, no. 3, p. 70–97.

Dean, K.G., Dehn, J., Papp, K.R., Smith, S., Izbekov, P., Peterson, R., Kearney, C., and Steffke, A., 2004, Integrated satellite observations of the 2001 eruption of Mt. Cleveland, Alaska: Journal of Volcanology and Geothermal Research, v. 135, no. 1-2, p. 51–73, https://doi.org/10.1016/j.jvolgeores.2003.12.013.

DeGrandpre, K.G., Pesicek, J.D., Lu, Z., DeShon, H.R., and Roman, D.C., 2019, High rates of inflation during a noneruptive episode of seismic unrest at Semisopochnoi Volcano, Alaska in 2014–2015: Geochemistry, Geophysics, Geosystems, v. 20, no. 12, 24 p., https://doi.org/10.1029/2019GC008720.

DeGrandpre, K., Wang, T., Lu, Z., and Freymueller, J.T., 2017, Episodic inflation and complex surface deformation of Akutan volcano, Alaska revealed from GPS time-series: Journal of Volcanology and Geothermal Research, v. 347, p. 337–359, https://doi.org/10.1016/j.jvolgeores.2017.10.003.

Dixon, J.P., Cameron, C.E., Iezzi, A.M., Power, J.A., Wallace, K., and Waythomas, C.F., 2020, 2017 Volcanic activity in Alaska—Summary of events and response of the Alaska Volcano Observatory: U.S. Geological Survey Scientific Investigations Report 2020–5102, 61 p., https://doi.org/10.3133/sir20205102.

Dixon, J.P., Cameron, C., McGimsey, R.G., Neal, C.A., and Waythomas, C., 2015, 2013 Volcanic activity in Alaska—Summary of events and response of the Alaska Volcano Observatory: U.S. Geological Survey Scientific Investigations Report 2015–5110, 92 p., https://doi.org/10.3133/sir20155110.

Dixon, J.P., Stihler, S.D., Haney, M.M., Lyons, J.J., Ketner, D.M., Mulliken, K.M., Parker, T., and Power, J.A., 2019, Catalog of earthquake parameters and description of seismographic and acoustic stations at Alaskan volcanoes—January 1, 2013, through December 31, 2017: U.S. Geological Survey Data Series 1115, 92 p., https://doi.org/10.3133/ds1115.

Fee, D., Haney, M.M., Matoza, R.S., Van Eaton, A.R., Cervelli, P., Schneider, D.J., and Iezzi, A.M., 2017, Volcanic tremor and plume height hysteresis from Pavlof Volcano, Alaska: Science, v. 355, no. 6320, p. 45–48, https://doi.org/10.1126/science.aah6108.

Fee, D., Steffke, A., and Garces, M., 2010, Characterization of the 2008 Kasatochi and Okmok eruptions using remote infrasound arrays: Journal of Geophysical Research, Atmospheres, v. 115, no. D2, article D00L10, 15 p., https://doi.org/10.1029/2009JD013621.

Freymueller, J.T., and Kaufman, A.M., 2010, Changes in the magma system during the 2008 eruption of Okmok volcano, Alaska, based on GPS measurements: Journal of Geophysical Research, Solid Earth, v. 115, no. B12, article B12415, 14 p., https://doi.org/10.1029/2010JB007716.

Gardner, C.A., and Guffanti, M.C., 2006, U.S. Geological Survey's alert notification system for volcanic activity: U.S. Geological Survey Fact Sheet 2006–3139, 4 p., https://doi.org/10.3133/fs20063139.

Hadley, D., Hufford, G.L., and Simpson, J.J., 2004, Resuspension of relic volcanic ash and dust from Katmai—Still an aviation hazard: Weather and Forecasting, v. 19, no. 5, p. 829–840, https://doi.org/10.1175/1520-0434(2004)019<0829:RORVAA>2.0.CO;2.

Hildreth, W., and Fierstein, J., 2012, The Novarupta-Katmai eruption of 1912—Largest eruption of the twentieth century—Centennial perspectives: U.S. Geological Survey Professional Paper 1791, 259 p., https://doi.org/10.3133/pp1791.

Keith, T.E.C., ed., 1995, The 1992 eruptions of Crater Peak Vent, Mount Spurr volcano, Alaska: U.S. Geological Survey Bulletin 2139, 220 p., https://doi.org/10.3133/b2139.

Larsen, J.F., Neal, C., Schaefer, J., Beget, J., and Nye, C., 2007, Late Pleistocene and Holocene caldera-forming eruptions of Okmok Caldera, Aleutian Islands, Alaska, *in* Eichelberger, J., Gordeev, E., Izbekov, P., Kasahara, M., and Lees, J., eds., Volcanism and subduction—The Kamchatka region: American Geophysical Union, Geophysical Monograph Series, v. 172, p. 343–364, https://doi.org/10.1029/172GM24.

Lee, C.-W., Lu, Z., Jung, H., Won, J.-S., and Dzurisin, D., 2010, Surface deformation of Augustine Volcano, 1992–2005, from multiple-interferogram processing using a refined Small Baseline Subset (SBAS) Interferometric Synthetic Aperture Radar (InSAR) approach, chap. 18 *of* Power, J.A., Coombs, M.L., and Freymueller, J.T., eds., The 2006 eruption of Augustine Volcano, Alaska: U.S. Geological Survey Professional Paper 1769, p. 453–465, https://doi.org/10.3133/pp176918.

Loewen, M.W., Dietterich, H.R., Graham, N., and Izbekov, P., 2021, Evolution in eruptive style of the 2018 eruption of Veniaminof volcano, Alaska, reflected in groundmass textures and remote sensing: Bulletin of Volcanology, v. 83, no. 11, article 72, 19 p., https://doi.org/10.1007/s00445-021-01489-6.

Lopez, T., Carn, S., Werner, C., Fee, D., Kelly, P., Doukas, M., Pfeffer, M., Webley, P., Cahill, C., and Schneider, D., 2013, Evaluation of Redoubt Volcano's sulfur dioxide emissions by the Ozone Monitoring Instrument: Journal of Volcanology and Geothermal Research, v. 259, p. 290–307, https://doi.org/10.1016/j.jvolgeores.2012.03.002.

Lu, Z., and Dzurisin, D., 2014, InSAR imaging of Aleutian volcanoes: Chichester, United Kingdom, Springer-Praxis, 390 p., https://doi.org/10.1007/978-3-642-00348-6.

Lu, Z., Wicks, C.J., Jr., Dzurisin, D., Power, J.A., Thatcher, W.R., and Masterlark, T., 2003, Interferometric synthetic aperture radar studies of Alaska volcanoes: Earth Observation Magazine, v. 12, no. 3, p. 8–10.

Lu, Z., Wicks, C., Jr., Power, J.A., and Dzurisin, D., 2000, Ground deformation associated with the March 1996 earthquake swarm at Akutan volcano, Alaska, revealed by satellite radar interferometry: Journal of Geophysical Research, v. 105, no. B9, p. 21,483–21,496, https://doi.org/10.1029/2000JB900200.

McConnell, V.S., Beget, J.E., Roach, A.L., Bean, K.W., and Nye, C.J., 1998, Geologic map of the Makushin volcanic field, Unalaska Island, Alaska: Alaska Division of Geological & Geophysical Surveys Report of Investigations 97-20, 2 sheets, scale 1:63,360, https://doi.org/10.14509/2576.

McGimsey, R.G., Neal, C.A., and Doukas, M.P., 1995, Volcanic activity in Alaska—Summary of events and response of the Alaska Volcano Observatory, 1992: U.S. Geological Survey Open-File Report 95–83, 26 p., https://doi.org/10.3133/ofr9583.

McGimsey, R.G., and Neal, C.A., 1996, 1995 Volcanic activity in Alaska and Kamchatka—Summary of events and response of the Alaska Volcano Observatory: U.S. Geological Survey Open-File Report 96–738, 23 p., https://doi.org/10.3133/ofr96738.

Miller, T.P., McGimsey, R.G., Richter, D.H., Riehle, J.R., Nye, C.J., Yount, M.E., and Dumoulin, J.A., 1998, Catalog of the historically active volcanoes of Alaska: U.S. Geological Survey Open-File Report 98–582, 104 p., https://doi.org/10.3133/ofr98582.

Miller, T.P., and Smith, R.L., 1987, Late Quaternary caldera-forming eruptions in the eastern Aleutian arc, Alaska: Geology, v. 15, no. 5, p. 434–438, https://doi.org/10.1130/0091-7613(1987)15<434:LQCEIT>2.0.CO;2.

Neal, C.A., Herrick, J., Girina, O.A., Chibisova, M., Rybin, A., McGimsey, R.G., and Dixon, J., 2014, 2010 Volcanic activity in Alaska, Kamchatka, and the Kurile Islands—Summary of events and response of the Alaska Volcano Observatory: U.S. Geological Survey Scientific Investigations Report 2014–5034, 76 p., https://doi.org/10.3133/sir20145034.

Neal, C.A., McGimsey, R.G., Dixon, J.P., Cameron, C.E., Nuzhdaev, A.A., and Chibisova, Marina, 2011, 2008 Volcanic activity in Alaska, Kamchatka, and the Kurile Islands—Summary of events and response of the Alaska Volcano Observatory: U.S. Geological Survey Scientific Investigations Report 2010–5243, 94 p., https://doi.org/10.3133/sir20105243.

Nichols, D.R., and Yehle, L.A., 1961, Analyses of gas and water from two mineral springs in the Copper River basin, Alaska, chap. D *of* Short papers in the geologic and hydrologic sciences, articles 293-435: U.S. Geological Survey Professional Paper 424-D, p. D191–D194, https://doi.org/10.3133/pp424D.

Nye, C.J., and Turner, D.L., 1990, Petrology, geochemistry, and age of the Spurr volcanic complex, eastern Aleutian Arc: Bulletin of Volcanology, v. 52, no. 3, p. 205–226, https://doi.org/10.1007/BF00334805.

Pesicek, J.D., Wellik, J.J., II, Prejean, S.G., and Ogburn, S.E., 2018, Prevalence of seismic rate anomalies preceding volcanic eruptions in Alaska: Frontiers in Earth Science, v. 6, article 100, 15 p., https://doi.org/10.3389/feart.2018.00100.

Petersen, T., Caplan-Auerbach, J., and McNutt, S.R., 2006, Sustained long-period seismicity at Shishaldin Volcano, Alaska: Journal of Volcanology and Geothermal Research, v. 151, no. 4, p. 365–381, https://doi.org/10.1016/j.jvolgeores.2005.09.003.

Power, J.A., Haney, M.M., Botnick, S.M., Dixon, J.P., Fee, D., Kaufman, A.M., Ketner, D.M., Lyons, J.J., Parker, T., Paskievitch, J.F., Read, C.W., Searcy, C., Stihler, S.D., Tepp, G., and Wech, A.G., 2020, Goals and development of the Alaska Volcano Observatory seismic network and application to forecasting and detecting volcanic eruptions: Seismological Research Letters, v. 91, no. 2A, p. 647–659, https://doi.org/10.1785/0220190216.

Power, J.A., Stihler, S.D., White, R.A., and Moran, S.C., 2004, Observations of Deep Long-Period (DLP) Seismic Events Beneath Aleutian Arc Volcanoes; 1989–2002: Journal of Volcanology and Geothermal Research, v. 138, no. 3-4, p. 243–266, https://doi.org/10.1016/j.jvolgeores.2004.07.005.

Prejean, S.G., Werner, C.A., Buurman, H., Doukas, M.P., Kelly, P.J., Kern, C., Ketner, D.M., Stihler, S.D., Thurber, C.H., and West, M.E., 2012, Seismic and gas analyses imply magmatic intrusion at Iliamna Volcano, Alaska in 2012 [abs.]: Eos, Transactions, American Geophysical Union, Fall meeting supplement, Abstract number V53B-2826.

Quezada-Reyes, A., Lesage, P., Valdés-Gonzalez, C., and Perrioer, L., 2013, An analysis of the seismic activity of Popocatépetl Volcano, Mexico, associated with the eruptive period of December 2002 to February 2003—Looking for precursors, *in* Rose, W.I., Palma, J.L., Granados, H.D., and Varley, N., eds., Understanding open-vent volcanism and related hazards: Geological Society of America Special Paper 498, p. 89–106, https://doi.org/10.1130/2013.2498(06).

Reeder, J.W., 1990, Sugarloaf, in Annual report of the world volcanic eruptions in 1987: Bulletin of Volcanic Eruptions [Bulletin of Volcanology], Supplement, v. 52, no. 1., article 87-34, p. 36, https://doi.org/10.1007/BF00261307.

Richter, D.H., Symonds, R.B., Rosenkrans, D.S., McGimsey, R.G., Evans, W.C., and Poreda, R.J., 1998a, Report on the 1997 activity of Shrub mud volcano, Wrangell-St. Elias National Park and Preserve, southcentral Alaska: U.S. Geological Survey Open-File Report 98–128, 13 p., https://doi.org/10.3133/ofr98128.

Richter, D.H., Waythomas, C.F., McGimsey, R.G., and Stelling, P.L., 1998b, Geologic map of Akutan Island, Alaska: U.S. Geological Survey Open-File Report 98–135, 1 sheet, scale 1:48,00, 22-p. pamphlet, https://doi.org/10.3133/ofr98135.

Riehle, J.R., 1985, A reconnaissance of the major Holocene tephra deposits in the upper Cook Inlet region, Alaska: Journal of Volcanology and Geothermal Research, v. 26, no. 1-2, p. 37–74, https://doi.org/10.1016/0377-0273(85)90046-0.

Roman, D.C., Power, J.A., Moran, S.C., Cashman, K.V., Doukas, M.P., Neal, C.A., and Gerlach, T.M., 2004, Evidence for dike emplacement at Iliamna Volcano, Alaska in 1996: Journal of Volcanology and Geothermal Research, v. 130, no. 3-4, p. 265–284, https://doi.org/10.1016/S0377-0273(03)00302-0.

Searcy, C.K., and Power, J.A., 2020, Seismic character and progression of explosive activity during the 2016–2017 eruption of Bogoslof volcano, Alaska: Bulletin of Volcanology, v. 82, no. 1, article 12, 12 p., https://doi.org/10.1007/s00445-019-1343-4.

Siebert, L., Simkin, T., and Kimberly, P., 2010, Volcanoes of the World (3d ed.): Berkley, Calif., University of California Press, 568 p.

Simons, F.S., and Mathewson, D.E., 1955, Geology of Great Sitkin Island, Alaska: U.S. Geological Survey Bulletin 1028–B, https://doi.org/10.3133/b1028B.

Thelen, W.A., Allstadt, K., De Angelis, S., Malone, S.D., Moran, S.C., and Vidale, J., 2013, Shallow repeating seismic events under an alpine glacier at Mount Rainier, Washington, USA: Journal of Glaciology, v. 59, no. 214, p. 345–356, https://doi.org/10.3189/2013JoG12J111.

Wallace, K.L., and Schwaiger, H.F., 2019, Volcanic ash resuspension from the Katmai region: Alaska Park Science, v. 18, no. 1, p. 63–70, accessed March 12, 2020, at https://www.nps.gov/articles/aps-18-1-8.htm.

Waythomas, C.F., and Miller, T.P., 1999, Preliminary volcano-hazard assessment for Iliamna Volcano, Alaska: U.S. Geological Survey Open-File Report 99–373, 31-p. pamphlet, 1 sheet, scale unknown, https://doi.org/10.3133/ofr99373.

Waythomas, C.F., Miller, T.P., and Nye, C.J., 2003a, Preliminary geologic map of Great Sitkin Volcano, Alaska: U.S. Geological Survey Open-File Report 03–36, 1 sheet, scale 1:63,360, https://doi.org/10.3133/ofr0336.

Waythomas, C.F., Miller, T.P., and Nye, C.J., 2003b, Preliminary volcano-hazard assessment for Great Sitkin Volcano, Alaska: U.S. Geological Survey Open-File Report 03–112, 25-p. pamphlet, 1 sheet, https://doi.org/10.3133/ofr03112.

Waythomas, C.F., Miller, T.P., and Mangan, M.T., 2006, Preliminary volcano-hazard assessment for the Emmons Lake volcanic center, Alaska: Anchorage, Alaska, U.S. Geological Survey Scientific Investigations Report 2006–5248, 33-p. pamphlet, 1 sheet, https://doi.org/10.3133/sir20065248.

Waythomas, C.F., Power, J.A., Richter, D.H., and McGimsey, R.G., 1998, Preliminary volcano-hazard assessment for Akutan Volcano, east-central Aleutian Islands, Alaska: U.S. Geological Survey Open-File Report 98–360, 36-p. pamphlet, 1 plate, scale 1:82,000, https://doi.org/10.3133/ofr98360.

Waythomas, C.F., Dietterich, H., Tepp, G., Lopez, T. and Loewen, M., 2022, The 2018 eruption of Veniaminof Volcano, Alaska: U.S. Geological Survey Scientific Investigations Report 2022–5075, 32 p., https://doi.org/10.3133/sir20225075.

Werner, C.A., Doukas, M.P., and Kelly, P.J., 2011, Gas emission from failed and actual eruptions from Cook Inlet Volcanoes, Alaska, 1989–2006: Bulletin of Volcanology, v. 73, no. 2, p. 155–173, https://doi.org/10.1007/s00445-011-0453-4.

# Glossary of Selected Terms and Acronyms

**andesite** Volcanic rock composed of about 57–63 percent silica ($SiO_2$).

**ash** Fine fragments (less than 2 millimeters across) of rock formed in an explosive volcanic eruption.

**basalt** Volcanic rock composed of about 45–52 weight percent silica ($SiO_2$).

**basaltic andesite** Volcanic rock composed of about 52–57 weight percent silica ($SiO_2$).

**caldera** A large, roughly circular depression typically caused by a volcanic collapse or explosion.

**dacite** Volcanic rock composed of about 63–69 weight percent silica ($SiO_2$).

**fallout** A general term for debris that falls to the Earth from an eruption cloud.

**fumarole** A small opening or vent from which hot gases are emitted.

**Holocene** Geologic epoch that extends from 10,000 years ago the present.

**infrasound** Low-frequency sound waves, below the threshold of human hearing.

**intracaldera** Adjective referring to within the caldera.

**juvenile** Adjective describing volcanic material created from magma reaching the surface.

**lahar** A flow comprising saturated mixtures of volcaniclastic sediment and water.

**Landsat-8** An American Earth observation satellite; the eighth in the Landsat program.

**lava** Molten rock that has reached the Earth's surface.

**long-period earthquake** An earthquake with dominant frequency content between 1 and 5 hertz. Used interchangeably with the term low-frequency earthquake.

**$M_L$** Local magnitude; an earthquake magnitude scale based on the amplitude of ground motion as measured by a standard seismograph.

**magma** Molten rock below the Earth's surface.

**phreatic activity** An explosive eruption caused by the sudden heating of groundwater as it contacts hot volcanic rock or magma, leading to a steam-driven explosion.

**phreatic ash** Fine fragments of rock expelled during phreatic activity; this ash is typically derived from existing rock and not from new magma.

**pixel** One of the many discrete rectangular elements that form a digital image. In a satellite image, resolution describes the size of a pixel in relation to area covered on the ground. More pixels per unit area on the ground means a higher resolution.

**Pleistocene** A geologic epoch that extends from about 11,700 to 2.6 million years ago.

**pyroclast** An individual particle ejected during a volcanic eruption; typically classified by size, for example, ash and lapilli.

**regional earthquake** Earthquake generated by fracture or slippage along a fault; not caused by volcanic activity.

**real-time seismic amplitude measurement** Amplitude of ground shaking caused by earthquakes and volcanic tremor averaged over 10-minute intervals.

**satellite vent** A subsidiary volcanic vent located on the flank of a larger volcano.

**seismic swarm** A flurry of closely spaced earthquakes or other ground shaking activity; commonly precedes an eruption.

**spatter cone** A low, steep-sided cone of spatter built up on a fissure or vent.

**stratovolcano** Also called a stratocone or composite cone; a steep-sided volcano, typically conical in shape, built of interbedded lava flows and fragmental deposits from explosive eruptions.

**Strombolian** A type of volcanic eruption characterized by intermittent bursts of fluid lava, typically basalt, from a vent or crater. Produced by gas bubbles rising through a conduit and bursting at the surface.

**Tertiary** A geologic period that extends from about 2.6 million to 66 million years ago.

**tremor** Low-amplitude, continuous earthquake activity commonly associated with magma movement.

**vent** An opening in the Earth's surface through which magma erupts or volcanic gasses are emitted.

**volcano-tectonic earthquake** An earthquake generated within or near a volcano by brittle rock failure resulting from strain induced by volcanic processes.

# Appendixes 1–3

# Appendix 1. Citations for Alaska Volcano Observatory Annual Summaries from 1992 to 2017.

**Table 1.1.** Citations for Alaska Volcano Observatory annual summaries from 1992 to 2017.

| Year | Citation | URL |
|---|---|---|
| 1992 | McGimsey, R.G., Neal, C.A., and Doukas, M.P., 1995, Volcanic activity in Alaska—Summary of events and response of the Alaska Volcano Observatory, 1992: U.S. Geological Survey Open-File Report 95–83, 26 p. | https://doi.org/10.3133/ofr9583 |
| 1993 | Neal, C.A., McGimsey, R.G., and Doukas, M.P., 1996, Volcanic activity in Alaska—Summary of events and response of the Alaska Volcano Observatory, 1993: U.S. Geological Survey Open-File Report 96–24, 21 p. | https://doi.org/10.3133/ofr9624 |
| 1994 | Neal, C.A., Doukas, M.P., and McGimsey, R.G., 1995, 1994 Volcanic activity in Alaska—Summary of events and response of the Alaska Volcano Observatory: U.S. Geological Survey Open-File Report 95–271, 18 p. | https://doi.org/10.3133/ofr95271 |
| 1995 | McGimsey, R.G., and Neal, C.A., 1996, 1995 Volcanic activity in Alaska and Kamchatka—Summary of events and response of the Alaska Volcano Observatory: U.S. Geological Survey Open-File Report 96–738, 22 p. | https://doi.org/10.3133/ofr96738 |
| 1996 | Neal, C.A., and McGimsey, R.G., 1997, 1996 Volcanic activity in Alaska and Kamchatka—Summary of events and response of the Alaska Volcano Observatory: U.S. Geological Survey Open-File Report 97–433, 34 p. | https://doi.org/10.3133/ofr97433 |
| 1997 | McGimsey, R.G., and Wallace, K.L., 1999, 1997 Volcanic activity in Alaska and Kamchatka—Summary of events and response of the Alaska Volcano Observatory: U.S. Geological Survey Open-File Report 99–448, 42 p. | https://doi.org/10.3133/ofr99448 |
| 1998 | McGimsey, R.G., Neal, C.A., and Girina, O., 2003, 1998 Volcanic activity in Alaska and Kamchatka—Summary of events and response of the Alaska Volcano Observatory: U.S. Geological Survey Open-File Report 03–423, 35 p. | https://doi.org/10.3133/ofr03423 |
| 1999 | McGimsey, R.G., Neal, C.A., and Girina, O., 2004a, 1999 Volcanic activity in Alaska and Kamchatka—Summary of events and response of the Alaska Volcano Observatory: U.S. Geological Survey Open-File Report 2004–1033, 49 p | https://doi.org/10.3133/ofr20041033 |
| 2000 | Neal, C.A., McGimsey, R.G., and Chubarova, O., 2004, 2000 Volcanic activity in Alaska and Kamchatka—Summary of events and response of the Alaska Volcano Observatory: U.S. Geological Survey Open-File Report 2004–1034, 37 p. | https://doi.org/10.3133/ofr20041034 |
| 2001 | McGimsey, R.G., Neal, C.A., and Girina, O., 2004b, 2001 Volcanic activity in Alaska and Kamchatka—Summary of events and response of the Alaska Volcano Observatory: U.S. Geological Survey Open-File Report 2004–1453, 53 p. | https://doi.org/10.3133/ofr20041453 |
| 2002 | Neal, C.A., McGimsey, R.G., and Girina, O., 2005, 2002 Volcanic activity in Alaska and Kamchatka—Summary of events and response of the Alaska Volcano Observatory: U.S. Geological Survey Open-File Report 2004–1058, 51 p. | https://doi.org/10.3133/ofr20041058 |
| 2003 | McGimsey, R.G., Neal, C.A., and Girina, O., 2005, 2003 Volcanic activity in Alaska and Kamchatka—Summary of events and response of the Alaska Volcano Observatory: U.S. Geological Survey Open-File Report 2005–1310, 58 p. | https://doi.org/10.3133/ofr20051310 |
| 2004 | Neal, C.A., McGimsey, R.G., Dixon, J.P., and Melnikov, D., 2005, 2004 Volcanic activity in Alaska and Kamchatka—Summary of events and response of the Alaska Volcano Observatory: U.S. Geological Survey Open-File Report 2005–1308, 67 p. | https://doi.org/10.3133/ofr20051308 |
| 2005 | McGimsey, R.G., Neal, C.A., Dixon, J.P., and Ushakov, S., 2007, 2005 Volcanic activity in Alaska, Kamchatka, and the Kurile Islands—Summary of events and response of the Alaska Volcano Observatory: U.S. Geological Survey Scientific Investigations Report 2007–5269, 94 p. | https://doi.org/10.3133/sir20075269 |

**Table 1.1.**—Continued

| Year | Citation | URL |
|---|---|---|
| 2006 | Neal, C.A., McGimsey, R.G., Dixon, J.P., Manevich, A., and Rybin, A., 2009, 2006 Volcanic activity in Alaska, Kamchatka, and the Kurile Islands—Summary of events and response of the Alaska Volcano Observatory: U.S. Geological Survey Scientific Investigations Report 2008–5214, 102 p. | https://doi.org/10.3133/sir20085214 |
| 2007 | McGimsey, R.G., Neal, C.A., Dixon, J.P., Malik, N., and Chibisova, M., 2011, 2007 Volcanic activity in Alaska, Kamchatka, and the Kurile Islands—Summary of events and response of the Alaska Volcano Observatory: U.S. Geological Survey Scientific Investigations Report 2010–5242, 110 p. | https://doi.org/10.3133/sir20105242 |
| 2008 | Neal, C.A., McGimsey, R.G., Dixon, J.P., Cameron, C.E., Nuzhaev, A.A., and Chibisova, M., 2011, 2008 Volcanic activity in Alaska, Kamchatka, and the Kurile Islands—Summary of events and response of the Alaska Volcano Observatory: U.S. Geological Survey Scientific Investigations Report 2010–5243, 94 p. | https://doi.org/10.3133/sir20105243 |
| 2009 | McGimsey, R.G., Neal, C.A., Girina, O.A., Chibisova, M., and Rybin, A., 2014, 2009 Volcanic activity in Alaska, Kamchatka, and the Kurile Islands—summary of events and response of the Alaska Volcano Observatory: U.S. Geological Survey Scientific Investigations Report 2013–5213, 125 p. | https://doi.org/10.3133/sir20135213 |
| 2010 | Neal, C.A., Herrick, J., Girina, O.,A., Chibisova, M., Rybin, A., McGimsey, R.G., and Dixon, J., 2014, 2010 Volcanic activity in Alaska, Kamchatka, and the Kurile Islands—Summary of events and response of the Alaska Volcano Observatory: U.S. Geological Survey Scientific Investigations Report 2014–5034, 76 p. | https://doi.org/10.3133/sir20145034 |
| 2011 | McGimsey, R.G., Maharrey, J.Z., and Neal, C.A., 2014, 2011 Volcanic activity in Alaska—Summary of events and response of the Alaska Volcano Observatory: U.S. Geological Survey Scientific Investigations Report 2014–5159, 50 p. | https://doi.org/10.3133/sir20145159 |
| 2012 | Herrick, J.A., Neal, C.A., Cameron, C., Dixon, J., and McGimsey, R.G., 2014, 2012 Volcanic activity in Alaska—Summary of events and response of the Alaska Volcano Observatory: U.S. Geological Survey Scientific Investigations Report 2014–5160, 80 p. | https://doi.org/10.3133/sir20145160 |
| 2013 | Dixon, J.P., Cameron, C., McGimsey, R.G., Neal, C.A., and Waythomas, C., 2015, 2013 Volcanic activity in Alaska—Summary of events and response of the Alaska Volcano Observatory: U.S. Geological Survey Scientific Investigations Report 2015–5110, 92 p. | https://doi.org/10.3133/sir20155110 |
| 2014 | Cameron, C.E., Dixon, J.P., Neal, C.A., Waythomas, C.F., Schaefer, J.R., and McGimsey, R.G., 2017, 2014 Volcanic activity in Alaska—Summary of events and response of the Alaska Volcano Observatory: U.S. Geological Survey Scientific Investigations Report 2017–5077, 81 p. | https://doi.org/10.3133/sir20175077 |
| 2015 | Dixon, J.P., Cameron, C.E., Iezzi, A.M., and Wallace, K., 2017, 2015 Volcanic activity in Alaska—Summary of events and response of the Alaska Volcano Observatory: U.S. Geological Survey Scientific Investigations Report 2017–5104, 81 p. | https://doi.org/10.3133/sir20175104 |
| 2016 | Cameron, C.E., Dixon, J.P., Waythomas, C.F., Iezzi, A.M., Wallace, K.L., McGimsey, R.G., and Bull, K.F., 2020, 2016 Volcanic activity in Alaska—Summary of events and response of the Alaska Volcano Observatory: U.S. Geological Survey Scientific Investigations Report 2020–5125, 63 p. | https://doi.org/10.3133/sir20205125 |
| 2017 | Dixon, J.P., Cameron, C.E., Iezzi, A.M., Power, J.A., Wallace, K., and Waythomas, C.F., 2020, 2017 Volcanic activity in Alaska—Summary of events and response of the Alaska Volcano Observatory: U.S. Geological Survey Scientific Investigations Report 2020–5102, 61 p. | https://doi.org/10.3133/sir20205102 |

# Appendix 2. Volcanoes Included in Previous Alaska Volcano Observatory Annual Summaries

**Table 2.1.** Compilation by year of volcanoes included in Alaska Volcano Observatory annual summaries from 1992 to 2018.

[Volcanoes of each year listed in geographic order, from east to west along the Wrangell-Aleutian volcanic arc]

| Volcanoes mentioned |
|---|
| **1992** |
| Mount Spurr (Crater Peak) |
| Redoubt Volcano |
| Iliamna Volcano |
| Mount Mageik |
| Westdahl volcano |
| Akutan Volcano |
| Bogoslof volcano |
| Pyre Peak |
| **1993** |
| Mount Churchill |
| Mount Sanford |
| Mount Spurr (Crater Peak) |
| Mount Veniaminof |
| Shishaldin Volcano |
| Makushin Volcano |
| Pyre Peak |
| Atka volcanic complex (Mount Kliuchef) |
| Kanaga Volcano |
| **1994** |
| Mount Sanford |
| Iliamna Volcano |
| Trident Volcano |
| Mount Martin |
| Mount Mageik |
| Mount Veniaminof |
| Mount Kupreanof |
| Shishaldin Volcano |
| Makushin Volcano |
| Mount Cleveland |
| Kanaga Volcano |
| **1995** |
| Mount Martin |
| Mount Veniaminof |
| Shishaldin Volcano |
| Makushin Volcano |
| Atka volcanic complex (Mount Kliuchef) |
| Kanaga Volcano |
| **1996** |
| Mount Wrangell |
| Iliamna Volcano |
| Mount Martin |
| Mount Mageik |
| Pavlof Volcano |
| Shishaldin Volcano |
| Westdahl volcano |
| Akutan Volcano |
| Amukta Island |
| Atka volcanic complex (Korovin Volcano) |
| Kanaga Volcano |
| **1997** |
| Mount Wrangell |
| Mount Sanford |
| Shrub mud volcano |
| Iliamna Volcano |
| Kukak Volcano |
| Snowy Mountain |
| Mount Martin |
| Mount Mageik |
| Mount Chiginagak |
| Pavlof Volcano |
| Shishaldin Volcano |
| Mount Okmok |
| Mount Cleveland |
| Amukta Island |
| **1998** |
| Shrub mud volcano |
| Augustine Volcano |
| Becharof Lake area |
| Mount Chiginagak |
| Shishaldin Volcano |
| Akutan Volcano |
| Atka volcanic complex (Korovin Volcano) |
| **1999** |
| Mount Wrangell |
| Shrub mud volcano |
| Iliamna Volcano |
| Mount Veniaminof |
| Pavlof Volcano |
| Shishaldin Volcano |
| Mount Vsevidof |
| **2000** |
| Mount Wrangell |
| Snowy Mountain |
| Mount Chiginagak |
| Shishaldin Volcano |
| **2001** |
| Kukak Volcano |
| Snowy Mountain |
| Pavlof Volcano |
| Frosty Peak |
| Shishaldin Volcano |
| Makushin Volcano |
| Mount Okmok |
| Mount Cleveland |
| Great Sitkin Volcano |
| **2002** |
| Mount Wrangell |
| Mount Martin |
| Mount Mageik |
| **2002—continued** |
| Mount Veniaminof |
| Mount Hague |
| Shishaldin Volcano |
| Great Sitkin Volcano |
| **2003** |
| Mount Wrangell |
| Redoubt Volcano |
| Iliamna Volcano |
| Augustine Volcano |
| Mount Mageik |
| Mount Veniaminof |
| Pavlof Volcano |
| Mount Hague |
| Shishaldin Volcano |
| Akutan Volcano |
| **2004** |
| Mount Crillon (nonvolcanic peak) |
| Mount Spurr |
| Mount Martin |
| Mount Veniaminof |
| Shishaldin Volcano |
| Westdahl volcano |
| **2005** |
| Mount Spurr |
| Iliamna Volcano |
| Augustine Volcano |
| Mount Katmai (Novarupta) |
| Trident Volcano |
| Mount Martin |
| Mount Mageik |
| Mount Chiginagak |
| Aniakchak Crater |
| Mount Veniaminof |
| Mount Hague |
| Shishaldin Volcano |
| Mount Cleveland |
| Atka volcanic complex (Korovin Volcano) |
| Kasatochi Island |
| Tanaga Volcano |
| **2006** |
| Klawasi group mud volcanoes (unnamed vent) |
| Mount Spurr |
| Augustine Volcano |
| Fourpeaked Mountain |
| Mount Martin |
| Mount Veniaminof |
| Mount Cleveland |
| Atka volcanic complex (Korovin Volcano) |
| Kasatochi Island |

**Table 2.1.—Continued**

| Volcanoes mentioned |
|---|
| 2007 |
| Redoubt Volcano |
| Augustine Volcano |
| Fourpeaked Mountain |
| Mount Veniaminof |
| Pavlof Volcano |
| Akutan Volcano |
| Mount Cleveland |
| Atka volcanic complex (Korovin Volcano) |
| 2008 |
| Redoubt Volcano |
| Aniakchak Crater |
| Mount Veniaminof |
| Shishaldin Volcano |
| Mount Okmok |
| Mount Cleveland |
| Kasatochi Island |
| 2009 |
| Mount Sanford |
| Redoubt Volcano |
| Fourpeaked Mountain |
| Aniakchak Crater |
| Mount Veniaminof |
| Shishaldin Volcano |
| Mount Okmok |
| Mount Cleveland |
| 2010 |
| Mount Wrangell |
| Mount Sanford |
| Redoubt Volcano |
| Fourpeaked Mountain |
| Mount Katmai (Novarupta) |
| Becharof Lake area |
| Aniakchak Crater |
| Mount Veniaminof |
| Westdahl volcano |
| Makushin Volcano |
| Mount Cleveland |
| Kasatochi Island |
| 2011 |
| Aniakchak Crater |
| Mount Okmok |
| Mount Cleveland |
| 2012 |
| Mount Wrangell |
| Mount Spurr |
| Redoubt Volcano |
| Iliamna Volcano |
| Augustine Volcano |
| Fourpeaked Mountain |
| Mount Martin |
| Aniakchak Crater |
| Mount Cleveland |
| Kanaga Volcano |
| Little Sitkin Island |

| Volcanoes mentioned |
|---|
| 2013 |
| Redoubt Volcano |
| Iliamna Volcano |
| Fourpeaked Mountain |
| Mount Peulik |
| Aniakchak Crater |
| Mount Veniaminof |
| Pavlof Volcano |
| Shishaldin Volcano |
| Akutan Volcano |
| Makushin Volcano |
| Mount Okmok |
| Mount Cleveland |
| Atka volcanic complex (Korovin Volcano) |
| Great Sitkin Volcano |
| Mount Gareloi |
| 2014 |
| Mount Spurr |
| Redoubt Volcano |
| Iliamna Volcano |
| Fourpeaked Mountain |
| Mount Katmai (Novarupta) |
| Mount Martin |
| Mount Chiginagak |
| Aniakchak Crater |
| Mount Veniaminof |
| Pavlof Volcano |
| Shishaldin Volcano |
| Akutan Volcano |
| Mount Okmok |
| Mount Recheshnoi |
| Mount Cleveland |
| Kanaga Volcano |
| Tanaga Volcano |
| Semisopochnoi Island |
| 2015 |
| Mount Spurr |
| Redoubt Volcano |
| Iliamna Volcano |
| Augustine Volcano |
| Mount Katmai (Novarupta) |
| Becharof Lake area |
| Ugashik caldera |
| Aniakchak Crater |
| Mount Veniaminof |
| Mount Kupreanof |
| Pavlof Volcano |
| Shishaldin Volcano |
| Mount Recheshnoi |
| Mount Cleveland |
| Semisopochnoi Island |
| 2016 |
| Mount Wrangell |
| Mount Spurr |
| Iliamna Volcano |

| Volcanoes mentioned |
|---|
| 2016—continued |
| Augustine Volcano |
| Mount Douglas |
| Mount Katmai (Novarupta) |
| Aniakchak Crater |
| Pavlof Volcano |
| Frosty Peak |
| Shishaldin Volcano |
| Makushin Volcano |
| Bogoslof volcano |
| Mount Okmok |
| Mount Cleveland |
| Atka volcanic complex (Korovin Volcano) |
| 2017 |
| Mount Spurr |
| Redoubt Volcano |
| Iliamna Volcano |
| Augustine Volcano |
| Mount Katmai (Novarupta) |
| Pavlof Volcano |
| Shishaldin Volcano |
| Akutan Volcano |
| Makushin Volcano |
| Bogoslof volcano |
| Mount Okmok |
| Mount Cleveland |
| Great Sitkin Volcano |
| Takawangha volcano |
| Mount Gareloi |
| Kiska Volcano |
| 2018 |
| Shrub mud volcano |
| Mount Spurr |
| Iliamna Volcano |
| Mount Katmai (Novarupta) |
| Mount Veniaminof |
| Pavlof Volcano |
| Shishaldin Volcano |
| Westdahl volcano |
| Akutan Volcano |
| Makushin Volcano |
| Mount Okmok |
| Mount Cleveland |
| Great Sitkin Volcano |
| Mount Gareloi |
| Semisopochnoi Island (Mount Young) |

**Table 2.2.** Compilation of volcanic activity described in previous Alaska Volcano Observatory annual summaries from 1992 to 2018.

[Volcanic centers listed in geographic order from east to west along the Wrangell-Aleutian volcanic arc. Official volcano names may not reflect the geographic or geologic extent of the volcanic features. $CO_2$, carbon dioxide; PIREP, pilot weather report]

| Volcano | Year mentioned | Type of activity |
|---|---|---|
| Mount Crillon (nonvolcanic) | 2004 | Anomalous clouds from avalanches |
| Mount Churchill | 1993 | Anomalous tectonic seismicity |
| Mount Wrangell | 1996 | Robust steam emissions |
| | 1997 | Steam emissions |
| | 1999 | Steam and possible ash emissions |
| | 2000 | Steam emissions |
| | 2002 | Anomalous clouds possibly associated with resuspended ash |
| | 2003 | Anomalous clouds |
| | 2007 | Triggered seismicity; steam emissions; resuspended ash |
| | 2010 | Anomalous weather clouds |
| | 2012 | Steam emissions |
| | 2013 | Resuspended ash; steam emissions |
| | 2016 | Snow melt prompts false report of new summit ash deposit |
| Mount Sanford | 1993 | Anomalous clouds, likely from avalanches |
| | 1994 | Anomalous cloud, likely from avalanche |
| | 1997 | Anomalous cloud, likely from avalanche |
| | 2009 | Anomalous weather cloud |
| | 2010 | Anomalous cloud related to weather or avalanche |
| Shrub mud volcano | 1997 | Eruption at Shrub mud volcano with energetic ejection of saline mud and $CO_2$ |
| | 1998 | Eruption of saline mud and $CO_2$ at Shrub mud volcano continues |
| | 1999 | Eruption of saline mud and $CO_2$ at Shrub mud volcano continues |
| | 2018 | Eruption at Shrub mud volcano continues; new mud eruption on southeast flank |
| Unnamed Klawasi group vent | 2006 | Possible new mud vent between Upper Klawasi and Lower Klawasi mud volcanoes |
| Mount Spurr | 1992 | Subplinian eruption with ash fall, pyroclastic flows, and lahars |
| | 1993 | Seismicity associated with glacial outburst |
| | 2004 | Elevated seismicity and heat flux; lahars; ice cauldron forms; steam emissions; increased $CO_2$ emissions |
| | 2005 | Elevated seismicity and heat flux; debris flows; cauldron evolves; steam emissions |
| | 2006 | Declining seismicity and heat flux; cauldron evolves; steam emissions |
| | 2012 | Glacial outburst flood; elevated seismicity |
| | 2014 | Earthquake swarm; glacial outburst flood |
| | 2015 | Earthquake swarm |
| | 2016 | Earthquake swarms |
| | 2017 | Earthquake swarm |
| | 2018 | Elevated seismicity, likely related to glacial movement |
| Redoubt Volcano | 1992 | Eruption false alarm |
| | 2003 | Anomalous weather cloud |
| | 2007 | Steam emissions; increased heat flux |
| | 2008 | Increased gas and thermal flux; debris flows |
| | 2009 | Major magmatic eruption; dome extrusion; lahars; ash and tephra fall; pyroclastic flows |
| | 2010 | Gas and steam emissions; seismicity briefly elevated; thermal anomalies |
| | 2012 | Robust steam emissions |
| | 2013 | Steam emissions |
| | 2014 | Steam emissions |
| | 2015 | Outburst flood caused by melting from avalanche |
| | 2017 | Steam emissions |
| Iliamna Volcano | 1992 | Robust steam emissions; eruption false alarm |
| | 1994 | Vigorous steam emissions; ice and rock avalanche |
| | 1996 | Earthquake swarms related to magmatic intrusion; increased $SO_2$ and $CO_2$ flux |

**Table 2.2.**—Continued

| Volcano | Year mentioned | Type of activity |
|---|---|---|
| Iliamna Volcano—continued | 1997 | Earthquake swarm; ice and rock avalanche |
| | 1999 | Ice and rock avalanche |
| | 2003 | Ice and rock avalanche |
| | 2005 | Avalanche |
| | 2012 | Steam emissions; seismic swarms; ice and rock avalanches |
| | 2013 | Ice and rock avalanches |
| | 2014 | Ice and rock avalanches |
| | 2015 | Large tectonic earthquake |
| | 2016 | Steam emissions; ice and rock avalanche |
| | 2017 | Ice and rock avalanche |
| | 2018 | Ice and rock avalanche |
| Augustine Volcano | 1998 | Spine of 1986 dome partially collapses and generates mudflow |
| | 2003 | Steam emissions |
| | 2005 | Elevated seismicity; weak phreatic eruptive activity; steam and ash emissions; deformation |
| | 2006 | Explosive and effusive eruption; steam and ash emissions; pyroclastic flows; ash fall; lahars; dome extrusion |
| | 2007 | Elevated seismicity; steam emissions |
| | 2012 | Steam emissions; sulfur odor; elevated seismicity |
| | 2015 | Steam emissions; rockfalls |
| | 2016 | Earthquake swarm |
| | 2017 | Elevated seismicity |
| Mount Douglas | 2013 | Steam emissions |
| | 2016 | Earthquake swarm |
| Fourpeaked Mountain | 2006 | Phreatic eruption; steam and ash emissions; debris flows; glacial outburst flood |
| | 2007 | Steam emissions; declining seismicity |
| | 2009 | Declining steam and gas emissions |
| | 2010 | Declining steam and gas emissions; sporadic earthquake swarms |
| | 2012 | Elevated seismicity |
| | 2013 | Elevated seismicity |
| | 2014 | Long-lasting seismic network outage |
| | 2016 | Earthquake swarm |
| Kukak Volcano | 1997 | Steam emissions |
| | 2001 | Steam emissions |
| Snowy Mountain | 1997 | Steam emissions |
| | 2000 | Steaming hole in glacier; sulfur odor |
| | 2001 | Steaming hole in glacier |
| Mount Katmai | | |
| Novarupta | 2003 | Resuspension of 1912 ash |
| | 2005 | Resuspension of 1912 ash |
| | 2010 | Resuspension of 1912 ash |
| | 2014 | Resuspension of 1912 ash |
| | 2015 | Resuspension of 1912 ash |
| | 2016 | Resuspension of 1912 ash; deployment of particulate monitors |
| | 2017 | Resuspension of 1912 ash |
| | 2018 | Resuspension of 1912 ash |
| Trident Volcano | 1994 | Anomalous weather cloud |
| | 2005 | New crater |
| Mount Mageik | 1992 | Anomalous weather cloud |
| | 1994 | Anomalous weather cloud |

**Table 2.2.**—Continued

| Volcano | Year mentioned | Type of activity |
|---|---|---|
| Mount Mageik—continued | 1996 | Seismicity related to glacial activity; earthquake swarm |
| | 1997 | Steam emissions |
| | 2002 | Steam emissions |
| | 2003 | Steam emissions |
| | 2005 | Steam emissions |
| Mount Martin | 1994 | Anomalous weather cloud |
| | 1995 | Robust steam emissions |
| | 1996 | Seismicity related to glacial activity; earthquake swarm |
| | 1997 | Steam emissions |
| | 2002 | Steam emissions |
| | 2003 | Steam emissions |
| | 2004 | Robust steam emissions |
| | 2005 | Steam emissions |
| | 2006 | Earthquake swarm |
| | 2010 | Resuspended ash |
| | 2012 | Elevated seismicity; steam emissions |
| | 2014 | Earthquake swarm; steam emissions |
| Becharof Lake area | 1998 | Earthquake swarm |
| | 2010 | Earthquake swarm |
| | 2015 | Large earthquake with aftershocks |
| Mount Peulik | 2013 | Steam emissions; sulfur odor |
| Ugashik caldera | 2015 | Discolored water |
| Mount Chiginagak | 1997 | Steam emissions and sulfur odor from new fumarole field |
| | 1998 | Steam emissions and sulfur odor |
| | 2000 | Steam emissions |
| | 2005 | Increased summit heat flux; crater lake forms; acidic outburst flood |
| | 2014 | Increased fumarolic activity; thermal anomalies |
| Aniakchak Crater | 2005 | Elevated seismicity; thermal anomaly |
| | 2008 | Weather-related seismicity |
| | 2009 | Anomalous seismicity |
| | 2010 | Low frequency earthquake swarms |
| | 2011 | Drainage of maar lake; destructive downstream flooding |
| | 2012 | Elevated seismicity |
| | 2013 | Earthquake swarms |
| | 2014 | Long-lasting seismic network outage |
| | 2015 | Seismic network reestablished |
| | 2016 | Notable nonvolcanic earthquake with aftershocks |
| Mount Veniaminof | 1993 | Strombolian eruptive activity; lava flows; steam and ash emissions |
| | 1994 | Strombolian eruptive activity; lava flows; steam and ash emissions |
| | 1995 | Strombolian eruptive activity; lava flows; steam and ash emissions |
| | 1999 | Increased glacial discharge; turbid river |
| | 2002 | Increased seismicity; weak phreatic activity; steam and ash emissions |
| | 2003 | Increased seismicity; weak phreatic activity; steam and ash emissions |
| | 2004 | Intermittent phreatic and Strombolian eruptive activity; steam and ash emissions |
| | 2005 | Intermittent phreatic and Strombolian eruptive activity; steam and ash emissions |
| | 2006 | Intermittent phreatic and Strombolian eruptive activity; steam and ash emissions |
| | 2007 | Decline in steam emissions |
| | 2008 | Weak phreatic eruptive activity; steam and ash emissions |
| | 2009 | Weak phreatic eruptive activity; steam emissions |
| | 2010 | Sporadic elevated seismicity; steam emissions |
| | 2013 | Strombolian eruptive activity; elevated seismicity; ash emissions; lava flows |

**Table 2.2.**—Continued

| Volcano | Year mentioned | Type of activity |
|---|---|---|
| Mount Veniaminof—continued | 2014 | Declining seismicity; thermal anomalies; steam emissions |
| | 2015 | Elevated seismicity |
| | 2018 | Intermittent minor eruption |
| Mount Kupreanof | 1994 | Steam emissions |
| | 2015 | Steam emissions |
| Pavlof Volcano | 1996 | Strombolian eruptive activity; fountaining; lava flows; lahars, ash emissions |
| | 1997 | Strombolian eruptive activity |
| | 1999 | Summit snow melt; steam emissions; possible resuspended ash |
| | 2001 | Steam and possible ash emissions; steam emissions and sulfur odor from Mount Hague misattributed to Pavlof Volcano |
| | 2003 | Steam emissions from Mount Hague misattributed to Pavlof Volcano |
| | 2005 | Steam emissions from Mount Hague misattributed to Pavlof Volcano |
| | 2007 | Strombolian eruptive activity; ash emissions; lava flows; lahars |
| | 2013 | Strombolian eruptive activity; elevated seismicity; ash emissions; lava flows; lahars |
| | 2014 | Strombolian eruptive activity; lava fountaining; steam and ash emissions; lava flows; lahars |
| | 2015 | End of 2014 eruptive unrest |
| | 2016 | Substantial eruption; ash emissions; pyroclastic flows; lahars |
| | 2017 | End of intermittent eruptive activity; elevated seismicity; steam emissions; thermal anomalies |
| | 2018 | Elevated seismicity |
| Mount Hague | 2001 | Steam emissions and sulfur odor misattributed to Pavlof Volcano |
| | 2002 | Elevated seismicity; steam emissions |
| | 2003 | Crater lake drains and refills; steam emissions misattributed to Pavlof Volcano |
| | 2005 | Steam emissions misattributed to Pavlof Volcano |
| Frosty Peak | 2001 | Rockfall avalanches mistaken for eruptive activity |
| | 2016 | Ice and rock avalanche |
| Shishaldin Volcano | 1993 | Weak eruptive activity; steam and ash emissions |
| | 1994 | Anomalous cloud |
| | 1995 | Weak eruptive activity; steam and ash emissions |
| | 1996 | Weak eruptive activity; steam and ash emissions |
| | 1997 | Weak eruptive activity; steam and ash emissions |
| | 1998 | Weak eruptive activity; steam and ash emissions |
| | 1999 | Subplinian eruption; ash emissions and ash fall; Strombolian eruptive activity; steam emissions |
| | 2000 | Weak eruptive activity; steam emissions |
| | 2001 | Increased seismicity; steam emissions |
| | 2002 | Increased seismicity; steam emissions |
| | 2003 | Steam emissions |
| | 2004 | Elevated seismicity; steam and ash emissions |
| | 2005 | Elevated seismicity; steam emissions |
| | 2008 | Possible ash emission; steam emissions |
| | 2009 | Elevated seismicity; steam emissions; thermal anomalies |
| | 2013 | Elevated seismicity; steam emissions |
| | 2014 | Intermittent low-level eruptive activity; steam and ash emissions |
| | 2015 | Intermittent low-level eruptive activity; steam and ash emissions |
| | 2016 | Weak eruptive activity; thermal anomalies; steam emissions |
| | 2017 | Elevated seismicity; steam emissions; thermal anomalies |
| | 2018 | Declining volcanic unrest |
| Westdahl volcano | 1992 | Fissure eruption; lava fountaining; ash emissions; lava flows |
| | 1996 | Anomalous weather cloud |
| | 2004 | Earthquake swarm |
| | 2010 | Elevated lower crustal seismicity |
| | 2018 | Long-term inflation |

**Table 2.2.**—Continued

| Volcano | Year mentioned | Type of activity |
|---|---|---|
| Akutan Volcano | 1992 | Steam and ash emissions |
| | 1996 | Intense earthquake swarms; ground cracking |
| | 1998 | Tremor-like seismicity related to weather |
| | 2003 | Anomalous steam emissions |
| | 2007 | Triggered seismicity; inflation; anomalous steam emissions |
| | 2013 | Triggered seismicity; intermittent tectonic tremor |
| | 2014 | Earthquake swarm; uplift; probable magmatic inflation |
| | 2017 | Earthquake swarm |
| | 2018 | Long-term inflation |
| Makushin Volcano | 1993 | Minor phreatic activity; steam and ash emissions |
| | 1994 | Minor phreatic activity; steam and ash emissions |
| | 1995 | Steam and ash emissions |
| | 2001 | Elevated seismicity; steam emissions; sulfur odor |
| | 2008 | Discolored seawater and bubbles in Unalaska Bay (nonvolcanic) |
| | 2010 | Elevated seismicity; robust steam emissions |
| | 2013 | Intermittent tremor; steam emissions |
| | 2016 | Earthquake swarms |
| | 2017 | Earthquake swarm; steam emissions |
| | 2018 | Earthquake swarms; steam emissions |
| Bogoslof volcano | 1992 | Dome extrusion; ash and steam emissions |
| | 2016 | Substantial explosive eruptive activity; steam and ash emissions; pyroclastic flows |
| | 2017 | Substantial explosive eruptive activity; steam and ash emissions; pyroclastic flows |
| Mount Okmok | 1997 | Strombolian eruptive activity; fountaining; steam and ash emissions; lava flows |
| | 2001 | Earthquake swarm |
| | 2008 | Major phreatomagmatic eruption; ash emissions and ash fall; pyroclastic flows; lahars |
| | 2009 | Tremor bursts; inflation |
| | 2011 | Inflation |
| | 2013 | Inflation; earthquake swarm; sporadic tremor |
| | 2014 | Inflation |
| | 2016 | Seismic tremor |
| | 2017 | Inflation |
| | 2018 | Inflation |
| Mount Recheshnoi | 2014 | Earthquake swarm |
| | 2015 | Elevated seismicity |
| Mount Vsevidof | 1999 | Steam emissions after regional earthquake |
| Mount Cleveland | 1994 | Small explosion; steam and ash emissions |
| | 1997 | Small explosion; steam and ash emissions |
| | 2001 | Explosive eruption; steam and ash emissions; lava flows; debris flows |
| | 2005 | Intermittent explosive eruptions; steam and ash emissions |
| | 2006 | Intermittent explosive eruptions; ash emissions |
| | 2007 | Intermittent explosive eruptions; steam, ash, and $SO_2$ emissions; ballistics; lahars |
| | 2008 | Intermittent explosive eruptions; ash emissions and ash fall; debris flows; ballistics; lava effusion |
| | 2009 | Intermittent explosive eruptions; ash emissions; debris flows; thermal anomalies |
| | 2010 | Intermittent explosive eruptions; steam and ash emissions; debris flows; thermal anomalies |
| | 2011 | Thermal anomalies; lava dome extrusion; minor ash emissions |
| | 2012 | Intermittent explosive activity; ash emissions; lava dome extrusion; thermal anomalies |
| | 2013 | Intermittent explosive activity; ash emissions; debris flows; pyroclastic flows; thermal anomalies |
| | 2014 | Intermittent explosive activity; steam and ash emissions; lava dome extrusion; pyroclastic flows |

**Table 2.2.**—Continued

| Volcano | Year mentioned | Type of activity |
|---|---|---|
| Mount Cleveland—continued | 2015 | Intermittent explosive activity; steam and ash emissions; dome extrusion; thermal anomalies |
| | 2016 | Intermittent explosive activity; steam and ash emissions; dome extrusion; thermal anomalies |
| | 2017 | Intermittent explosive activity; steam and ash emissions; dome extrusion; thermal anomalies |
| | 2018 | Intermittent explosive activity; steam and ash emissions; dome extrusion; thermal anomalies |
| Amukta Island | 1996 | Small eruption; ash emissions |
| | 1997 | Small eruption; ash emissions |
| Pyre Peak | 1992 | Weak eruptive activity; steam and ash emissions |
| | 1993 | Fissure eruption; lava flow; ash emissions |
| Atka volcanic complex | | |
| Mount Kliuchef | 1993 | Audible rumbling, strong sulfur odor, and increased steam emissions following earthquake |
| | 1995 | Anomalous cloud; strong sulfur odor |
| Korovin Volcano | 1995 | Thermal anomaly |
| | 1996 | Anomalous weather cloud |
| | 1998 | Eruption; ash emissions and ashfall |
| | 2005 | Minor eruption; steam and ash emissions; elevated seismicity |
| | 2006 | Earthquake swarms; tremor; uplift; steam emissions |
| | 2007 | Triggered seismicity; tremor bursts; steam and ash emissions |
| | 2013 | Earthquake swarm; tremor |
| | 2016 | Seismic tremor; steam emissions |
| Kasatochi Island | 2005 | Unusual bubbling and floating scum on crater lake |
| | 2006 | Continued bubbling in intracaldera lake |
| | 2008 | Major explosive eruption; ash emissions and ash fall; pyroclastic flows; crater widening; local tsunami |
| | 2010 | Waning seismicity; diffuse soil degassing; coastal erosion; lake refilling |
| Great Sitkin Volcano | 2001 | Elevated seismicity |
| | 2002 | Earthquake swarm; tremor |
| | 2013 | Earthquake swarms; thermal anomaly |
| | 2017 | Earthquake swarm; explosion |
| | 2018 | Earthquake swarm; explosions |
| Kanaga Volcano | 1993 | Steam emissions; sulfur odor |
| | 1994 | Eruption; steam and ash emissions; lava flows; debris flows |
| | 1995 | Weak eruptive activity; steam and ash emissions |
| | 1996 | Steam and possible ash emissions; sulfur odor |
| | 2012 | Phreatic eruption; ash emissions; new summit fissure |
| | 2014 | Earthquake swarm |
| Tanaga Volcano | 2005 | Elevated seismicity |
| | 2014 | Earthquake swarm |
| Takawangha volcano | 2005 | Tremor |
| | 2017 | Earthquake swarm |
| Mount Gareloi | 2013 | Felt earthquakes; steam emissions |
| | 2017 | Steam emissions |
| | 2018 | Increased seismicity |
| Semisopochnoi Island | | |
| | 2014 | Earthquake swarm; likely magmatic intrusion |
| | 2015 | Earthquake swarm |
| Mount Young | 2018 | Minor eruption |
| Little Sitkin Island | 2012 | Earthquake swarms; likely magmatic intrusion |
| Kiska Volcano | 2017 | Steam emissions |

# Appendix 3. Aviation Color Codes and Volcano Alert Levels Used by United States Volcano Observatories

The Aviation Color Code addresses the hazards to aviation posed by a volcano, whereas the Volcano Alert Level addresses the hazards on the ground. There could be situations where a volcano is producing lava flows that are dangerous on the ground and merit a **WATCH** or **WARNING**, but where the hazard to aviation is minimal, meriting an Aviation Color Code of **GREEN** or **YELLOW**. Where possible, Volcano Alert Level announcements contain additional explanations of volcanic activity and expected hazards (Gardner and Guffanti, 2006).

**Table 3.1.** Definitions of the Aviation Color Codes used by United States volcano observatories.

| Aviation Color Code | Definition |
|---|---|
| **GREEN** | Volcano is in typical background, noneruptive state.<br>**Or, after a change from a higher level:**<br>Volcanic activity has ceased, and volcano reverted to its noneruptive state. |
| **YELLOW** | Volcano is showing signs of elevated unrest above known background level.<br>**Or, after a change from a higher level:**<br>Volcanic activity has decreased considerably but continues to be closely monitored for possible renewed increase. |
| **ORANGE** | Volcano is showing heightened or escalating unrest with increased potential of eruption, timeframe uncertain.<br>**Or:**<br>Eruption is underway but poses limited hazards. |
| **RED** | Eruption is imminent with considerable emission of volcanic ash into the atmosphere likely.<br>**Or:**<br>Eruption is underway or suspected with considerable emission of volcanic ash into the atmosphere (ash-plume height specified, if possible). |
| **UNASSIGNED** | Ground-based instrumentation is insufficient to establish that a volcano is in a typical background level (GREEN/NORMAL). When activity at such a volcano increases to the point of being detected by remote sensing, distant seismic networks, or eyewitness reports, an alert level and color code are then assigned accordingly. When activity decreases, the volcano goes back to UNASSIGNED without going through GREEN/NORMAL. |

**Table 3.2.** Definitions of the Volcano Alert Levels used by United States volcano observatories.

| Volcano Alert Level | Definition |
|---|---|
| **NORMAL** | Volcano is in typical background, noneruptive state.<br>**Or, after a change from a higher level:**<br>Volcanic activity has ceased, and volcano reverted to its noneruptive state. |
| **ADVISORY** | Volcano is showing signs of elevated unrest above known background level.<br>**Or, after a change from a higher level:**<br>Volcanic activity has decreased considerably but continues to be closely monitored for possible renewed increase. |
| **WATCH** | Volcano is showing heightened or escalating unrest with increased potential of eruption, timeframe uncertain.<br>**Or:**<br>Eruption is underway but poses limited hazards. |
| **WARNING** | Highly hazardous eruption is imminent, underway, or suspected. |
| **UNASSIGNED** | Ground-based instrumentation is insufficient to establish that a volcano is in a typical background level (GREEN/NORMAL). When activity at such a volcano increases to the point of being detected by remote sensing, distant seismic networks, or eyewitness reports, an alert level and color code are then assigned accordingly. When activity decreases, the volcano goes back to UNASSIGNED without going through GREEN/NORMAL. |

Moffett Field Publishing Service Center
Manuscript approved March 9, 2023
Edited by Claire Ashcraft
Illustration support by Katie Sullivan
Layout and design by Cory Hurd

USGS

Cameron and others—**2018 Volcanic Activity in Alaska—Summary of Events and Response of the Alaska Volcano Observatory**—Scientific Investigations Report 2023–5029

ISSN 2328-0328 (online)
https://doi.org/10.3133/sir20235029